5-2011

Thermo- and pH-Sensitive Hydrophilic Block Copolymers: Synthesis, Micellization, Gelation, and Application

Thomas G. O'Lenick
University of Tennessee - Knoxville, olenick@ion.chem.edu

To the Graduate Council:

I am submitting herewith a dissertation written by Thomas G. O'Lenick entitled "Thermo- and pH-Sensitive Hydrophilic Block Copolymers: Synthesis, Micellization, Gelation, and Application." I have examined the final electronic copy of this dissertation for form and content and recommend that it be accepted in partial fulfillment of the requirements for the degree of Doctor of Philosophy, with a major in Chemistry.

Bin Zhao, Major Professor

We have read this dissertation and recommend its acceptance:

Jimmy W. Mays, Michael D. Best, Hong Guo

Accepted for the Council:

Carolyn R. Hodges

Vice Provost and Dean of the Graduate School

(Original signatures are on file with official student records.)

To the Graduate Council:

I am submitting herewith a dissertation written by Thomas G. O'Lenick entitled "Thermo- and pH-Sensitive Hydrophilic Block Copolymers: Synthesis, Micellization, Gelation, and Application." I have examined the final electronic copy of this dissertation for form and content and recommend that it be accepted in partial fulfillment of the requirements for the degree of Doctor of Philosophy, with a major in Chemistry.

Bin Zhao, Major Professor

We have read this dissertation
and recommend its acceptance:

Jimmy W. Mays

Michael D. Best

Hong Guo

Accepted for the council:

Carolyn R. Hodges
Vice Provost and Dean of the Graduate School

(Original signatures are on file with official student records.)

Thermo- and pH-Sensitive Hydrophilic Block Copolymers: Synthesis, Micellization, Gelation, and Application

A Dissertation

Presented for the

Doctor of Philosophy Degree

The University of Tennessee, Knoxville

Thomas G. O'Lenick

May 2011

Acknowledgements

I would like to thank Dr. Bin Zhao for his advisement, patience, instruction, and support throughout my graduate studies. Graduate school was a very difficult time in my life and I would not have been able to complete my studies without Dr. Zhao's understanding, patience, and guidance. From his instruction and guidance I feel I have become a professional chemist that is well rounded in both organic and polymer chemistry.

I would also like to thank Dr. Mike Best, Dr. Jimmy Mays, and Dr. Hong Guo for serving on my doctoral committee. I would also like to thank Dr. Miller and Dr. Dai for their support and collaboration during the spring semester of 2009.

I would like to thank my fellow group members who have been working with me during my tenure at the University of Tennessee: Dr. Dejin Li, Dr. Xueguang Jiang, Dr. Xiaoming Jiang, Jeremiah Woodcock, Jon Horton, Naixiong Jin, and Roger Wright. Without their friendship and cooperation I would not have my sanity.

I would also like to thank my parents for their love, guidance, and support. They provided me with every tool I needed to succeed in life both as a parent and a chemist. I would also like to thank my dad for being a role model for me not only as a chemist but also as a great dad.

Most importantly, I would like to thank my wife Courtney, son Ty, and daughter Harper for their love and support. My son Ty has taught me to enjoy the little things in life and no matter what life throws at me it is okay to smile and laugh. My daughter Harper has taught me to be strong and never stop fighting for what I want, no matter how

bad the odds may be for my success. My wife Courtney has been my rock when I needed someone to lean on, my inspiration when I wanted to quit, and loving arms when I was in need. Thank you all so much for everything you do and I love you.

Finally, I want to thank the University of Tennessee and the National Science Foundation for the financial support through out my studies.

Abstract

This dissertation presents the synthesis of a series of thermo- and pH-sensitive hydrophilic block copolymers and the study of their solution behavior in water. By incorporating a small amount of weak acid or base groups into the thermosensitive block(s) of a hydrophilic block copolymer, the LCST of the thermosensitive block(s) can be modified by changing the solution pH. Accordingly, the critical micellization temperature (CMT) and the sol-gel transition temperature ($T_{sol\text{-}gel}$) of the block copolymer in water can be tuned.

Chapter 1 describes the synthesis of thermo- and pH-sensitive poly(methoxydi(ethylene glycol) methacrylate-*co*-methacrylic acid)-*b*-PEO-*b*-poly(methoxydi(ethylene glycol) methacrylate-*co*-methacrylic acid) and the study of sol-gel transitions of its aqueous solutions at various pH values. The CMT of the 0.2 wt% solution and the $T_{sol\text{-}gel}$ of the 12.0 wt% solution of this copolymer can be varied over a large temperature range. By judiciously controlling temperature and pH, multiple sol-gel-sol transitions were realized. Chapter 2 presents a systematic study of pH effect on rheological properties of micellar gels formed from 10.0 wt% aqueous solutions of thermo- and pH-sensitive poly(ethoxydi(ethylene glycol) acrylate-*co*-acrylic acid)-*b*-PEO-*b*-poly(ethoxydi(ethylene glycol) acrylate-*co*-acrylic acid). With the increase of pH, the sol-gel transition became broader. The plateau moduli (G_N) evaluated from frequency sweeps at $T/T_{sol\text{-}gel}$ of 1.025, 1.032, and 1.039 decreased with the increase of pH from 3.00 to 5.40 with the largest drop observed at pH = ~ 4.7. The decrease in G_N reflects the reduction of the number of bridging chains. The ionization of carboxylic acid introduced

charges onto the thermosensitive blocks and made the polymer more hydrophilic, facilitating the formation of loops and dangling chains.

Chapter 3 presents the synthesis of PEO-*b*-poly(methoxydi(ethylene glycol) methacrylate-*co*-2-(*N*-methyl-*N*-(4-pyridyl)amino)ethyl methacrylate) with the thermosensitive block containing a catalytic 4-*N*,*N*-dialkylaminopyridine and the study of the effect of thermo-induced micellization on its activity in the hydrolysis of *p*-nitrophenyl acetate. The CMTs of this copolymer at pH of 7.06 and 7.56 were 40 and 37 °C, respectively. Below CMT, the logarithm of initial hydrolysis rate changed linearly with $1/T$. Above CMT, the reaction rate leveled off, which is presumably because it was controlled by mass transport to the core of micelles above CMT.

Contents

List of Tables

List of Schemes

List of Figures

Chapter 1. Thermosensitive Aqueous Gels with Tunable Sol-Gel Transition Temperatures from Thermo- and pH-Responsive Hydrophilic ABA Triblock Copolymer

Abstract

This chapter describes the synthesis of a well-defined hydrophilic ABA triblock copolymer composed of a poly(ethylene oxide) (PEO) middle block and thermo- and pH-sensitive outer blocks and the study of sol-gel transitions of its aqueous solutions at various pH values. The doubly responsive linear triblock copolymer, poly(methoxydi(ethylene glycol) methacrylate-*co*-methacrylic acid)-*b*-PEO-*b*-poly(methoxydi(ethylene glycol) methacrylate-*co*-methacrylic acid) (P(DEGMMA-*co*-MAA)-*b*-PEO-*b*-P(DEGMMA-*co*-MAA)), was prepared by atom transfer radical polymerization of a mixture of DEGMMA and *t*-butyl methacrylate with a molar ratio of 100 : 5 from a difunctional PEO macroinitiator and subsequent removal of *t*-butyl groups using trifluoroacetic acid. Dynamic light scattering studies showed that the critical micellization temperature (CMT) of this ABA triblock copolymer in a 0.2 wt % aqueous solution was dependent on the solution pH and can be varied in a large temperature range (> 20 °C). To study the sol-gel transitions, a 12.0 wt% aqueous solution of the triblock copolymer with a pH of 4.89 was made; its pH value can be readily changed and well controlled by the injection of either a 1.0 M HCl or a 1.0 M KOH solution. From rheological measurements, the sol-gel transition temperature ($T_{sol\text{-}gel}$) versus pH curve was found to closely trace the CMT versus pH curve, though there was a shift. By cycling the solution pH between 3.2 and 5.4, we showed that the $T_{sol\text{-}gel}$ at a specific pH was reproducible. Moreover, multiple sol-gel-sol transitions were realized by judiciously controlling the temperature and pH simultaneously, demonstrating the possibility of achieving on-demand sol-gel transitions by using two external stimuli. In addition, the effect of polymer concentration on $T_{sol\text{-}gel}$ at pH = 4.0 was investigated. The sol-gel

transition temperature increased with the decrease of polymer concentration and the critical gelation concentration was found to be between 4 and 6 wt%.

1.1 Introduction

ABA triblock copolymers, composed of a permanently water-soluble B block and stimuli-responsive hydrophilic A blocks, can self-assemble in a dilute aqueous solution into flower micelles with the outer blocks associating into the core and the central blocks forming loops in the corona layer upon application of an external stimulus.[1,2] When the polymer concentration is sufficiently high, i.e., above the critical gelation concentration (CGC), a 3-dimensional micellar network is formed, in which the central block forming bridges among neighboring micelles. Consequently, the free-flowing solution is transformed into a free-standing micellar gel triggered by the environmental stimulus.[1-4] The block copolymer micellar gels have received growing interest in recent years and have found applications, e.g., in controlled release of drugs and tissue engineering.[3-6] Compared with chemically crosslinked hydrogels, stimuli-sensitive aqueous micellar gels are more advantageous for many biomedical applications because the in situ sol-gel transition and the nature of physical crosslinking allow convenient delivery and removal of polymers.

There have been a number of reports on stimuli-sensitive hydrophilic ABA triblock and other multi-block copolymer micellar gels.[3-28] For example, using atom transfer radical polymerization (ATRP), Armes et al. synthesized a series of ABA triblock copolymers that can form gels in water in response to either pH or temperature changes.[8-13] These linear triblock copolymers were composed of a biocompatible phosphorylcholine-containing polymer as the central block and pH- or temperature-sensitive polymers as outer blocks. Kirkland et al. prepared poly(*N*-isopropylacrylamide)-*b*-poly(*N*,*N*-dimethyacrylamide)-*b*-poly(*N*-isopropylacrylamide) (PNIPAm-*b*-PDMA-*b*-

PNIPAm) by reversible addition fragmentation chain transfer (RAFT) polymerization.[14] Above the lower critical solution temperature (LCST) of PNIPAm, the triblock copolymer aqueous solutions underwent sol-gel transitions that led to the formation of micellar gels with mechanical properties similar to collagen, a naturally occurring polypeptide that has been used as a cell growth scaffold.[14]

Of particular interest to us are aqueous block copolymer micellar gels that can respond to multiple stimuli, i.e., the sol-gel transition can be induced by at least two distinct physical or chemical stimuli.[3,4,15-28] Such gels would provide a greater design flexibility that is needed in many technological uses including biomedical applications. Up to date, there are only a few reports in the literature on multi-sensitive block copolymer aqueous gels. Notably, Li et al. reported the synthesis of thermo- and redox-sensitive ABA triblock copolymers by ATRP using a difunctional initiator that contained a redox-sensitive disulfide bond.[15] The sol-gel transitions can be triggered biochemically and thermally. Temperature- and pH-sensitive block copolymer aqueous gels are probably the most studied multi-responsive micellar gels.[18-28] The block copolymers were usually prepared by either growing pH-sensitive blocks from or introducing pH-responsive groups to the chain ends of an ABA triblock copolymer that can form thermoreversible gels in water (e.g., PEO-*b*-PPO-*b*-PEO).[18-25] Suh et al. used pyromellitic dianhydride to couple PEO-*b*-PPO-*b*-PEO to make multiblock copolymers with carboxylic acid groups being incorporated at the junction points.[26] Very recently, Lee et al. reported pH- and thermo-sensitive aqueous gels of multiblock copolymers composed of PEO and poly(amino urethane).[27,28]

Here we present a new type of thermo- and pH-responsive ABA triblock copolymer aqueous micellar gels. Different from those reported in the literature, our approach is to incorporate carboxylic acid groups into the thermosensitive outer blocks of an ABA triblock copolymer. The key feature of this type of doubly responsive hydrophilic block copolymers is that the LCST of the thermosensitive block can be modulated by application of a second stimulus.[29-31] It has been reported in the literature that the LCST transition temperature of a thermosensitive polymer that contains a small amount of weak acid or base groups can be precisely and reversibly tuned by adjusting the solution pH,[31-44] allowing one to reversibly tune the sol-gel transition temperature in a wide temperature range. In this work, we synthesized a thermo- and pH-sensitive ABA triblock copolymer, poly(methoxydi(ethylene glycol)-*co*-methacrylic acid)-*b*-poly(ethylene oxide)-*b*-poly(methoxydi(ethylene glycol)-*co*-methacrylic acid) (P(DEGMMA-*co*-MAA)-*b*-PEO-*b*-P(DEGMMA-*co*-MAA)), by ATRP of a mixture of DEGMMA and *t*-butyl methacrylate (*t*BMA) with a molar ratio of 100 : 5 from a difunctionalized PEO macroinitiator and subsequent removal of *t*-butyl groups of *t*BMA units (Scheme 1.1). PDEGMMA is a biocompatible thermosensitive water-soluble polymer with a LCST at 25 °C in water, which belongs to a new class of thermo-responsive hydrophilic polymers with a short oligo(ethylene glycol) pendant from each repeating unit.[45-65] We show that the sol-gel transition temperature ($T_{sol\text{-}gel}$) of aqueous solutions of this ABA triblock copolymer can be controlled by pH and multiple sol-gel-sol transitions can be realized via the combination of temperature and pH triggers. It should be noted here that very recently Lutz and coworkers reported the synthesis of thermosensitive linear triblock copolymers and four-arm star-block copolymers by ATRP of mixtures of DEGMMA and

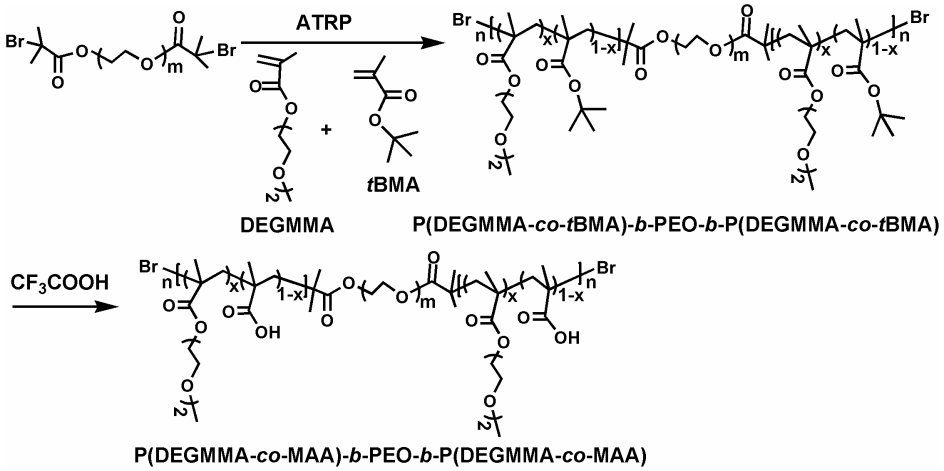

Scheme 1.1. Synthesis of Thermo- and pH-Sensitive ABA Triblock Copolymer P(DEGMMA-*co*-MAA)-*b*-PEO-*b*-P(DEGMMA-*co*-MAA).

oligo(ethylene glycol) methacrylate from linear and 4-arm star PEO macroinitiators, respectively. The thermo-induced sol-gel transitions of aqueous solutions of these copolymers were investigated.[64,65]

1.2 Experimental Part

1.2.1 Materials

Methoxydi(ethylene glycol) methacrylate (DEGMMA, or di(ethylene glycol) methyl ether methacrylate, 95%, Aldrich), *N,N,N′,N′,N″*-pentamethyldiethylenetriamine (PMDETA, Aldrich), and ethyl 2-bromoisobutyrate (EBiB, Aldrich) were dried over calcium hydride and distilled under reduced pressure. CuBr (98%, Aldrich) was purified according to the procedure described in the literature[66,67] and was stored in a desiccator. Potassium hydrogen phthalate (KHP) and trifluoroacetic acid (99%) were obtained from Acros and used without further treatment. Dichloromethane and anisole (99%, Acros) were dried with calcium hydride, distilled, and stored in solvent storage flasks. *tert*-Butyl methacrylate (99%, Aldrich) was passed through a basic aluminum oxide column prior to use. Poly(ethylene glycol) (HO-PEO-OH, MW = 20,000 g/mol) was obtained from Aldrich. All other chemicals were purchased from either Aldrich or Fisher and used without further purification.

1.2.2 General Characterization

Gel permeation chromatography (GPC) was carried out at ambient temperature using PL-GPC 20 (an integrated GPC system from Polymer Laboratories, Inc) with a differential refractive index detector, one PLgel 5 μm guard column (50 × 7.5 mm), and two PLgel 5 μm mixed-C columns (each 300 × 7.5 mm, linear range of molecular weight

from 200 to 2,000,000 according to Polymer Laboratories). The data were processed using Cirrus^{TM} GPC/SEC software (Polymer Laboratories). THF was used as the carrier solvent at a flow rate of 1.0 mL/min. Polystyrene standards (Polymer Laboratories) were used for calibration. The ^{1}H (300 MHz) NMR spectra were recorded on a Varian Mercury 300 NMR spectrometer and the residual solvent proton signal was used as the internal standard.

1.2.3. Synthesis of Difunctional PEO Macroinitiator (Br-PEO-Br)

Poly(ethylene oxide) (PEO) with a molecular weight of 20,000 g/mol (21.257 g, 1.063 mmol) was added into a three-necked flask and dissolved in toluene (250 mL). The trace amount of water in PEO was removed by azeotropic distillation of toluene (~ 150 mL) under the normal atmospheric pressure. After the solution was cooled to room temperature, triethylamine (0.934 g, 9.2 mmol) was added and the mixture was stirred for 30 min under the protection of N_2. 2-Bromoisobutyryl bromide (4.208 g, 18.3 mmol) was added dropwise from an addition funnel. After the reaction mixture was stirred overnight at ambient temperature, the precipitate was removed by vacuum filtration. The filtrate was concentrated and precipitated in diethyl ether (200 mL). The polymer was purified by precipitation in diethyl ether three times from its dichloromethane solution. The macroinitiator was then dissolved in water with a pH of ~ 8. Dichloromethane was used to extract the PEO macroinitiator. The organic extracts were combined and dried over anhydrous magnesium sulfate overnight. After the removal of magnesium sulfate by filtration, the solution was concentrated and precipitated in diethyl ether. The macroinitiator was then recrystallized in ethanol twice and dried under high vacuum at an

elevated temperature. The difunctional macroinitator Br-PEO-Br was obtained as a white solid.

1.2.4. Synthesis of P(DEGMMA-*co*-*t*BMA)-*b*-PEO-*b*-P(DEGMMA-*co*-*t*BMA)

Copper (I) bromide (14.4 mg, 1.00 $\times 10^{-4}$ mol) and the difunctional PEO macroinitiator Br-PEO-Br (1.003 g, 4.95 $\times 10^{-5}$ mol) were weighed into a two-necked flask, followed by addition of DEGMMA (3.721 g, 19.8 mmol), *t*BMA (0.147 g, 1.04 mmol), and anisole (7.811 g). *N,N,N′,N′,N″*-Pentamethyldiethylenetriamine (17.2 mg, 9.89 $\times 10^{-5}$ mol) was then injected into the flask via a microsyringe. Three freeze-pump-thaw cycles were employed to degas the reaction mixture. The reaction was started by placing the flask into a 75 °C oil bath. The polymerization was monitored by GPC. After 100 min, the polymerization was stopped by opening the flask to air and diluting the reaction mixture with THF. The copper catalyst was removed from the reaction mixture by passing the solution through a short neutral aluminum oxide/silica gel column. The polymer was precipitated four times in hexanes and then dried under high vacuum. GPC analysis results (polystyrene standards): $M_{n,GPC}$ = 43000 g/mol, polydispersity (PDI) = 1.13. The numbers of DEGMMA and *t*BMA units in the block copolymer were 235 and 12, respectively, calculated from the ^{1}H NMR spectrum.

1.2.5. Synthesis of P(DEGMMA-*co*-MAA)-*b*-PEO-*b*-P(DEGMMA-*co*-MAA)

P(DEGMMA-*co*-*t*BMA)-*b*-PEO-*b*-P(DEGMMA-*co*-*t*BMA) (2.000 g) was added into a 50 mL round bottom flask and dissolved with dichloromethane (10 mL). The solution was stirred at room temperature for 2 h to ensure complete dissolution. Trifluoroacetic acid (5.470 g) was then added into the flask. After the reaction mixture was stirred at ambient temperature for 46 h, the volatiles were removed by a rotavapor.

The polymer was precipitated four times in a mixture of hexanes and diethyl ether (10/1, v/v), and then dried under high vacuum.

1.2.6. Preparation of 12.0 wt% Aqueous Solution of P(DEGMMA-*co*-MAA)-*b*-PEO-*b*-P(DEGMMA-*co*-MAA)

P(DEGMMA-*co*-MAA)-*b*-PEO-*b*-P(DEGMMA-*co*-MAA) was added into a pre-weighed round bottom flask and dried under high vacuum at 70 °C for 5 h. The weight of the dried polymer was 1.143 g. Milli-Q water (8.361 g) was added into the flask and the mixture was then sonicated in an ice/water ultrasonic bath (Fisher Scientific Model B200 Ultrasonic Cleaner) to dissolve the ABA triblock copolymer in water. The flask was then stored in a refrigerator (~ 4 °C) overnight and the solution was filtered with a 0.45 μm Nylon filter. We then injected 103.5 μL of a 1.0 M KOH aqueous solution to make the polymer solution a buffer (-COOH/-COOK). The pH of the obtained polymer solution, measured by a pH meter (Accumet AB15 pH meter from Fisher Scientific, calibrated with pH = 4.01, 7.00, and 10.01 standard buffer solutions), was 4.89, which is close to the pK_a value (pK_a = 5.59) of carboxylic acid groups in a random copolymer P(DEGMMA-*co*-MAA) with a molar ratio of DEGMMA to MAA similar to that in the ABA triblock copolymer.[68] This 12.0 wt% polymer aqueous solution was used as the starting point for all experiments in this work.

1.2.7 Dynamic Light Scattering Study of Thermo-Induced Micellization of 0.2 wt% Aqueous Solutions of P(DEGMMA-*co*-MAA)-*b*-PEO-*b*-P(DEGMMA-*co*-MAA) in 10 mM KHP Buffers with Various pH Values

The thermo-induced micellization of P(DEGMMA-*co*-MAA)-*b*-PEO-*b*-P(DEGMMA-*co*-MAA) at a concentration of 0.2 wt% in 10 mM KHP buffers with

various pH values was studied by dynamic light scattering (DLS). The KHP buffers were prepared by dissolving KHP in Milli-Q water (KHP concentration: 10 mM) and the pH values were adjusted by the addition of a 1.0 M KOH aqueous solution or a 1.0 M HCl aqueous solution. A series of 0.2 wt% aqueous solutions of P(DEGMMA-*co*-MAA)-*b*-PEO-*b*-P(DEGMMA-*co*-MAA) with different pH values were prepared by diluting a certain amount of the aforementioned 12.0 wt% aqueous polymer solution with KHP buffers (e.g., 3.357 g of the pH = 3.20 KHP buffer was added into a vial that contained 56.0 mg of the 12.0 wt% polymer solution). All 0.2 wt% polymer solutions were sonicated in an ice/water ultrasonic bath for 2 min to ensure that the solutions were homogeneous. The pH values of the solutions were re-measured by a pH meter (essentially the same as the pH values of KHP buffers)

DLS measurements were conducted with a Brookhaven Instruments BI-200SM goniometer equipped with a PCI BI-9000AT digital correlator, a temperature controller, and a solid-state laser (model 25-LHP-928-249, λ = 633 nm) at a scattering angle of 90^{o}. The polymer solutions were filtered into borosilicate glass tubes with an inner diameter of 7.5 mm by the use of 0.2 μm filters. The glass tubes were then sealed with PE stoppers. The solutions were gradually heated from room temperature. At each temperature, the solutions were equilibrated for 30 min prior to data recording. The time correlation functions were analyzed with a Laplace inversion program (CONTIN).

1.2.8 Titration of 12.0 wt% Aqueous Solution of P(DEGMMA-*co*-MAA)-*b*-PEO-*b*-P(DEGMMA-*co*-MAA) with a 1.0 M KOH Solution

A portion of the aforementioned 12.0 wt% triblock copolymer solution (2.887 g) was added into a small vial, followed by the injection of the same amount of a 1.0 M HCl

solution as that of the previously injected KOH solution for this portion of the polymer solution. The pH of the obtained solution was 2.58, measured by a pH meter. 5.0 μL of a 1.0 M KOH solution was then injected into the vial via a microsyringe. The vial was sonicated in an ultrasonic water bath for 2 min and the pH was recorded. This process was repeated until a total of 100 μL of 1.0 M KOH solution was added. The total volume increased by 3.5 %. A plot of pH versus the amount of KOH was made, which was used as a guide to determine the amount of KOH, or equivalently the amount of HCl, that is needed to achieve particular pH values and vice versa.

1.2.9 Rheological Measurements

Rheological experiments were conducted using a stress-controlled rheometer (TA Instruments Model TA AR2000ex). A cone-plate geometry with a cone diameter of 20 mm and an angle of 2° (truncation 52 μm) was employed; the temperature was controlled by the bottom Peltier plate. In each measurement, ~ 85 μL of a polymer solution was loaded onto the plate by a micropipette. The solvent trap was filled with water and a solvent trap cover was used to minimize water evaporation. Dynamic viscoelastic properties (dynamic storage modulus G' and loss modulus G") of polymer solutions were measured by oscillatory shear experiments performed at a fixed frequency of 1 Hz in a heating ramp at a heating rate of 2 ^{o}C/min. The frequency dependences of G' and G" of a polymer solution at selected temperatures were obtained by frequency sweep tests from 0.1 to 100 Hz. A strain amplitude of γ = 0.2 % was used in all dynamic tests to ensure that the deformation was within the linear viscoelastic regime. At each temperature, the solution was equilibrated for at least 2 min prior to data recording.

1.3 Results and Discussion

1.3.1 Synthesis of P(DEGMMA-*co*-MAA)-*b*-PEO-*b*-P(DEGMMA-*co*-MAA)

The thermo- and pH-sensitive ABA triblock copolymer, P(DEGMMA-*co*-MAA)-*b*-PEO-*b*-P(DEGMMA-*co*-MAA), was synthesized from P(DEGMMA-*co*-*t*BMA)-*b*-PEO-*b*-P(DEGMMA-*co*-*t*BMA) by the removal of *t*-butyl groups. P(DEGMMA-*co*-*t*BMA)-*b*-PEO-*b*-P(DEGMMA-*co*-*t*BMA) was prepared by ATRP of a mixture of DEGMMA and *t*BMA with a molar ratio of 100 : 5 from a difunctional PEO macroinitiator (MW = 20000 g/mol) at 75 °C in anisole using CuBr/PMDETA as catalyst. The block copolymer was purified by repetitive precipitation in hexanes, dried in high vacuum, and characterized by GPC and ^{1}H NMR spectroscopy analysis. Figure 1.1a shows the GPC traces of macroinitiator Br-PEO-Br and P(DEGMMA-*co*-*t*BMA)-*b*-PEO-*b*-P(DEGMMA-*co*-*t*BMA); the $M_{n,GPC}$ and polydispersity index of the obtained ABA triblock copolymer were 43000 g/mol and 1.13, respectively (relative to polystyrene standards). Trifluoroacetic acid was then used to remove the *t*-butyl groups in the copolymer. Note that our group previously confirmed that CF_3COOH does not affect other ester linkages in the polymer.[31] The cleavage reaction was conducted in dichloromethane with excess trifluoroacetic acid at room temperature for 46 h. ^{1}H NMR spectroscopy analysis shows that the *t*-butyl peak located at 1.39 ppm disappeared (Figure 1.1b).[69] The numbers of DEGMMA and *t*BMA units in the copolymer were calculated from the ^{1}H NMR spectra using the integral values of the peaks at 4.08 ppm (-COOCH_2CH$_2$- of DEGMMA units), the peak located at 1.39 ppm (COOC(CH_3)$_3$ of *t*BMA units, excluding the integral value of the small broad peak shown in the ^{1}H NMR spectrum (ii) after the cleavage[69]), and the peaks from 3.45 to 3.94 ppm (OCH_2 from the

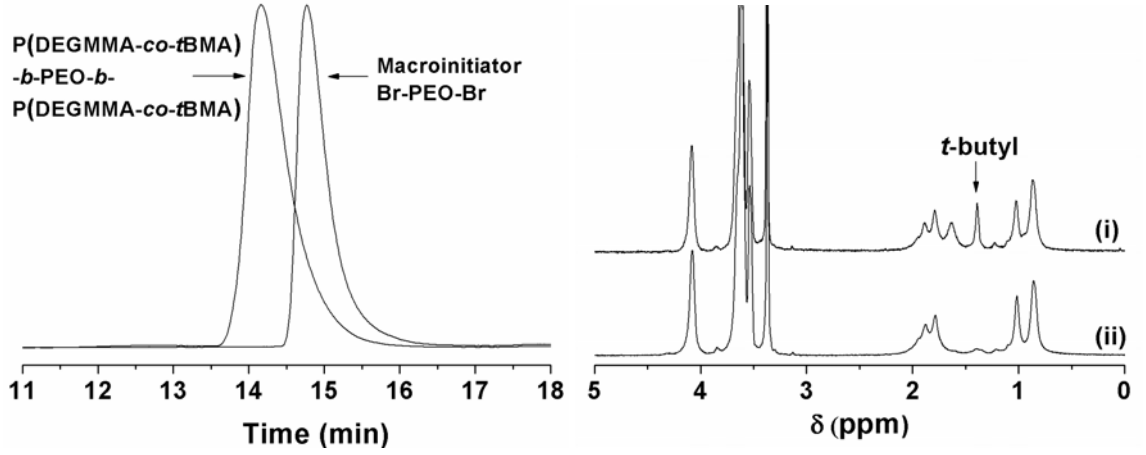

(a) (b)

Figure 1.1. (a) Gel permeation chromatography analysis of difunctional PEO macroinitiator Br-PEO-Br and the ABA triblock copolymer P(DEGMMA-*co*-*t*BMA)-*b*-PEO-*b*-P(DEGMMA-*co*-*t*BMA), and (b) ^{1}H NMR spectra of (i) P(DEGMMA-*co*-*t*BMA)-*b*-PEO-*b*-P(DEGMMA-*co*-*t*BMA) and (ii) P(DEGMMA-*co*-MAA)-*b*-PEO-*b*-P(DEGMMA-*co*-MAA). $CDCl_3$ was used as the solvent.

central PEO block and $OCH_2CH_2OCH_2CH_2OCH_3$ of DEGMMA units). The numbers of DEGMMA and *t*BMA units (MAA units) were 235 and 12, respectively.

1.3.2 pH Dependence of Critical Micellization Temperature of P(DEGMMA-*co*-MAA)-*b*-PEO-*b*-P(DEGMMA-*co*-MAA) at a Concentration of 0.2 wt% in 10 mM KHP Aqueous Buffers

Using dynamic light scattering (DLS), we first investigated how the critical micellization temperature (CMT) of P(DEGMMA-*co*-MAA)-*b*-PEO-*b*-P(DEGMMA-*co*-MAA) in 10 mM aqueous KHP buffers changed with the solution pH. Figure 1.2 shows representative data from DLS studies: the intensity of scattered light at scattering angle of 90° and the hydrodynamic size, obtained by CONTIN analysis, as a function of temperature for a 0.2 wt% aqueous solution of P(DEGMMA-*co*-MAA)-*b*-PEO-*b*-P(DEGMMA-*co*-MAA) in a pH = 4.93 KHP buffer in the heating process. Below 36 °C, the scattering intensity was very low and the hydrodynamic diameter was < 10 nm, indicating that the polymer was dissolved molecularly in water, i.e., in the unimer state. Above 36 °C, the scattering intensity began to increase; the CMT was 37.5 °C, determined from Figure 1.2a. While multiple size distributions were observed in the temperature range of 37 – 40 °C, a single size distribution with an average hydrodynamic diameter of ~ 72 nm was found at 41 °C and above. Clearly, the thermosensitive P(DEGMMA-*co*-MAA) blocks underwent a hydration-to-dehydration transition and self-assembled into a hydrophobic core with the central PEO blocks forming loops in the corona layer, yielding flower micelles. The single size distribution observed at $T \geq 41$ °C suggests the absence of PEO bridges among micelles. The thermo-induced micellization behaviors of P(DEGMMA-*co*-MAA)-*b*-PEO-*b*-P(DEGMMA-*co*-MAA) at other pH

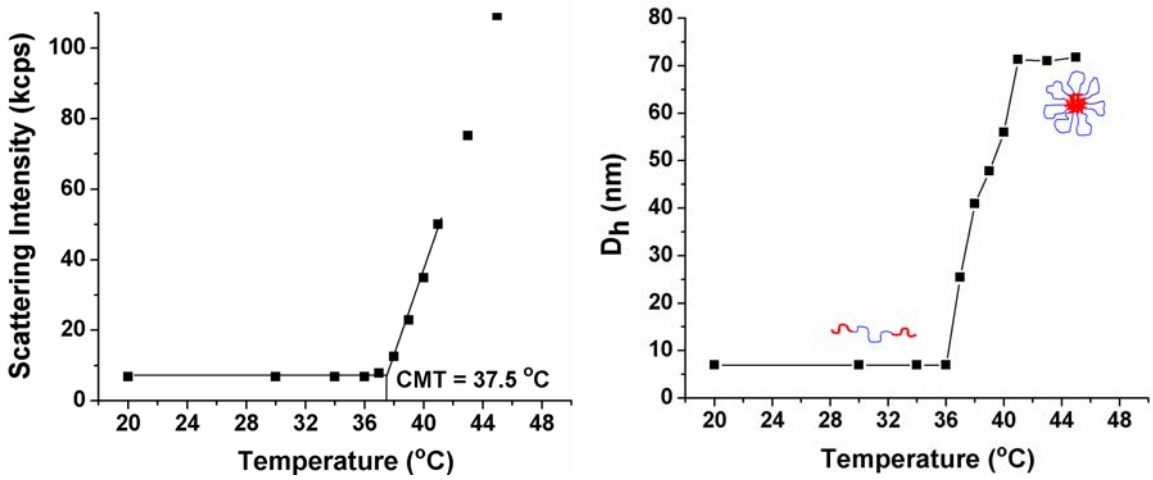

(a) (b)

Figure 1.2. (a) Scattering intensity at the scattering angle of 90° and (b) apparent hydrodynamic diameter, D_h, as a function of temperature, obtained from a DLS study of a 0.2 wt% solution of P(DEGMMA-*co*-MAA)-*b*-PEO-*b*-P(DEGMMA-*co*-MAA) in the pH = 4.93 KHP buffer.

values were also studied and the results are summarized in Figure 1.3. Evidently, the CMT of this triblock copolymer initially increased slowly with the increase of pH (only 2 °C from pH 3.32 to 4.93). Above pH = 5.0, the CMT increased appreciably faster; it jumped more than 12 °C in just one pH unit. At pH = 6.60, no CMT was observed in the experimentally studied temperature range from room temperature to 70 °C. Thus, the CMT of this triblock copolymer can be varied in a wide temperature range by adjusting the solution pH. This tunability stems from the behavior of carboxylic acid groups. At low pH values, the pendant carboxylic acid groups are protonated and form acid-ether complexes via hydrogen bonding with the ether linkages of neighboring DEGMMA monomer units,[70-72] which depresses the LCST of thermosensitive blocks. With the increase of pH, the COOH groups begins to ionize and the acid-ether complexes decompose, making thermosensitive P(DEGMMA-*co*-MAA) blocks more hydrophilic and thus resulting in a high LCST for the thermosensitive blocks and a high CMT for P(DEGMMA-*co*-MAA)-*b*-PEO-*b*-P(DEGMMA-*co*-MAA). From the titration of a random copolymer P(DEGMMA-*co*-MAA) with a molar ratio of DEGMMA to MAA similar to that in the ABA triblock copolymer, the pK_a of COOH groups in P(DEGMMA-*co*-MAA) was determined to be 5.59.[68] Thus, it appears that when the degree of ionization (α) of carboxylic acid groups is < 50 %, the LCST changes slowly. At α > 50 %, the LCST increases drastically. At even higher pH values, nearly all carboxylic acid groups are ionized, causing the polymer chain to be highly hydrophilic and consequently exhibit no thermoresponsive property in the studied temperature range.

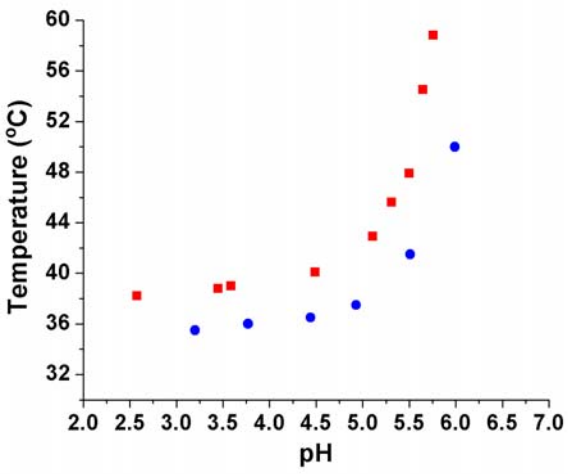

Figure 1.3. Plots of critical micellization temperature (CMT, ●) of P(DEGMMA-*co*-MAA)-*b*-PEO-*b*-P(DEGMMA-*co*-MAA) in dilute aqueous buffer solutions (polymer concentration: 0.2 wt%) and sol-gel transition temperature ($T_{sol\text{-}gel}$, ■) of 12.0 wt% aqueous solution of P(DEGMMA-*co*-MAA)-*b*-PEO-*b*-P(DEGMMA-*co*-MAA) versus solution pH. The CMTs were determined by DLS and the $T_{sol\text{-}gel}$s were measured by rheometry experiments.

1.3.3 Rheometry Study of Sol-Gel Transitions of 12.0 wt% Aqueous Solutions of P(DEGMMA-*co*-MAA)-*b*-PEO-*b*-P(DEGMMA-*co*-MAA) at Various pH Values

To study the pH-dependence of sol-gel transition, a 12.0 wt% aqueous solution was made by dissolving P(DEGMMA-*co*-MAA)-*b*-PEO-*b*-P(DEGMMA-*co*-MAA) in Milli-Q water. A small amount of a 1.0 M KOH aqueous solution was then injected to raise the pH to 4.89, which is close to the pK_a value (5.59) of COOH groups in a random copolymer P(DEGMMA-*co*-MAA) with a molar ratio of DEGMMA to MAA similar to that in the triblock copolymer.[68] Thus, the solution was an aqueous buffer composed of COOH/COOK, allowing the pH value to be well controlled and easily tuned by injection of HCl and KOH solutions. In the following rheometry experiments, this solution was used as the starting point. Since we needed to change the solution pH, especially in the multiple sol-gel-sol transition experiment, and it was not convenient to use a pH meter to determine the pH of a small amount of a solution, we studied how the pH of the 12.0 wt% polymer solution varied with the addition of HCl or KOH. We took 2.887 g of the 12.0 wt% polymer solution, added the same amount of a 1.0 M HCl solution as that of the previously injected KOH solution for this portion of the polymer solution, and then conducted a titration by injecting 5.0 μL of a 1.0 M KOH solution each time and subsequently measuring the solution pH with a pH meter. A plot of solution pH versus number of μmols of added KOH was constructed and is shown in Figure 1.4. Note that after the completion of titration, the solution volume increased by only 3.5 %. To confirm that the solution pH can be precisely controlled, we injected calculated amounts of a 1.0 M HCl solution, which can be viewed as negative amounts of KOH, at the end of titration and found from pH measurements that the pH values were right on the curve (the red

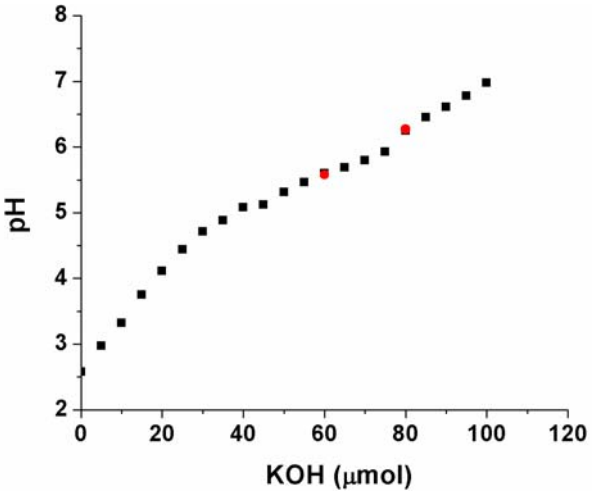

Figure 1.4. The plot of solution pH versus number of μmols of KOH injected into a 12.0 wt% aqueous solution of P(DEGMMA-*co*-MAA)-*b*-PEO-*b*-P(DEGMMA-*co*-MAA) (2.887 g). The KOH solution was added stepwise; each time, 5.0 μL of a 1.0 M aqueous KOH solution was injected via a microsyringe, followed by the measurement of pH with a pH meter (solid square symbols, ■). After the completion of titration, calculated amounts of 1.0 M HCl solutions were added and the pH values were measured (red solid circle symbols, ●).

solid circles in Figure 1.4). Figure 1.4 was used as a guide to determine the amount of KOH or HCl needed to achieve a particular pH value.

Rheological measurements were conducted to study the thermo-induced sol-gel transitions and rheological properties of aqueous solutions of P(DEGMMA-*co*-MAA)-*b*-PEO-*b*-P(DEGMMA-*co*-MAA) at various pH values. Figure 1.5 shows the data from an oscillatory shear measurement of the 12.0 wt% aqueous solution with a pH of 3.59 at a constant frequency of 1 Hz in a heating ramp with a heating rate of 2 °C/min. A strain amplitude of γ = 0.2 % was used to ensure that the measurement was taken in the linear viscoelastic regime. Below 30 °C, both dynamic storage modulus G' and loss modulus G" were small and the data points were scattered. In the temperature range of 30 - 39 °C, both G' and G" increased sharply with the increase of temperature. The fact that G" was larger than G' in this zone indicates that the solution was a viscoelastic liquid. Above 39 °C, G' became greater than G", suggesting that the triblock copolymer solution turned into a gel. The crossover, G' = G", is commonly used as an indicator of the sol-to-gel or gel-to-sol transition. Thus, the sol-to-gel transition temperature ($T_{sol\text{-}gel}$) of this polymer solution was 39.0 °C, which is slightly higher than the CMT of the same polymer in a 0.2 wt % aqueous solution at a similar pH (CMT = 35.5 °C at pH = 3.20 from Figure 1.3). Compared with the sharp transitions of 20 wt% aqueous solutions of thermosensitive AB diblock copolymers (1 - 2 °C),[30] the sol-to-gel transition of the ABA triblock copolymer shown here is much broader. This can be attributed to the different gelation mechanisms for the two types of block copolymers in solutions. For AB diblock copolymers, gelation occurs when the volume fraction of spherical micelles exceeds a critical value. For ABA triblock copolymers in moderately concentrated solutions, when the thermosensitive

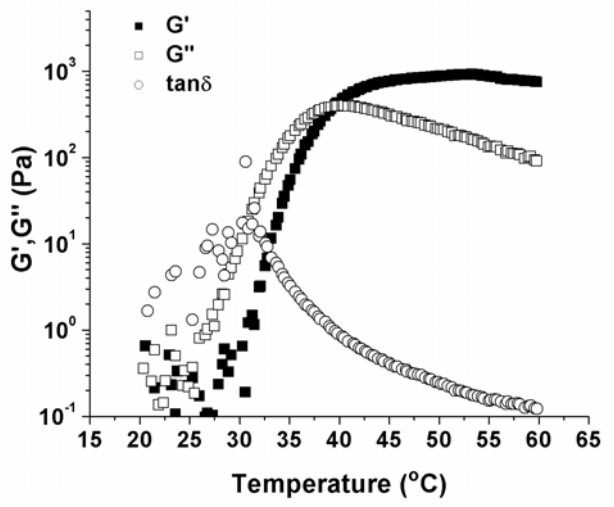

Figure 1.5. Plot of dynamic storage modulus G' (■), dynamic loss modulus G'' (□), and tanδ versus temperature for the 12.0 wt% aqueous solution of P(DEGMMA-*co*-MAA)-*b*-PEO-*b*-P(DEGMMA-*co*-MAA) at pH = 3.59. The data were collected from a temperature ramp experiment with a heating rate of 2 °C/min. A strain amplitude of 0.2 % and an oscillation frequency of 1 Hz were used.

outer blocks become dehydrated and associate into hydrophobic domains, bridges are formed by the hydrophilic PEO blocks among neighboring micelles, yielding a 3-dimensional network gel. This process is not as sharp as the jamming of spherical micelles of AB diblock copolymers.

The transition from a viscoelastic liquid to a 3-dimensional network gel was also evidenced by the data collected from frequency sweep experiments (Figure 1.6). At 32 °C, the solution was a transparent liquid that can flow when tilted. The storage modulus G' was smaller than G" in the range from 0.1 to 50 Hz and both exhibited power law dependencies on frequency f in the low frequency window: G' ~ f^2 and G" ~ f. This is the typical rheological behavior of a liquid.[73-75] At 36 °C, which is close to the sol-gel transition temperature, G' and G" were of similar magnitudes in the low frequency range of 0.1 to 10 Hz and were ~ $f^{0.5}$. This is the signature of the transition between liquid-like and solid-like behavior and the temperature closely approximates the gelation temperature.[73-75] At 50 °C, the sample was a transparent free-standing gel. G' was significantly greater than G" and was nearly independent of f in the frequency range of 0.1 to 60 Hz, spanning nearly three orders in magnitude, which is a characteristic of solid-like behavior.

The sol-to-gel transitions of 12.0 wt% aqueous solutions of P(DEGMMA-*co*-MAA)-*b*-PEO-*b*-P(DEGMMA-*co*-MAA) at other pH values, ranging from 2.58 to 5.76, were also studied by rheological measurements. These solutions were obtained by injecting calculated amounts of either a 1.0 M HCl or a 1.0 M KOH solution into the 12.0 wt% polymer solution with a pH of 4.89. The pH values of the obtained solutions,

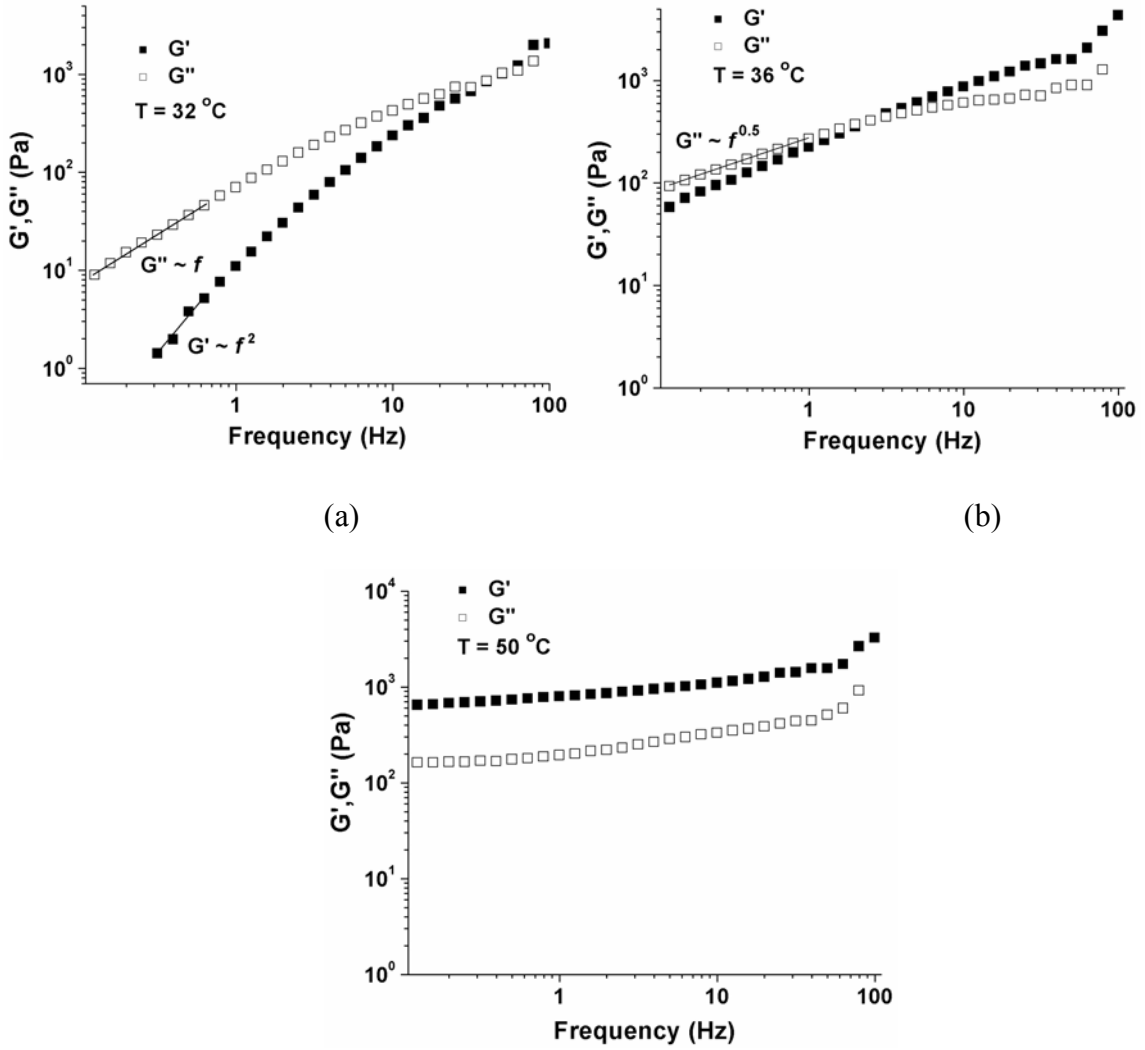

Figure 1.6. Frequency dependences of dynamic storage modulus G' (■) and loss modulus G" (□) of the 12.0 wt% aqueous solution of P(DEGMMA-*co*-MAA)-*b*-PEO-*b*-P(DEGMMA-*co*-MAA) with a pH of 3.59 at (a) 32, (b) 36 , and (c) 50 °C. A strain amplitude of 0.2 % was used in the frequency sweep experiments.

determined by a pH meter, were in good agreement with those predicted from the titration curve shown in Figure 1.4. The results from dynamic viscoelastic measurements are summarized in Figure 1.3. Similar to the trend for CMT of the triblock copolymer in dilute solutions, the $T_{sol\text{-}gel}$ initially increased slowly with the increase of pH in the pH range from 2.58 ($T_{sol\text{-}gel}$ = 38.2 °C) to 4.49 ($T_{sol\text{-}gel}$ = 40.1 °C). Above pH = 4.5, the increase of the sol-gel transition temperature with pH became faster. In just 1.3 pH units, the sol-gel transition temperature jumped by nearly 20 °C, from 40.1 °C at pH = 4.49 to 58.8 °C at pH 5.76. Thus, the sol-gel transition temperature of an aqueous solution of P(DEGMMA-*co*-MAA)-*b*-PEO-*b*-P(DEGMMA-*co*-MAA) can be tuned in a large temperature range by adjusting the solution pH. A striking feature of Figure 1.3 is that the CMT curve of the triblock copolymer in 0.2 wt% aqueous solutions and the $T_{sol\text{-}gel}$ curve for 12.0 wt% solutions follow the same trend, though there is a shift. At pH < 5.0, the $T_{sol\text{-}gel}$ is higher than the CMT at the same pH by 3 – 4 °C. With the increase of pH, the difference between $T_{sol\text{-}gel}$ and CMT becomes larger, which can be attributed to the different effects of the charges on the thermosensitive blocks on CMT and $T_{sol\text{-}gel}$. The ionization of carboxylic acid groups at a higher pH makes the polymer chain more hydrophilic. Different from the micellization of the ABA triblock copolymer in a dilute aqueous solution, the gelation requires the formation of an adequately strong 3-dimensional network, which should possess a sufficient mechanical strength to exhibit solid-like properties. Thus, for the 12.0 wt% solution at the same pH, a higher temperature is required to transform the solution into a solid-like gel.

1.3.4 Cycling the pH Value of 12.0 wt% Aqueous Solution of P(DEGMMA-*co*-MAA)-*b*-PEO-*b*-P(DEGMMA-*co*-MAA) between 3.2 and 5.4: Reproducibility of Sol-Gel Transition Temperature

Figure 1.4 shows that the pH of the 12.0 wt% aqueous solution of P(DEGMMA-*co*-MAA)-*b*-PEO-*b*-P(DEGMMA-*co*-MAA) can be readily tuned by injection of a 1.0 M HCl or KOH solution and can be well controlled. To study the reproducibility of the sol-gel transition tempeature, we cycled the pH value of a 12.0 wt% polymer solution between 3.2 and 5.4 three times by successive addition of HCl and KOH and determined $T_{sol\text{-}gel}$ by rheological measurements. A calculated amount of a 1.0 M HCl solution, based on the titration curve shown in Figure 1.4, was injected into 1.913 g of the 12.0 wt% solution with a pH of 4.89 to bring the pH value to 3.24 (Table 1). The temperature ramp performed at a strain amplitude of 0.2 %, a fixed frequency of 1 Hz, and a heating rate of 2 °C /min showed that the sol-gel transition temperature of the solution at this pH occurred at 38.5 °C, which was right on the $T_{sol\text{-}gel}$ curve in Figure 1.3. After weighing the remaining solution in the vial, we injected into the polymer solution the calculated amount of a 1.0 M KOH solution that was needed to change the pH to 5.36. The rheological measurement of the solution showed that the sol-gel transition temperature was 46.8 °C, which again fell right on the curve of $T_{sol\text{-}gel}$ versus pH. We then repeated this process for additional two cycles by successive addition of the calculated amounts of 1.0 M HCl and 1.0 M KOH solutions based on the titration curve in Figure 1.4. The results from rheological measurements are summarized in Table 1.1. As can be clearly seen, the $T_{sol\text{-}gel}$ is very reproducible at a given pH value. The sol-gel transition

Table 1.1 Sol-gel transition temperatures of a 12.0 wt% aqueous solution of P(DEGMMA-*co*-MAA)-*b*-PEO-*b*-P(DEGMMA-*co*-MAA) whose pH value was cycled between 3.2 and 5.4 by successive injection of calculated amounts of 1.0 M HCl and 1.0 M KOH solutions. The weight of the initial polymer solution was 1.913 g and its pH was 4.89.

	Solution weight	Targeted pH	Calculated [a]	Injected [b]	Measured pH [c]	$T_{sol\text{-}gel}$ [d]
Cycle-1-A	1.913 g	3.24	17.4 μL HCl	17 μL HCl	3.24	38.5 °C
Cycle-1-B	1.543 g	5.36	21.9 μL KOH	21 μL KOH	5.36	46.8 °C
Cycle-2-A	1.355 g	3.24	19.9 μL HCl	20 μL HCl	3.19	38.6 °C
Cycle-2-B	1.256 g	5.36	18.5 μL KOH	19 μL KOH	5.38	46.9 °C
Cycle-3-A	0.967 g	3.24	14.2 μL HCl	14 μL HCl	3.23	38.9 °C
Cycle-3-B	0.873 g	5.36	12.9 μL KOH	13 μL KOH	5.39	47.0 °C

[a] The amount of a 1.0 M HCl or a 1.0 M KOH solution that was needed to change the pH to the targeted value was calculated based on the titration curve shown in Figure 1.4.

[b] The amount of a 1.0 M HCl or 1.0 M KOH solution that was injected via a microsyringe.

[c] The solution pH was measured with a pH meter.

[d] The sol-gel transition temperature was determined by the rheological measurement performed in a temperature ramp with a strain amplitude of 0.2 %, a constant frequency of 1 Hz, and a heating rate of 2 °C/min.

temperatures at pH = 3.2 in the 1st, 2nd and 3rd cycles are 38.5, 38.6, and 38.9 °C, respectively, while at pH = 5.4 they are 46.8, 46.9, and 47.0 °C.

1.3.5 Multiple Sol-Gel-Sol Transitions by Simultaneously Controlling pH and Temperature

In this section, we demonstrated that multiple sol-gel-sol transitions can be realized by judiciously controlling both pH and temperature. We started with 0.994 g of the 12.0 wt% polymer solution and changed its pH value from 4.89 to 5.60 by injection of 8.5 μL of a 1.0 M KOH solution according to Figure 1.4. An oscillatory shear measurement performed in the temperature ramp mode using a constant frequency of 1 Hz, a strain amplitude γ of 0.2 %, and a heating rate of 2 °C/min indicated that the sol-gel transition temperature of this solution was 51.3 °C, consistent with the prediction from the $T_{sol\text{-}gel}$ versus pH curve in Figure 1.3. The vial was placed in a 55 °C bath and as expected the solution turned into a clear gel, which upon lowering the temperature from 55 to 45 °C was converted to a sol (see the digital pictures in Figure 1.7). From the temperature ramp, the ratio of G' to G" changed from 1.30 at 55 °C (in a gel state) to 0.47 at 45 °C (in a sol state). We then weighed the remaining solution in the vial (0.904 g solution) and injected the calculated amount of a 1.0 M HCl solution (5.0 μL), based on the titration curve in Figure 1.4, to change the pH from 5.60 to 5.12. The solution was allowed to equilibrate at 45 °C for 18 h. By visual inspection, the sol turned into a free-standing gel (Figure 1.7). A portion of the sample was then taken for the rheological experiment; the sol-gel transition temperature decreased to 43.5 °C, essentially the same as the $T_{sol\text{-}gel}$ (42.9 °C) for the same pH shown in Figure 1.3. We then decreased the temperature to 39 °C, which is below the $T_{sol\text{-}gel}$ for this pH (43.5 °C).

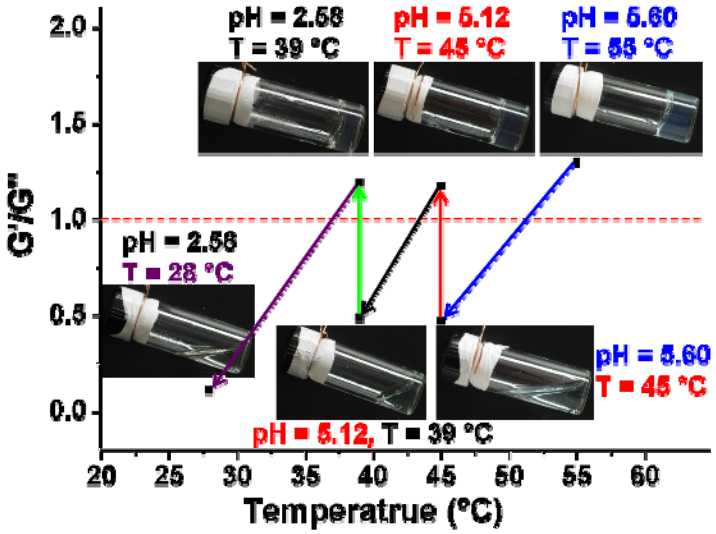

Figure 1.7. Ratio of dynamic storage modulus G' to loss modulus G" versus temperature in an experiment demonstrating multiple sol-gel-sol transitions of the 12.0 wt% aqueous solution of P(DEGMMA-*co*-MAA)-*b*-PEO-*b*-P(DEGMMA-*co*-MAA) that were achieved by simultaneously controlling temperature and pH. The ratios of G' to G" at given temperatures and pH values were obtained from the temperature ramps of the solutions at different pH values. The digital pictures show the states of the polymer solution at given temperatures and pH values.

After the equilibration at this temperature for 30 min, the gel became a viscous liquid (Figure 1.7).

The solution was weighed again (0.624 g), and the vial was placed back in the 39 °C water bath. The pH value was adjusted to 2.58 by injection of 10.0 μL of HCl (the amount calculated from Figure 1.4 was 9.7 μL) and the solution was equilibrated for 18 h. As can be seen from the picture in Figure 1.7, the sample turned into a gel. A dynamic viscoelastic measurement indicated that the sol-gel transition temperature was 38.0 °C, which is essentially identical to the $T_{sol\text{-}gel}$ (38.2 °C) at this pH in Figure 1.3. We then lowered the temperature to 28 °C; the gel was transformed into a free-flowing liquid (Figure 1.7). Thus, by judiciously controlling the solution pH and temperature, multiple sol-gel-sol transitions were achieved, demonstrating the great flexibility in tuning the sol-gel/gel-sol transitions of the doubly responsive hydrophilic ABA triblock copolymer in water by combining two external triggers.

1.3.6. Concentration Effect on the Sol-Gel Transition of Aqueous Solution of P(DEGMMA-*co*-MAA)-*b*-PEO-*b*-P(DEGMMA-*co*-MAA) at pH = 4.0

It is known that polymer concentration affects the sol-gel transition temperature and the gel characteristics.[74,75] To investigate the concentration effect on the sol-gel transition, we prepared a series of aqueous solutions of P(DEGMMA-*co*-MAA)-*b*-PEO-*b*-P(DEGMMA-*co*-MAA) with concentrations progressively decreasing from 15.0 wt% to 3.99 wt%. These solutions were made by concentrating the 12.0 wt% aqueous solution with a pH value of 4.0 via evaporation of water or diluting it using Milli-Q water. Because the dilution and concentration changed the pH slightly, the pH values of these solutions were maintained at pH = 4.0 by adding a very small amount of a 1.0 M HCl or

1.0 M KOH aqueous solution in order to eliminate the pH effect in the study of concentration effect. Dynamic viscoelastic measurements were performed on all samples. Figure 1.8 shows temperature ramps of four selected samples with concentrations of 13.9, 11.8, 9.0, and 7.0 wt %; the transition temperatures are 36.1, 39.0, 41.1, and 42.1 °C, respectively. The plot of $T_{sol\text{-}gel}$ versus concentration is presented in Figure 1.9. As expected, the sol-gel transition temperature increased with the decrease of polymer concentration, though the obtained curve is not smooth. Above 10 wt %, the change was nearly linear, while below 10 wt %, the increase of the sol-gel transition temperature was slowed down. Regardless, it is clear that a lower polymer concentration requires a higher degree of dehydration of thermosensitive blocks to form a sufficiently mechanically strong 3-dimensional network. For the 3.99 wt % aqueous polymer solution, although it was observed that G' was greater than G" at T > 46.4 °C, the values of both G' and G" were very small (< 4 Pa)[76] and no free-standing gel was observed but a viscous liquid, implying that the critical gelation concentration for this ABA triblock copolymer in water at pH = 4.0 is between 4 and 6 wt % (the lowest concentration in Figure 1.9). This is significantly smaller than the critical gelation concentration of AB diblock copolymer solutions, which is typically close to 20 wt %.

In the rheological experiments, we noticed that when the polymer concentration was above 10 wt%, G' increased with the increase of temperature and a plateau was observed up to the highest temperature in the experiment (Figure 1.8a and b). The gels were clear or nearly clear. For the solutions with concentrations below 10 wt%, both G' and G" exhibited a noticeable drop at an elevated temperature above the $T_{sol\text{-}gel}$. This phenomenon can be clearly seen from the temperature ramps for aqueous polymer

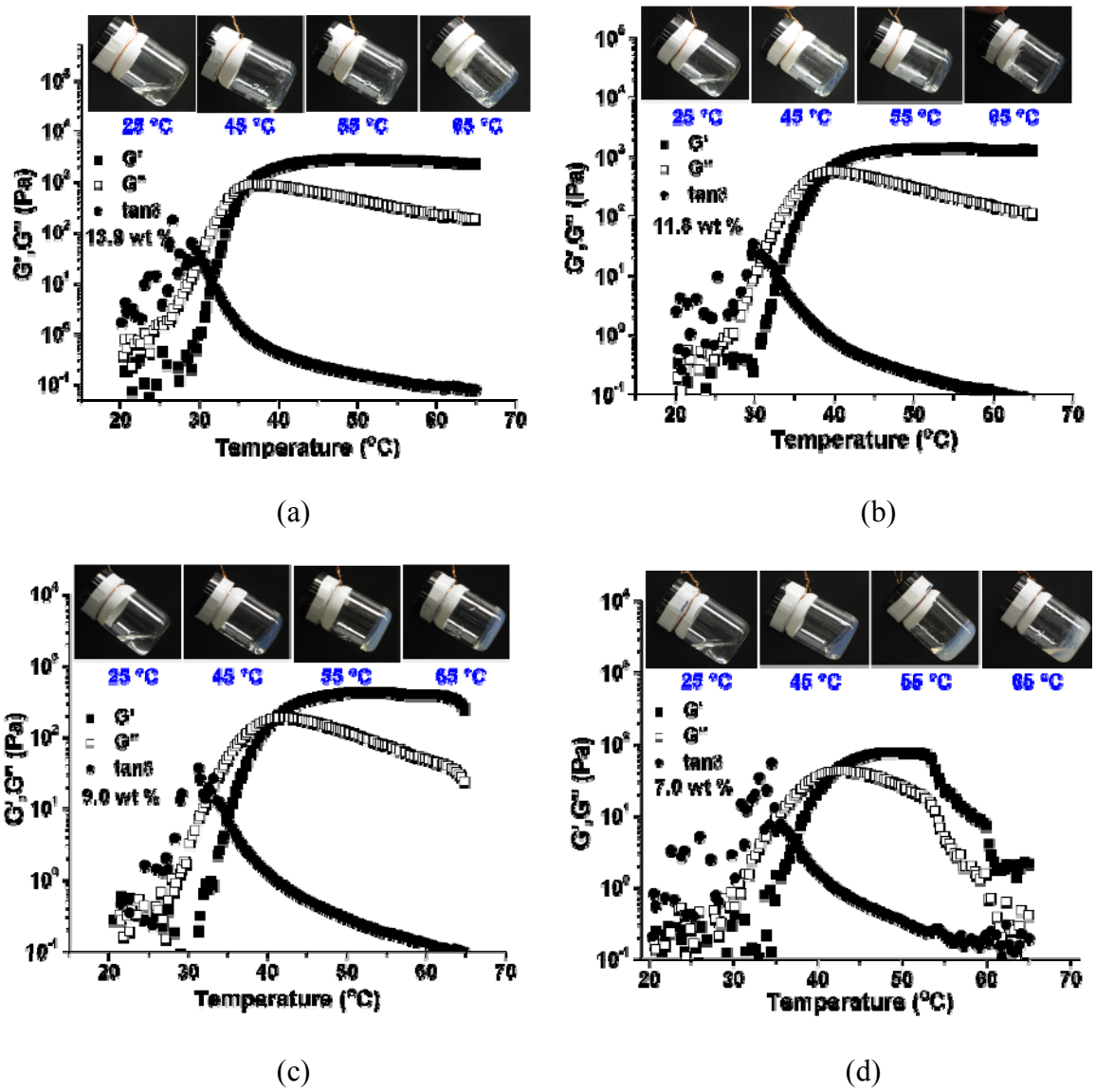

Figure 1.8. Temperature ramps for aqueous solutions of P(DEGMMA-*co*-MAA)-*b*-PEO-*b*-P(DEGMMA-*co*-MAA) with concentrations of (a) 13.9, (b) 11.8, (c) 9.0, and (d) 7.0 wt% at pH = 4.0. The rheological data were collected at a constant frequency of 1 Hz, a strain amplitude of 0.2 %, and a heating rate of 2 °C/min. The pictures show the states of each solution at four different temperatures.

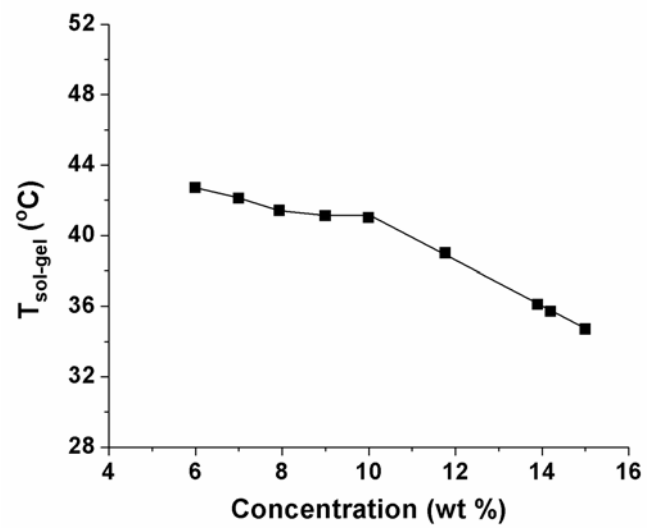

Figure 1.9. Concentration effect on the sol-gel transition temperature ($T_{sol-gel}$) of aqueous solution of P(DEGMMA-*co*-MAA)-*b*-PEO-*b*-P(DEGMMA-*co*-MAA) at pH = 4.0.

solutions with concentrations of 9.0 and 7.0 wt% in Figure 1.8c and d. In particular, the values of G' and G" of the 7.0 wt% sample dropped sharply at ~ 53 °C, but G' remained larger than G", indicating that the sample was still in a gel state. From the pictures shown in the Figure 1.8d, we can see that the sample was a slightly blue/whitish gel at 45 °C but became a white gel at 50 °C. With further increasing the temperature, both G' and G" continued to drop and phase separation occurred at 65 °C, where a clear solution layer and a white polymer precipitate were observed. We speculate that at such concentrations, there was a significant portion of PEO central blocks forming the loops in the corona (flower micelles), resulting in rather weak bridges among micelles. It is known that with the increase of temperature, the solubility of PEO in water becomes poor,[1,2] which means that the PEO bridges in the gel underwent shrinking, causing the macroscopic phase separation of polymer solutions.

1.4 Conclusion

In summary, we synthesized a thermo- and pH-sensitive ABA triblock copolymer P(DEGMMA-*co*-MAA)-*b*-PEO-*b*-P(DEGMMA-*co*-MAA) with the thermosensitive outer blocks incorporated with a small amount of carboxylic acid groups by ATRP of DEGMMA and *t*BMA from a difunctional PEO macroinitiator and subsequent removal of *t*-butyl groups of *t*BMA units.[77] DLS studies showed that the CMT of this triblock copolymer in KHP buffers at a 0.2 wt% concentration can be tuned in a wide temperature range by adjusting the solution pH. To study the sol-gel transition of the moderately concentrated polymer solution, a 12.0 wt% aqueous solution of P(DEGMMA-*co*-MAA)-*b*-PEO-*b*-P(DEGMMA-*co*-MAA) was made and the pH was raised to 4.89 by the

injection of a 1.0 M KOH solution. Since the solution was a buffer composed of COOH/COOK, its pH value can be readily changed by the injection of HCl or KOH and can be well controlled. Dynamic viscoelastic measurements showed that the sol-gel transition temperature of the 12.0 wt% polymer solution was determined by the solution pH and the $T_{sol\text{-}gel}$ versus pH curve exhibited a similar trend as the CMT vs. pH curve. By cycling the solution pH between pH = 3.2 and 5.4 three times, we demonstrated that the sol-gel transition temperature was very reproducible at a specific pH. We further showed that multiple sol-gel-sol transitions can be achieved by judiciously controlling both temperature and pH of the solution. The effect of the ABA triblock copolymer concentration on the sol-gel transition of its aqueous solution at pH = 4.0 was investigated; the $T_{sol\text{-}gel}$ was found to increase with the decrease of polymer concentration. When the concentration was above 10 wt%, a clear or nearly clear gel was observed up to 65 °C, while below 10 wt%, dynamic storage and loss moduli of the gel were observed to decrease at an elevated temperature above $T_{sol\text{-}gel}$. This is presumably because at a lower concentration, fewer PEO middle blocks form bridges among micelles and PEO is known to undergo shrinking at higher temperatures, causing the breakdown of the gel and eventually phase separation. The work reported here could provide a general principle for the design of multi-responsive hydrogels for biomedical applications (e.g., injectable gels for controlled release of drugs or as scaffolds for cell growth/tissue engineering) and other technological applications.

References

1. Hamley, I. W. *Block Copolymers in Solution: Fundamentals and Applications*, John Wiley & Sons: Chichester, 2005.
2. Hamley, I. W. *The Physics of Block Copolymers*, Oxford University Press: Oxford, 1998.
3. Joo, M. K.; Park, M. H.; Choi, B. G.; Jeong, B. *J. Mater. Chem.* **2009**, *19*, 5891-5905.
4. He, C. L.; Kim, S. W.; Lee, D. S. *J. Controlled Release* **2008**, *127*, 189-207.
5. Gil, E. S.; Hudson, S. M. *Prog. Polym. Sci.* **2004**, *29*, 1173-1222.
6. Jeong, B.; Kim, S. W.; Bae, Y. H. *Adv. Drug Delivery Rev.* **2002**, *54*, 37-51.
7. Mortensen, K.; Brown, W.; Jørgensen, E. *Macromolecules* **1994**, *27*, 5654.
8. Ma, Y.; Tang, Y.; Billingham, N. C.; Armes, S. P. Lewis, A. L. *Biomacromolecules* **2003**, *4*, 864-868.
9. Castelletto, V.; Hamley, I. W.; Ma, Y.; Bories-Azeau, X.; Armes, S. P.; Lewis, A. L. *Langmuir* **2004**, *20*, 4306-4309.
10. Li, C.; Tang, Y.; Armes, S. P.; Morris, C. J.; Rose, S. F.; Lloyd, A. W.; Lewis, A. L. *Biomacromolecules* **2005**, *6*, 994-999.
11. Li, C.; Buurma, N. J.; Haq, I.; Turner, C.; Armes, S. P. *Langmuir* **2005**, *21*, 11026-11033.
12. Madsen, J. Armes, S. P.; Lewis, A. L. *Macromolecules* **2006**, *39*, 7455-7457.
13. Madsen, J.; Armes, S. P.; Bertal, K.; Lomas, H.; MacNeil, S.; Lewis, A. L. *Biomacromolecules* **2008**, *9*, 2265-2275.

14. Kirkland, S. E.; Hensarling, R. M.; McConaught, S. D.; Guo, Y.; Jarrett, W. L.; McCormick, C. L. *Biomacromolecules* **2008**, *9*, 481-486.

15. Li, C.; Madsen, J.; Armes, S. P.; Lewis, A. L. *Angew. Chem. Int. Ed.* **2006**, *45*, 3510-3513.

16. Sun, K. H.; Sohn, Y. S.; Jeong, B. *Biomacromolecules* **2006**, *7*, 2871-2848.

17. Vogt, A. P.; Sumerlin, B. S. *Soft Mater* **2009**, *5*, 2347-2351.

18. Anderson, B. C.; Cox, S. M.; Bloom, P. D.; Sheares, V. V.; Mallapragada, S. K. *Macromolecules* **2003**, *36*, 1670-1676.

19. Determan, M. D.; Cox, J. P.; Seifert, S.; Thiyagarajan, P.; Mallapragada, S. K. *Polymer* **2005**, *46*, 6933-6946.

20. Determan, M. D.; Guo, L.; Thiyagarajan, P.; Mallapragada, S. K. *Langmuir* **2006**, *22*, 1469-1473.

21. Shim, W. S.; Yoo, J. S.; Bae, Y. H.; Lee, D. S. *Biomacromolecules* **2005**, *6*, 2930-2934.

22. Shim, W. S.; Kim, S. W.; Lee, D. S. *Biomacromolecules* **2006**, *7*, 1935-1941.

23. Shim, W.S.; Kim, J. H.; Park, H.; Kim, K.; Kwon, I. C.; Lee, D. S. *Biomaterials* **2006**, *27*, 5178-5185.

24. Dayananda, K.; Pi, B. S.; Kim, B. S.; Park, T. G.; Lee, D. S. *Polymer* **2007**, *48*, 758-762.

25. Park, S. Y.; Lee, Y.; Bae, K. H.; Ahn, C. H.; Park, T. G. *Macromol. Rapid Commun.* **2007**, *28*, 1172-1176.

26. Suh, J. M.; Bae, S. J.; Jeong, B. *Adv. Mater.* **2005**, *17*, 118-120.

27. Dayananda, K.; He, C. L.; Park, D. K.; Park, T. G.; Lee, D. S. *Polymer* **2008**, *49*, 4968-4973.

28. Huynh, D. P.; Nguyen, M. K.; Kim, B. S.; Lee, D. S. *Polymer* **2009**, *50*, 2565-2571.

29. Jiang, X. G., Lavender, C. A.; Woodcock, J. W.; Zhao, B. *Macromolecules* **2008**, *41*, 2632-2643.

30. Jiang, X. G.; Jin, S.; Zhong, Q. X.; Dadmun, M. D.; Zhao, B. *Macromolecules* **2009**, *42*, 8648-9476.

31. Jiang, X. G.; Zhao, B. *Macromolecules* **2008**, *41*, 9366-9375.

32. O'Lenick, T. G.; Jiang, X. M.; Zhao, B. *Polymer* **2009**, *50*, 4363-4371.

33. Yin, X.; Hoffman, A. S.; Stayton, P. S. *Biomacromolecules* **2006**, *7*, 1381-1385.

34. Chen, G.; Hoffman, A. S. *Nature* **1995**, *373*, 49-52.

35. Feil, H.; Bae, Y. H.; Feijen, J.; Kim, S. W. *Macromolecules* **1992**, *25*, 5528-5530.

36. Bulmus, V.; Ding, Z.; Long, C. J.; Stayton, P. S.; Hoffman, A. S. *Bioconjugate Chem.* **2000**, *11*, 78-83.

37. Zhou, S. Q.; Chu, B. *J. Phys. Chem. B.* **1998**, *102*, 1364-1371.

38. Olea, A. F.; Thomas, J. K. *Macromolecules* **1989**, *22*, 1165-1169.

39. Murthy, N.; Robichaud, J. R.; Tirrell, D. A.; Stayton, P. S.; Hoffman, A. S. *J. Controlled Release* **1999**, *61*, 137-143.

40. Lokitz, B. S.; York, A. W.; Stempka, J. E.; Treat, N. D.; Li, Y.; Jarrett, W. L.; McCormick, C. L. *Macromolecules* **2007**, *40*, 6473-6480.

41. Yamamoto, S.-I.; Pietrasik, J.; Matyjaszewski, K. *Macromolecules* **2008**, *41*, 7013-7020.

42. Wu, D.-C.; Liu, Y.; He, C. -B. *Macromolecules* **2008**, *41*, 18-20.

43. Jones, J. A.; Novo, N.; Flagler, K.; Pagnucco, C. D.; Carew, S.; Cheong, C.; Kong, X. Z.; Burke, N. A. D.; Stöver, H. D. H. *J. Polym. Sci. Part A: Polym. Chem.* **2005**, *43*, 6095-6104.

44. Feil, H.; Bbae, Y. H.; Feijen, J.; Kim, S. W. *Macromolecules* **1993**, *26*, 2496-2500.

45. Aoshima, S.; Kanaoka, S. *Adv. Polym. Sci.* **2008**, *210*, 169-208.

46. Allcock, H. R.; Dudley, G. K. *Macromolecules* **1996**, *29*, 1313-1319.

47. Chang, Y.; Powell, E. S.; Allcock, H. R.; Park, S. M.; Kim, C. *Macromolecules* **2003**, *36*, 2568-2570.

48. Han, S.; Hagiwara, M.; Ishizone, T. *Macromolecules* **2003**, *36*, 8312-8319.

49. Zhao, B.; Li, D. J.; Hua, F. J.; Green, D. R. *Macromolecules* **2005**, *38*, 9509-9517.

50. Hua, F. J.; Jiang, X. G.; Li, D. J.; Zhao, B. *J. Polym. Sci. Part A: Polym. Chem.* **2006**, *44*, 2454-2467.

51. Hua, F. J.; Jiang, X. G.; Zhao, B. *Macromolecules* **2006,** *39,* 3476-3479.

52. Aathimanikandan, S. V.; Savariar, E. N.; Thayumanavan, S. *J. Am. Chem. Soc.* **2005**, *127*, 14922-14929.

53. Li, D. J.; Jones, G. L.; Dunlap, J. R.; Hua, F. J.; Zhao, B. *Langmuir* **2006**, 22, 3344-3351.

54. Lutz, J.-F.; Hoth, A. *Macromolecules* **2006**, *39*, 893-896.

55. Lutz, J. F.; Weichenhan, K.; Akdemir, O.; Hoth, A. *Macromolecules* **2007**, *40*, 2503-2508.

56. Li, D. J.; Zhao, B. *Langmuir* **2007**, *23*, 2208-2217.

57. Jiang, X. G.; Zhao, B. *J. Polym. Sci. Part A: Polym. Chem.* **2007**, *45*, 3707-3721.

58. Li, D. J.; Dunlap, J. R.; Zhao, B. *Langmuir* **2008**, 24, 5911-5918.

59. Ishizone, T.; Seki, A.; Hagiwara, M.; Han, S.; Yokoyama, H.; Oyane, A.; Deffieux, A.; Carlotti, S. *Macromolecules* **2008**, *41*, 2963-2967.

60. Yamamoto, S.-I.; Pietrasik, J.; Matyjaszewski, K. *J. Polym. Sci. Part A: Polym. Chem.* **2008**, *46*, 194-202.

61. Jiang, X. W.; Smith, M. R.; Baker, G. L. *Macromolecules* **2008**, *41*, 318-324.

62. Wang, N.; Dong, A.; Radosz, M.; Shen, Y. Q. *J. Biomed. Mater. Res. Part A.* **2008**, *84A*, 148-157.

63. Jiang, X. M.; Wang, B. B.; Li, C. Y.; Zhao, B. *J. Polym. Sci. Part A: Polym. Chem.*, **2009**, *47*, 2853-2870.

64. Fechler, N.; Badi, N.; Schade, K.; Pfeifer, S.; Lutz, J.-F. *Macromolecules* **2009**, *42*, 33-36.

65. Badi, N.; Lutz, J.-F. *J. Controlled Release* **2009**, *140*, 224-229.

66. Zhao, B; He, T. *Macromolecules* **2003**, *36*, 8599-8602.

67. Matyjaszewski, K.; Miller, P. J.; Shukla, N.; Immaraporn, B.; Gelman, A.; Luokala, B. B. Siclovan, T. M.; Kickelbick, G.; Vallant, T.; Hoffmann, H.; Pakula, T. *Macromolecules* **1999**, *32*, 8716-8724.

68. A random copolymer P(DEGMMA-*co*-MAA) with a molar ratio of DEGMMA and MAA similar to that in the thermosensitive outer blocks of P(DEGMMA-*co*-MAA)-*b*-PEO-*b*-P(DEGMMA-*co*-MAA) was synthesized by the same procedure as for the ABA triblock copolymer except the use of ethyl 2-bromoisobutyrate as initiator. A 9.1 wt % aqueous solution of this random copolymer was made and titrated with 1.0 M KOH (see Appendix A). The pK_a was found to be 5.59.

69. The remaining weak broad peak in the same area is believed to come from the polymer backbone as a similar broad peak was observed in the ^{1}H NMR spectrum of homopolymer PDEGMMA (see Appendix A).

70. Mathur, A. M.; Drescher, B.; Scranton, A. B.; Klier, J. *Nature* **1998**, *392*, 367-370.

71. Poe, G. D.; Jarrett, W. L.; Scales, C. W.; McCormick, C. L. *Macromolecules* **2004**, *37*, 2603-2612.

72. Ye, M.; Zhang, D.; Han, L.; Tejada, J.; Ortiz, C. *Soft Matter* **2006**, *2*, 243-256.

73. He. Y. Y.; Lodge, T. P. *Chem. Commun.* **2007**, 2732-2734.

74. He, Y. Y.; Boswell, P. G.; Bühlmann, P.; Lodge, T. P. *J. Phys. Chem. B.* **2007**, *111*, 4645-4652.

75. He, Y. Y.; Lodge, T. P. *Macromolecules* **2008**, *41*, 167-174.

76. See Appendix A.

77. The work presented in this Chapter has been published in *Langmuir* (**2010**, *26*, 8787–8796. DOI: 10.1021/la9045308.)

Chapter 2. Rheological Properties of Thermo- and pH-Sensitive ABA Triblock Copolymer Aqueous Micellar Gels

Abstract

This chapter presents a systematic study of the effect of pH on rheological properties of aqueous micellar gels formed from 10.0 wt% aqueous solutions of a thermo- and pH-sensitive ABA triblock copolymer, poly(ethoxydi(ethylene glycol) acrylate-*co*-acrylic acid)-*b*-poly(ethylene oxide)-*b*-poly(ethoxydi(ethylene glycol) acrylate-*co*-acrylic acid) (P(DEGEA-*co*-AA)-*b*-PEO-*b*-P(DEGEA-*co*-AA)). The block copolymer was synthesized by atom transfer radical polymerization of DEGEA and *t*-butyl acrylate with a molar ratio of 100 : 5 from a difunctional PEO macroinitiator and subsequent removal of *t*-butyl groups using trifluoroacetic acid. PDEGEA is a thermosensitive water-soluble polymer with a cloud point of 9 °C in water. The thermo-induced sol-gel transition temperature ($T_{sol\text{-}gel}$) of the 10.0 wt% aqueous solution of P(DEGEA-*co*-AA)-*b*-PEO-*b*-P(DEGEA-*co*-AA) can be continuously and reversibly tuned over a wide temperature range by varying the solution pH. The sol-gel transition became broader with the increase of pH, which stemmed from the weaker and broader LCST transition of P(DEGEA-*co*-AA) blocks at higher pH values. The maximum value of dynamic storage modulus, obtained from heating ramp, and the plateau storage moduli (G_N), evaluated from frequency sweeps at three normalized temperatures ($T/T_{sol\text{-}gel}$ = 1.025, 1.032, and 1.039), decreased with the increase of pH from 3.00 to 5.40 with the largest drop observed at pH = ~ 4.7. The decrease in G_N reflects the reduction of the number of bridging polymer chains and simultaneously the increase of numbers of loops and dangling polymer chains. The ionization of carboxylic acid groups at higher pH values introduced charges onto the thermosensitive blocks and made the polymer chains more hydrophilic, facilitating the formation of loops and dangling chains in the gels. The increase in the number of

dangling polymer chains with the increase of pH was supported by fluorescence spectroscopy studies, which showed that the critical micelle concentration of P(DEGEA-*co*-AA)-*b*-PEO-*b*-P(DEGEA-*co*-AA) at a temperature corresponding to $T_{sol\text{-}gel}$ was higher at a higher pH value. The results obtained from this work showed that both $T_{sol\text{-}gel}$ and gel strength can be tuned by varying the solution pH, providing greater design flexibility for potential applications.

2.1 Introduction

Moderately concentrated aqueous solutions of thermosensitive ABA triblock copolymers are known to undergo reversible sol-gel transitions upon temperature changes.[1-3] If the A blocks are permanently water soluble and the B block is thermosensitive exhibiting a lower critical solution temperature (LCST) in water, the polymer molecules self-assemble into discrete, often spherical, micelles at temperatures above the LCST and the sol-to-gel transition is brought about by the packing of micelles into an ordered structure. Usually, a concentration of ~ 20 wt% is needed for the formation of this type of micellar gels. Representative examples of such polymers are poly(ethylene oxide)-*b*-poly(propylene oxide)-*b*-poly(ethylene oxide) (PEO-*b*-PPO-*b*-PEO) triblock copolymers with various compositions; these polymers have been intensively investigated in the past decades.[1-4] On the other hand, if the A blocks are thermosensitive and the B block is permanently water-soluble, a three-dimensional network is produced at elevated temperatures with the dehydrated A blocks associated into micellar cores and the central B blocks forming bridges. Compared with the first type of micellar gels, 3-D network gels can be more advantageous for some applications because the critical gelation concentration (CGC) is significantly lower.[5-7] For example, Kirkland et al. reported that a 7.5 wt% aqueous solution of poly(*N*-isopropylacrylamide)-*b*-poly(*N*,*N*-dimethyacrylamide)-*b*-poly(*N*-isopropylacrylamide) formed a free-standing gel upon heating. Note that poly(*N*-isopropylacrylamide) exhibits an LCST at 32 °C in water[8] and poly(*N*,*N*-dimethyacrylamide) is water soluble. These thermosensitive micellar gels have been investigated for applications in controlled release of substances

and tissue engineering because of their unique thermo-induced in situ sol-gel transition and the nature of physical crosslinking.[9-11]

We have been particularly interested in aqueous micellar gels of block copolymers that can respond to two or more physical or chemical stimuli.[12-28] Such gels would offer greater design flexibility that is needed in many applications. There have been a number of reports on multi-responsive block copolymer aqueous micellar gels;[9,10,12-28] one common feature of these gels is that they are thermosensitive. For example, thermo- and redox-sensitive hydrophilic block copolymers have been reported by several research groups.[14-16] Such polymers can be prepared from a difunctional initiator that contains a redox-sensitive disulfide bond; the thermally and biochemically induced sol-gel transitions of their aqueous solutions have been demonstrated.[15] Temperature- and pH-sensitive block copolymer aqueous gels are probably the most studied multi-responsive gels.[17-27] The block copolymers were usually prepared by either growing pH-sensitive blocks from or introducing pH-responsive groups to the chain ends of an ABA triblock copolymer that can form thermoreversible gels in water (e.g., PEO-*b*-PPO-*b*-PEO).[17-24] Suh et al. used pyromellitic dianhydride to couple PEO-*b*-PPO-*b*-PEO to make multiblock copolymers with carboxylic acid groups incorporated at the junction points.[25] Lee et al. recently reported pH- and thermo-sensitive aqueous gels of multiblock copolymers composed of PEO and poly(amino urethane).[26,27]

We previously reported a new type of thermo- and pH-sensitive block copolymer aqueous micellar gels.[28] A small amount of weak acid groups was incorporated into the thermsensitive outer blocks of an ABA triblock copolymer, poly(methoxydi(ethylene glycol) methacrylate-*co*-methacrylic acid)-*b*-PEO-*b*-poly(methoxydi(ethylene glycol)

methacrylate-*co*-methacrylic acid) (P(DEGMMA-*co*-MAA)-*b*-PEO-*b*-P(DEGMMA-*co*-MAA)). PDEGMMA is a biocompatible thermosensitive water-soluble polymer with a LCST of 25 °C in water, which belongs to a new class of thermosensitive polymers with a short oligo(ethylene glycol) pendant from each repeating unit.[28-49] A characteristic feature of thermosensitive polymers that contain a small amount of weak acid or base is that the LCST is controlled by the solution pH.[50-59] We showed that the sol-gel transition temperature ($T_{sol\text{-}gel}$) of a 12.0 wt% aqueous solution of P(DEGMMA-*co*-MAA)-*b*-PEO-*b*-P(DEGMMA-*co*-MAA) can be precisely, reversibly, and continuously tuned in a wide temperature range by varying the solution pH. Moreover, multiple sol-to-gel/gel-to-sol transitions were realized by controlling both temperature and pH, demonstrating the possibility of achieving on-demand sol-gel transition by combining two external stimuli.[28]

In the present work, we carried out a systematic study on rheological properties of 10.0 wt% aqueous solutions of a thermo- and pH-sensitive ABA triblock copolymer, poly(ethoxydi(ethylene glycol) acrylate)-*co*-acrylic acid)-*b*-PEO-*b*-poly(ethoxydi(ethylene glycol) acrylate-*co*-acrylic acid)) (P(DEGEA-*co*-AA)-*b*-PEO-*b*-P(DEGEA-*co*-AA)). The triblock copolymer was prepared from a difunctional PEO macroinitiator with a molecular weight of 20000 g/mol by atom transfer radical polymerization of DEGEA and *t*-butyl acrylate (*t*BA) with a molar ratio of 100 : 5 and subsequent removal of *t*-butyl groups of *t*BA units using trifluoroacetic acid (Scheme 2.1). We chose PDEGEA rather than PDEGMMA in this work because the LCST of PDEGEA in water is 9 °C and thus the sol-to-gel transition occurred in a more convenient temperature range for rheological measurements. Consistent with the previous

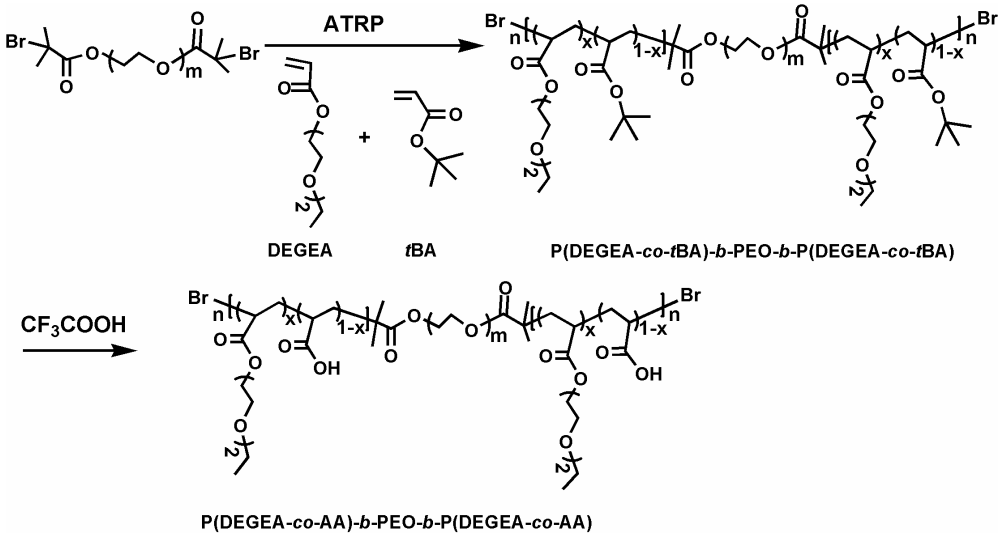

Scheme 2.1. Synthesis of Thermo- and pH-Sensitive ABA Triblock Copolymer P(DEGEA-*co*-AA)-*b*-PEO-*b*-P(DEGEA-*co*-AA) by ATRP of DEGEA and *t*BA from a Difunctional PEO Macroinitiator and Subsequent Treatment with Trifluoroacetic Acid.

report, the $T_{sol\text{-}gel}$ of the 10.0 wt% aqueous solution of P(DEGEA-*co*-AA)-*b*-PEO-*b*-P(DEGEA-*co*-AA) was dependent on pH. The sol-to-gel transition became broader with the increase of pH. Moreover, we found that the plateau dynamic storage moduli, obtained from frequency sweeps, decreased with the increase of solution pH with the largest drop observed at pH of ~ 4.7. The results showed that both $T_{sol\text{-}gel}$ and gel strength can be tuned by varying the pH of the polymer solution.

2.2 Experimental Part

2.2.1 Materials

Ethoxydi(ethylene glycol) acrylate (or di(ethylene glycol) ethyl ether acrylate, DEGEA, 90%, Aldrich) and *tert*-butyl acrylate (*t*BA, 99%, Fisher Scientific) were dried with calcium hydride overnight, distilled under reduced pressure, and stored in a refrigerator prior to use. CuBr (98%, Aldrich) was stirred in glacial acetic acid, filtered, and washed with absolute ethanol and diethyl ether. The purified CuBr was then dried in vacuum and stored in a desiccator. *N,N,N′,N′,N″*-pentamethyldiethylenetriamine (99%, Aldrich), dichloromethane, and anisole (99%, Acros) were dried with calcium hydride, vacuum distilled, and stored in storage flasks. Potassium hydrogen phthalate (KHP, primary standard, p.a.), trifluoroacetic acid (99%), acetone (HPLC grade), and Nile Red (99%) were obtained from Acros and used as received. Poly(ethylene oxide) (HO-PEO-OH, MW = 20,000 g/mol, Aldrich) was end-functionalized by reacting with 2-bromoisobutyryl bromide to give a difunctional PEO macroinitiator, Br-PEO-Br, as described in a previous publication.[28] Hexanes, diethyl ether, 1.0 M KOH solution (volumetric standard solution), and 1.0 M HCl solution (volumetric standard solution)

were obtained from Fisher Scientific. All other chemicals were purchased from either Aldrich or Fisher/Acros and used without further purification.

2.2.2 General Characterization

Size exclusion chromatography (SEC) was carried out at ambient temperature using PL-GPC 20 (an integrated GPC system from Polymer Laboratories, Inc) with a differential refractive index detector, one PLgel 5 μm guard column (50 × 7.5 mm), and two PLgel 5 μm mixed-C columns (each 300 × 7.5 mm, linear range of molecular weight from 200 to 2,000,000 according to Polymer Laboratories). THF was used as the carrier solvent at a flow rate of 1.0 mL/min. Polystyrene standards (Polymer Laboratories) were employed for calibration. The data were processed using Cirrus^{TM} GPC/SEC software (Polymer Laboratories). The ^{1}H (300 MHz) NMR spectra were recorded on a Varian Mercury 300 NMR spectrometer.

2.2.3 Synthesis of P(DEGEA-*co*-*t*BA)-*b*-PEO-*b*-P(DEGEA-*co*-*t*BA)

Copper (I) bromide (9.9 mg, 6.9 × 10^{-5} mol) and difunctional macroinitiator Br-PEO-Br (0.651 g, 3.26 × 10^{-5} mol) were weighed into a two-necked flask, followed by the addition of DEGEA (4.237 g, 22.5 mmol), *t*BA (0.152 g, 1.19 mmol), and anisole (2.147 g). The mixture was stirred under nitrogen atmosphere. *N,N,N′,N′,N″*-Pentamethyldiethylenetriamine (10.5 mg, 6.04 × 10^{-5} mol) was then injected into the flask via a microsyringe. After the reaction mixture was degassed by three freeze-pump-thaw cycles, the flask was placed into an oil bath with a preset temperature of 90 °C. The polymerization was monitored by SEC. After 180 min, the flask was removed from the oil bath and opened to air. The polymerization mixture was diluted with THF and the copper catalyst was removed by passing the solution through a short basic aluminum

oxide/silica gel column. The polymer was purified by precipitation in hexanes four times and then dried under high vacuum at 50 °C for 3 h. SEC analysis results (polystyrene standards): $M_{n,SEC}$ = 47,900 g/mol, polydispersity index (PDI) = 1.09.

2.2.4 Synthesis of P(DEGEA-*co*-AA)-*b*-PEO-*b*-P(DEGEA-*co*-AA)

P(DEGEA-*co*-*t*BA)-*b*-PEO-*b*-P(DEGEA-*co*-*t*BA) (1.277 g) was dried in a pre-weighed round bottom flask for 2 h. Dry dicholoromethane (6 mL) was added into the flask to dissolve the polymer, followed by the addition of trifluoroacetic acid (3.321 g). After the reaction mixture was stirred at ambient temperature for 67 h, the volatiles were removed by a rotary evaporator. The polymer was precipitated four times in a mixture of hexanes and diethyl ether (10/4, v/v) and then dried under high vacuum at 50 °C. ^{1}H NMR spectroscopy analysis showed that the *t*-butyl groups in the polymer were removed.

2.2.5 Preparation of 10.0 wt% Aqueous Solution of P(DEGEA-*co*-AA)-*b*-PEO-*b*-P(DEGEA-*co*-AA)

P(DEGEA-*co*-AA)-*b*-PEO-*b*-P(DEGEA-*co*-AA) was added into a pre-weighed round bottom flask and dried under high vacuum at 50 °C for > 3 h. The mass of the dried polymer was 0.958 g. Milli-Q water (8.641 g) was added into the flask and the mixture was sonicated in an ice/water ultrasonic bath (Fisher Scientific Model B200 Ultrasonic Cleaner) to dissolve the ABA triblock copolymer. The flask was then stored in a refrigerator (~ 4 °C) overnight and a homogeneous clear solution was obtained. The pH value of the polymer solution was 3.00, measured by a pH meter (Accumet AB15 pH meter from Fisher Scientific, calibrated with pH = 4.01, 7.00, and 10.01 standard buffer solutions) at 0 °C (the solution was placed in an ice/water bath).

2.2.6 Dynamic Light Scattering Study of Thermo-Induced Micellization of 0.02 wt% Aqueous Solutions of P(DEGEA-*co*-AA)-*b*-PEO-*b*-P(DEGEA-*co*-AA) in 10 mM KHP Buffers with Various pH Values

The thermo-induced micellization of P(DEGEA-*co*-AA)-*b*-PEO-*b*-P(DEGEA-*co*-AA) at a concentration of 0.02 wt% in 10 mM KHP buffers with various pH values was studied by dynamic light scattering (DLS). The pH values of 10 mM aqueous KHP buffers were adjusted by the addition of a 1.0 M KOH aqueous solution or a 1.0 M HCl aqueous solution. Four 0.02 wt% aqueous solutions of P(DEGEA-*co*-AA)-*b*-PEO-*b*-P(DEGEA-*co*-AA) with pH values of 3.00, 4.11, 5.07, and 6.00 were prepared by diluting a certain amount of the aforementioned 10.0 wt% aqueous polymer solution with corresponding KHP buffers. All 0.02 wt% polymer solutions were sonicated in an ice/water ultrasonic bath for 2 min to ensure that the solutions were homogeneous. The pH values of the solutions were re-measured by a pH meter (essentially the same as the pH values of KHP buffers)

DLS measurements were conducted with a Brookhaven Instruments BI-200SM goniometer equipped with a PCI BI-9000AT digital correlator, a temperature controller, and a solid-state laser (model 25-LHP-928-249, λ = 633 nm) at scattering angle of 90°. The polymer solutions were filtered into borosilicate glass tubes with an inner diameter of 7.5 mm by the use of 0.2 μm filters. The glass tubes were then sealed with PE stoppers. The solutions were gradually heated. At each temperature, the solutions were equilibrated for 30 min prior to data recording. The time correlation functions were analyzed with a Laplace inversion program (CONTIN).

2.2.7 Rheological Measurements

Rheological experiments were conducted on a stress-controlled rheometer (TA Instruments Model TA AR2000ex). A cone-plate geometry with a cone diameter of 20 mm and an angle of 2° (truncation 52 μm) was employed; the temperature was controlled by the bottom Peltier plate. In each measurement, 85 μL of a polymer solution was loaded onto the plate by a micropipette. The solvent trap was filled with water and a solvent trap cover was used to minimize water evaporation. Dynamic viscoelastic properties (dynamic storage modulus G' and loss modulus G") of polymer solutions were measured by oscillatory shear experiments performed at a fixed frequency of 1 Hz in a heating ramp at a heating rate of 3 °C/min. The frequency dependences of G' and G" of a polymer solution at selected temperatures were obtained by frequency sweep tests from 0.1 to 100 Hz (or 0.001 to 100 Hz at some selected temperatures). At each temperature, the solution was equilibrated for at least 2 min prior to data recording. A strain amplitude of $\gamma = 0.2$ % was used in all dynamic tests to ensure that the deformation was within the linear viscoelastic regime.

2.2.8 Determination of Critical Micelle Concentration (CMC) of P(DEGEA-*co*-AA)-*b*-PEO-*b*-P(DEGEA-*co*-AA) in Aqueous Buffers by Fluorescence Spectroscopy

The critical micelle concentration (CMC) of P(DEGEA-*co*-AA)-*b*-PEO-*b*-P(DEGEA-*co*-AA) in water at a specific pH and a temperature that corresponded to the sol-to-gel transition temperature of the 10.0 wt% aqueous polymer solution at that pH was determined by fluorescence spectroscopy using Nile Red as fluorescence probe. For each pH, a series of triblock copolymer solutions with different concentrations in a 10 mM KHP buffer were prepared by the following procedure. 10 μL of a stock solution of

Nile Red in acetone (concentration: 0.63 mg/g, 6.3 mg of Nile Red in 10.007 g of HPLC grade acetone) was added into empty vials using a micropipette. The vials were weighed immediately and then placed in vacuum for > 3 h to remove the solvent. A calculated amount of a stock polymer solution (concentration: 1.46 wt%) was injected into each vial via a microsyringe and weighed. A certain amount of the 10.0 mM KHP buffer was then added into each vial to bring the total weight of the solution to 2.000 g. The nominal concentration of Nile Red was 7.8×10^{-6} M. After the sonication in an ice/water ultrasonic bath for 30 min, the solutions were equilibrated overnight in an oil bath at a temperature that corresponded to the $T_{sol\text{-}gel}$ of 10.0 wt% polymer solution at the same pH. Fluorescence emission spectra of Nile Red in these solutions at a specific temperature were recorded from PerkinElmer LS 55 fluorescence spectrometer equipped with a 20 kW xenon discharge lamp. The excitation wavelength was 550 nm and the fluorescence emission spectra were recorded from 560 to 720 nm. The slit width was 10 nm. The sample cell was thermostated with an external water bath of a Fisher Scientific Isotemp refrigerated circulator for at least 20 min before data recording. The maximum fluorescence intensity was then plotted against the logarithm of polymer concentration for the determination of CMC.

2.2.9 Salt Effect on Sol-to-Gel Transition Temperature and Gel Properties of Aqueous Solution of P(DEGEA-*co*-AA)-*b*-PEO-*b*-P(DEGEA-*co*-AA) with pH of 4.64 and a Nominal Polymer Concentration of 10.0 wt%

The amount of COOH/COOK in a 10 wt% aqueous solution of the ABA triblock copolymer was calculated on the basis of the polymer composition and the polymer concentration. 1.0 M KCl aqueous solution was prepared by dissolving KCl (7.456 g, >

99.0 %, Fisher Scientific) in Milli-Q water in a 100 mL volumetric flask. The polymer solution used here was obtained by changing the pH value of the original 10.0 wt% aqueous solution of P(DEGEA-*co*-AA)-*b*-PEO-*b*-P(DEGEA-*co*-AA) to 6.43 by the addition of 1.0 M KOH solution and then to 3.10 by the addition of 1.0 M HCl solution, followed by the injection of 1.0 M KOH to increase the pH to 4.64. Calculated amounts of 1.0 M KCl aqueous solution were injected via a microsyringe into this polymer solution in a stepwise fashion until the total amount of the added KCl was twice that of COOH/COOK in the solution (excluding the amount of KCl produced in the processes of adding KOH and HCl). After each injection, the polymer solution was sonicated for 2 min in an ice/water bath to ensure that the solution was homogeneous. The sample was then subjected to rheological measurements.

2.2.10 Differential Scanning Calorimetry (DSC) Study of Thermo-Induced Phase Transitions of 10.0 wt% Aqueous Solutions of P(DEGEA-*co*-AA)-*b*-PEO-*b*-P(DEGEA-*co*-AA)

Differential scanning calorimetry analysis of polymer solutions was conducted on a TA Q-1000 DSC instrument that was calibrated with sapphire disks. Polymer solutions (20 μL, ~ 20 mg) were loaded into pre-weighed aluminum hermetic pans and sealed carefully. A heating rate of 1 °C/min was used to obtain DSC thermograms with an empty pan as reference.

2.3 Results and Discussion

2.3.1 Synthesis of Thermo- and pH-Sensitive ABA Triblock Copolymer P(DEGEA-*co*-AA)-*b*-PEO-*b*-P(DEGEA-*co*-AA)

The doubly responsive ABA triblock copolymer P(DEGEA-*co*-AA)-*b*-PEO-*b*-P(DEGEA-*co*-AA) was prepared by a two-step procedure (Scheme 2.1). The precursor polymer P(DEGEA-*co*-*t*BA)-*b*-PEO-*b*-P(DEGEA-*co*-*t*BA) was synthesized from a difunctional PEO macroinitiator by ATRP of DEGEA and *t*BA with a molar ratio of 100 : 5 at 90 °C using CuBr/*N,N,N′,N′,N″*-pentamethyldiethylenetriamine as catalyst. Figure 2.1A shows the SEC traces of PEO macroinitiator and P(DEGEA-*co*-*t*BA)-*b*-PEO-*b*-P(DEGEA-*co*-*t*BA). The peak shifted to the high molecular weight side and remained narrow, indicating that the polymerization was well controlled. The number average molecular weight and polydispersity index of the triblock copolymer were 47.9 kDa and 1.09, respectively (relative to polystyrene standards). The *t*-butyl groups in the copolymer were then removed using trifluoroacetic acid (TFA). We previously confirmed that other ester bonds were not affected by TFA.[28,29] Figure 2.1B shows the ^{1}H NMR spectra of the triblock copolymer before and after the treatment with TFA. The successful removal of *t*-butyl groups was evidenced by the disappearance of the *t*-butyl peak in the ^{1}H NMR spectrum. By using the integrals of the peak located at 1.2 ppm, which was from the methyl group of DEGEA unit, and the peak at 3.2 – 4.0 ppm, which was from the PEO block and –$OCH_2CH_2OCH_2CH_2OCH_2CH_3$ of DEGEA units, along with the difference between the integrals of the peaks at 1.3 – 1.5 ppm before and after the removal of *t*-butyl groups of *t*BA units, the numbers of DEGEA and *t*BA (or AA) units in the ABA triblock copolymer were calculated and they were 140 and 7, respectively. The molar ratio of *t*BA to DEGEA units in the copolymer was essentially the same as in the feed.

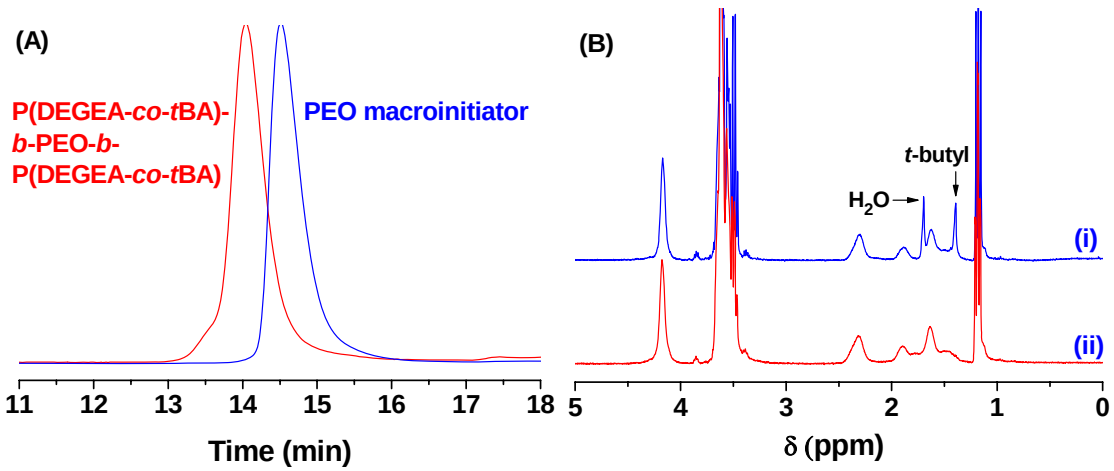

Figure 2.1. (A) Size exclusion chromatography traces of PEO macroinitiator and ABA triblock copolymer poly(ethoxydi(ethylene glycol) acrylate-*co*-*t*-butyl acrylate)-*b*-poly(ethylene oxide)-*b*-poly(ethoxydi(ethylene glycol) acrylate-*co*-*t*-butyl acrylate) (P(DEGEA-*co*-*t*BA)-*b*-PEO-*b*-P(DEGEA-*co*-*t*BA) and (B) ^{1}H NMR spectra of P(DEGEA-*co*-*t*BA)-*b*-PEO-*b*-P(DEGEA-*co*-*t*BA (i) before and (ii) after the removal of *t*-butyl groups using trifluoroacetic acid.

2.3.2 Thermo-Induced Sol-Gel Transition of 10.0 wt% Solution of P(DEGEA-*co*-AA)-*b*-PEO-*b*-P(DEGEA-*co*-AA) in Milli-Q water

A 10.0 wt% aqueous solution of P(DEGEA-*co*-AA)-*b*-PEO-*b*-P(DEGEA-*co*-AA) was made using Milli-Q water. The pH value of the solution was 3.00, measured with a pH meter (Accumet AB15 from Fisher Scientific) in an ice/water bath. The sample was a free-flowing liquid at ~ 0 °C; upon warming to room temperature, it turned into a clear gel that remained immobile even when the vial was inverted. This thermo-induced sol-gel transition was reversible; lowering the temperature converted the gel into a free-flowing liquid. To study its rheological properties, we carried out an oscillatory shear experiment at a fixed frequency of 1 Hz in a heating ramp at a heating rate of 3 °C/min. A strain amplitude of γ = 0.2 % was used to ensure that the measurement was taken in the linear viscoelastic regime. As shown in Figure 2.2, when the temperature was below 15 °C, the values of dynamic storage modulus G' and loss modulus G" were small and the data points were scattered. In the range of 15 – 23 °C, both G' and G" increased with the increase of temperature; the value of G" was larger than G', indicating that the sample was a viscous liquid. Above 23 °C, G' became greater than G", suggesting that the solution turned into a gel. The crossover, G' = G", has been commonly used as an indicator of the sol-gel transition. Therefore, the sol-to-gel transition temperature ($T_{\text{sol-gel}}$) of this 10.0 wt % aqueous solution is 23.1 °C.

This temperature-induced sol-gel transition stems from the LCST behavior of thermosensitive outer blocks of the ABA triblock copolymer. When the temperature is raised above the LCST of P(DEGEA-*co*-AA) blocks, they undergo a hydration-to-dehydration transition and self-assemble into hydrophobic domains (micellar cores). At a

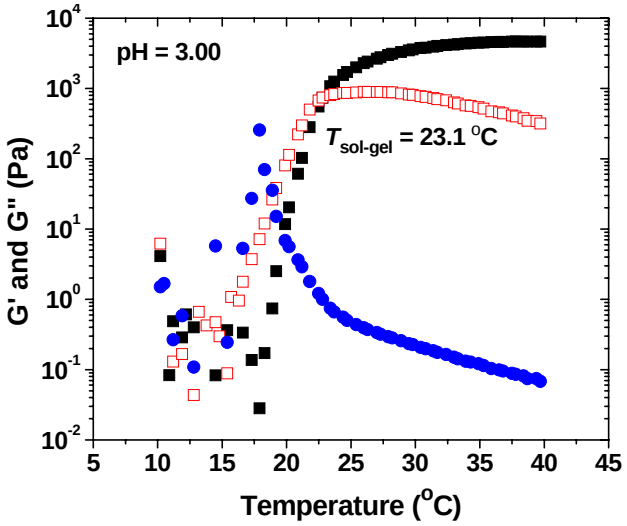

Figure 2.2. Plot of dynamic storage modulus G' (■), dynamic loss modulus G" (□), and tanδ (●) versus temperature for a 10.0 wt % aqueous solution of P(DEGEA-*co*-AA)-*b*-PEO-*b*-P(DEGEA-*co*-AA) with pH of 3.00. The data were collected from a temperature ramp experiment performed by using a fixed frequency of 1 Hz, a strain amplitude of 0.2 %, and a heating rate of 3 °C/min.

sufficiently high concentration (i.e., > CGC), a 3-dimensional network is formed with the central PEO blocks forming bridges among micellar cores. Decreasing temperature dissolves the P(DEGEA-*co*-AA) blocks and dissociates the network, resulting in a gel-to-sol transition. The origin of the thermo-induced gelation can be seen from the differential scanning calorimetry (DSC) analysis of the sample (Figure 2.3A). An endothermic peak was observed in the DSC thermogram with the onset temperature at ~ 8 °C and the peak position located at ~ 16 °C, indicating that the transition was an entropically driven process. To further confirm the thermo-induced micellization, we conducted a dynamic light scattering (DLS) study of a 0.02 wt% solution of P(DEGEA-*co*-AA)-*b*-PEO-*b*-P(DEGEA-*co*-AA) in an aqueous potassium hydrogen phthalate (KHP) buffer at pH = 3.00 (Figure 2.4). Below 15 °C, the scattering intensity was low and the apparent hydrodynamic size (D_h), obtained from CONTIN analysis, was < 10 nm, confirming that the triblock copolymer was dissolved molecularly in water. With the increase of temperature above 15 °C, the scattering intensity began to increase. The critical micellization temperature (CMT) determined from the plot of scattering intensity versus temperature was 15 °C, slightly higher than the onset temperature in the DSC thermogram (~ 8 °C), which can be attributed to the concentration effect. The apparent D_h of micelles at 25 °C was 64 nm. Note that the transition temperatures from both DSC and DLS studies were lower than the $T_{sol\text{-}gel}$ (23.1 °C) of the 10.0 wt% solution. This is understandable because the sol-gel transition is closely related to the mechanical property of the 3-D network gel and a slightly higher temperature is usually needed for the sample to exhibit a sufficient elastic property.

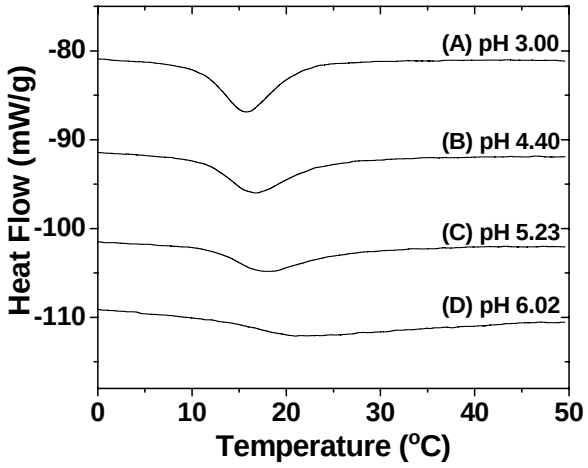

Figure 2.3. Differential scanning calorimetry thermograms of the 10.0 wt% aqueous solution of P(DEGEA-*co*-AA)-*b*-PEO-*b*-P(DEGEA-*co*-AA) at pH of (A) 3.00, (B) 4.40, (C) 5.23, and (D) 6.02. The heating rate was 1 °C/min. For the sake of clarity, the thermograms were shifted vertically.

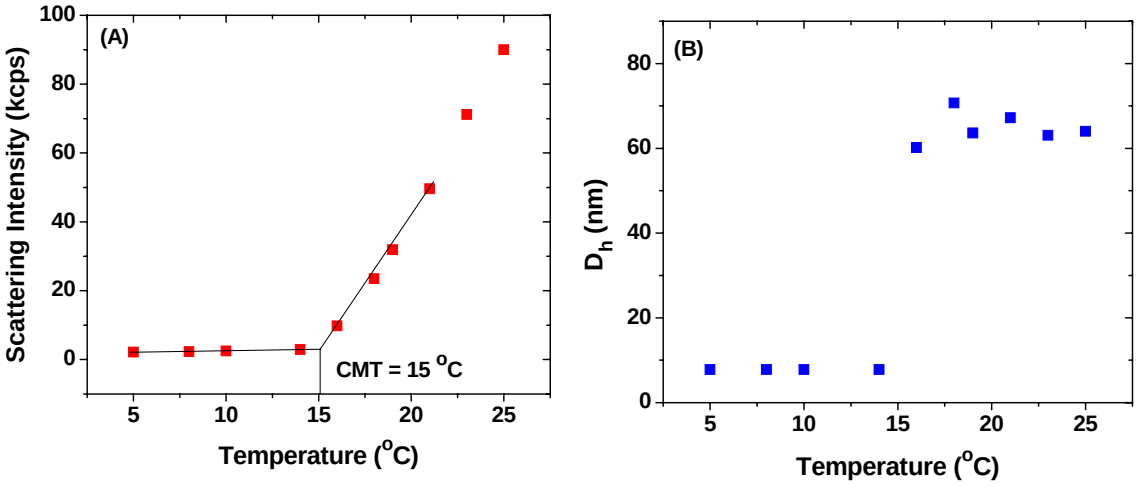

Figure 2.4. Scattering intensity at scattering angle of 90° (A) and apparent hydrodynamic size D_h (B), obtained from CONTIN analysis, as a function of temperature in a dynamic light scattering study of a 0.02 wt% solution of P(DEGEA-*co*-AA)-*b*-PEO-*b*-P(DEGEA-*co*-AA) in an aqueous KHP buffer with pH = 3.00.

A consequence of the formation of bridges by the midblock of an ABA triblock copolymer among micellar cores is that the gel exhibits stronger strain robustness compared with diblock copolymer micellar gels.[60] Figure 2.5 shows dynamic strain amplitude sweeps of the 10.0 wt% aqueous solution of P(DEGEA-*co*-AA)-*b*-PEO-*b*-P(DEGEA-*co*-AA) at pH of 3.00 and 30.5 °C at frequencies of 0.5, 1.0, 2.5, and 5.0 Hz. For all four frequencies, the gel exhibited a linear response up to at least 15 % strain, which was almost the same as supramolecular ABA triblock copolymer ion gels reported by Lodge et al.[60] In contrast, diblock copolymer ion gels showed nonlinear viscoelasticity above 4-5 % strain.[60] Thus, the dynamic strain sweep study also suggested the formation of a 3-dimensional network with the central PEO blocks forming bridges among micellar cores at temperatures above the $T_{sol\text{-}gel}$.

To further look into the sol-gel transition and gel characteristics, we conducted frequency sweeps at various temperatures using a strain amplitude of 0.2 % for the 10.0 wt% aqueous solution of the triblock copolymer. At 18 °C, G' and G" exhibited different power law dependences on frequency f in the low frequency region of 0.1 – 3 Hz: G' ~ f^2 and G" ~ f (Figure 2.6A). This is the typical rheological behavior of a viscous liquid.[61] At 24.5 °C, just above the $T_{sol\text{-}gel}$ (23.1 °C), a frequency sweep in a wider range (0.001 to 100 Hz, spanning five orders in magnitude) was collected and both the terminal flow and gel behavior were observed (Figure 2.6B). In the extremely low frequency region, G' and G" exhibited power law dependences on f, the characteristic of terminal flow behavior. At higher frequencies, G' became larger than G" and both G' and G" showed much weaker frequency dependences; these are the gel characteristics. Clearly, the gel was a transient network possessing physical crosslinks of a finite dissociation time. The crossover of G'

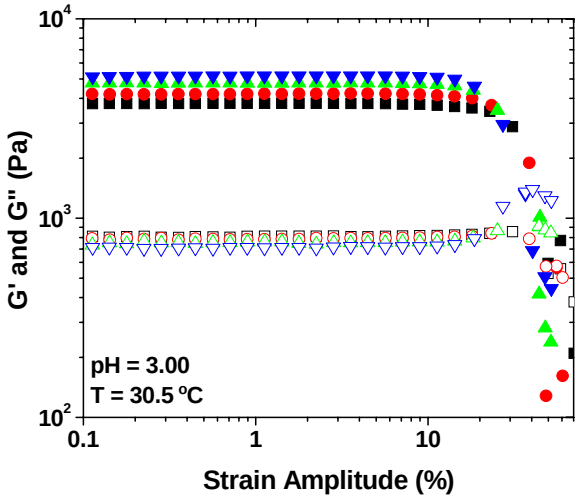

Figure 2.5. Dynamic strain amplitude sweeps for the 10.0 wt% aqueous solution of P(DEGEA-*co*-AA)-*b*-PEO-*b*-P(DEGEA-*co*-AA) with pH of 3.00 at 30.5 °C at frequencies of 0.50 Hz (dynamic storage modulus G', ■ and dynamic loss modulus G", □), 1.00 Hz (G', ● and G", ○), 2.50 Hz(G', ▲ and G", △), and 5.00 Hz (G', ▼ and G", ▽).

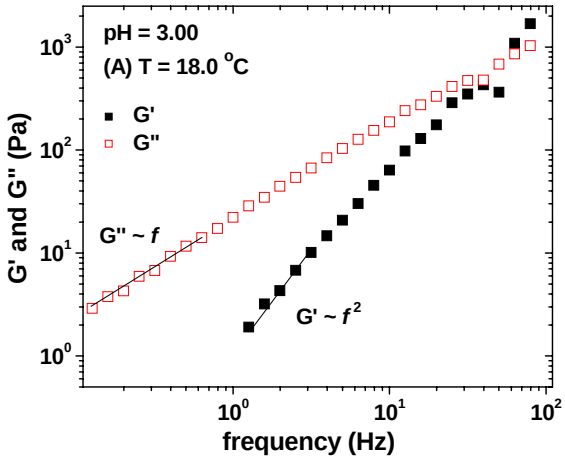
pH = 3.00
(A) T = 18.0 °C
G'
G"
G" ~ f
G' ~ f 2
G' and G" (Pa)
frequency (Hz)

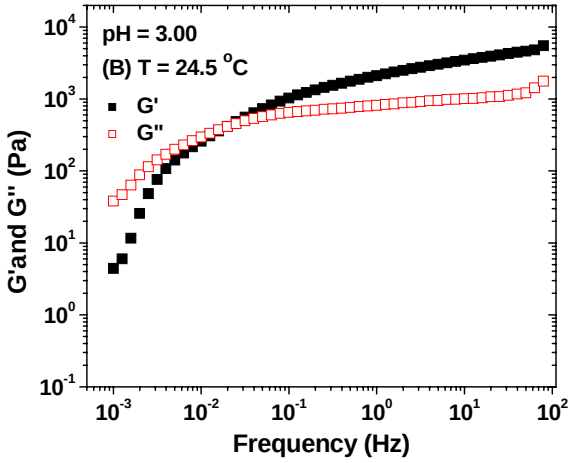
pH = 3.00
(B) T = 24.5 °C
G'
G"
G'and G" (Pa)
Frequency (Hz)

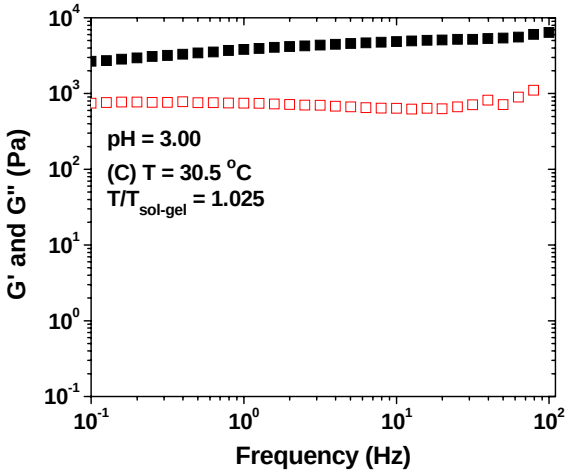
pH = 3.00
(C) T = 30.5 °C
T/T sol-gel = 1.025
G' and G" (Pa)
Frequency (Hz)

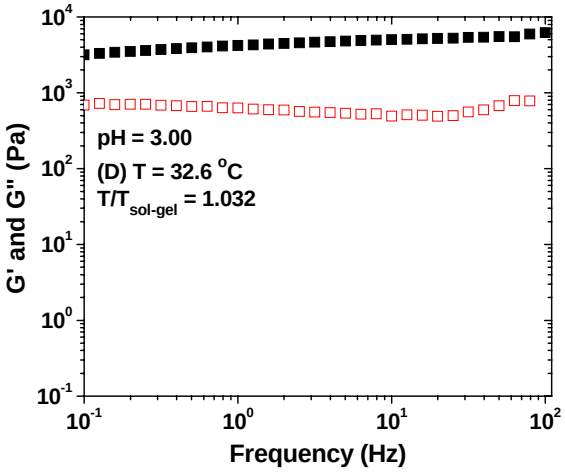
pH = 3.00
(D) T = 32.6 °C
T/T sol-gel = 1.032
G' and G" (Pa)
Frequency (Hz)

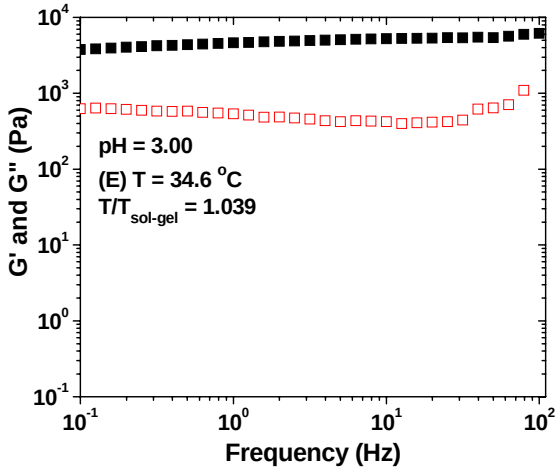

Figure 2.6. Frequency dependences of dynamic storage modulus G' (■) and loss modulus G" (□) of the 10.0 wt% aqueous solution of P(DEGEA-*co*-AA)-*b*-PEO-*b*-P(DEGEA-*co*-AA) with a pH of 3.00 at (A) 18, (B) 24.5, (C) 30.5, (D) 32.6, and (E) 34.6 °C. A strain amplitude of 0.2 % was used in the frequency sweep experiments.

and G" versus frequency curves occurred at f = 0.02 Hz, from which we can estimate the terminal relaxation time τ of polymer chains or the average life time of a thermosensitive P(DEGEA-*co*-AA) block in a micellar core at this temperature through

$$\tau = 1/(2\pi f)$$

where f is the frequency at the crossover point.[60] The estimated τ at this temperature was 8.0 s. With further increasing temperature, the relaxation time would become longer and the crossover point would shift to an even lower frequency.

At 30.5, 32.6, and 34.6 °C, the sample was a transparent gel. G' was significantly higher than G" and was nearly independent of f in the frequency range of 0.1 to 100 Hz (Figure 2.6C, D, and E), which are the characteristics of elastic solid-like behavior. The plateau modulus G_N of the gel can be obtained from the frequency sweep and it is known that the G_N of a transient gel is a measure of the number density of elastically active polymer chains (or effective gel network strands):

$$G_N = \upsilon k_B T$$

where υ is the number density of elastically active polymer chains (number of elastically active bridging chains per unit volume), k_B is Boltzmann constant, and T is the absolute temperature. The G_N is usually evaluated as the G' value at the frequency where G" exhibits the minimum value, because the increase of G" at higher frequencies indicates a fast relaxation process separate from the terminal flow process. This method for the determination of G_N is well established for the entangled homopolymer melts and has also been recently used in the study of thermoreversible transient gels.[62] The frequencies at which G" exhibited minimum values at 30.5, 32.6, and 34.6 °C were 12.59, 10, and 12.59 Hz, respectively; therefore, the values of G_N were 4.9×10^3 Pa, 5.0×10^3 Pa, and

5.3×10^3 Pa, respectively, which were close to the modulus in the plateau zone in the heating ramp (4.6×10^3 Pa, Figure 2.2). If the central block of every polymer chain is elastically active in the gel, calculations show that the value of G_N is 5.4×10^3 Pa at 30.5 °C, 5.4×10^3 Pa at 32.6 °C, and 5.5×10^3 Pa at 34.6 °C. This means that 91, 93, and 96% of polymer chains formed effective network strands in the gel at 30.5, 32.6, and 34.6 °C, respectively. The observed high percentages of polymer chains that were elastically active in the gels might result from the well-defined architecture of the ABA triblock copolymer and the relatively hydrophobic outer blocks (the LCST of PDEGEA is 9 °C).

2.3.3 pH Effect on Sol-Gel Transition of 10.0 wt% Aqueous Solution of P(DEGEA-*co*-AA)-*b*-PEO-*b*-P(DEGEA-*co*-AA)

To investigate the pH effects on sol-to-gel transition temperature ($T_{sol\text{-}gel}$) and gel properties, we gradually increased the pH value of the 10.0 wt% aqueous solution of P(DEGEA-*co*-AA)-*b*-PEO-*b*-P(DEGEA-*co*-AA) by injecting a small amount of 1.0 M KOH solution via a microsyringe in a stepwise fashion. Each time, the sample was sonicated in an ice/water ultrasonic bath for a few minutes to ensure that the solution was homogeneous before the pH value was measured. The sample was then subjected to dynamic viscoelastic measurements using the same conditions as for the original polymer solution. Figure 2.7 shows the sol-gel transition temperature as a function of pH (the original rheological data can be found in Appendix B). Similar to our previous observation for the 12.0 wt% aqueous solution of thermo- and pH-sensitive P(DEGMMA-*co*-MAA)-*b*-PEO-*b*-P(DEGMMA-*co*-MAA),[28] the $T_{sol\text{-}gel}$ initially increased slowly with the increase of pH, from 23.1 °C at pH = 3.00, to 26.4 °C at pH = 4.11, to 28.7 °C at pH = 4.40, to 30.1 °C at pH = 4.70, and 31.5 °C at pH = 4.95. Above

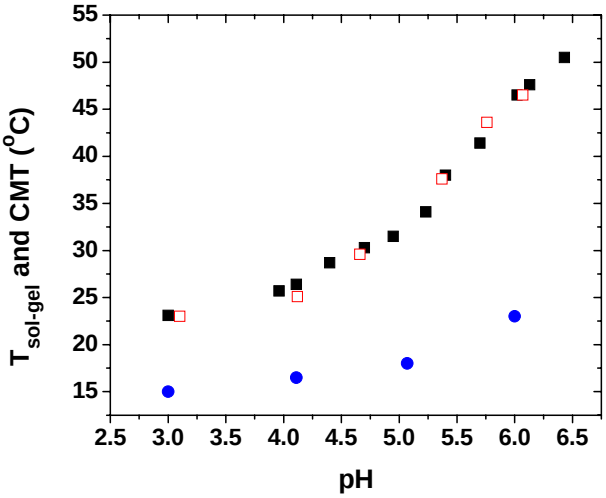

Figure 2.7. Sol-gel transition temperature ($T_{sol-gel}$) of 10.0 wt% aqueous solution of P(DEGEA-*co*-AA)-*b*-PEO-*b*-P(DEGEA-*co*-AA) as a function of pH in the processes of increasing (■) and decreasing pH (□), and the plot of critical micellization temperature (CMT, ●) of the triblock copolymer in the aqueous buffer at a concentration of 0.02 wt% versus pH. The sol-to-gel transition temperatures were determined by dynamic viscoelastic measurements using a heating rate of 3 °C/min, a strain amplitude of 0.2 %, and a fixed frequency of 1 Hz. The CMTs were determined by dynamic light scattering.

pH = 4.95, the increase of the sol-gel transition temperature with pH became slightly faster. In 1.5 pH units, the sol-gel transition temperature jumped by nearly 20 °C, from 31.5 °C at pH = 4.95 to 50.5 °C at pH 6.43. The pH of the polymer solution was then gradually brought back to 3.10 by injection of a 1.0 M HCl solution in a similar stepwise fashion. As shown in Figure 2.7, the sol-gel transition temperatures from the process of decreasing pH were essentially right on the curve of $T_{sol\text{-}gel}$ versus pH from the process of increasing pH, indicating that the $T_{sol\text{-}gel}$ can be precisely controlled by solution pH and can be continuously and reversibly tuned in a large temperature range.

To confirm that the tunability of $T_{sol\text{-}gel}$ of the 10.0 wt% aqueous solution of P(DEGEA-*co*-AA)-*b*-PEO-*b*-P(DEGEA-*co*-AA) originated from the pH dependence of the LCST of thermosensitive P(DEGEA-*co*-AA) blocks, we conducted DLS studies of the triblock copolymer in aqueous buffers with a concentration of 0.02 wt% at three more pH values. The CMT of P(DEGEA-*co*-AA)-*b*-PEO-*b*-P(DEGEA-*co*-AA) gradually increased with the increase of pH, from 15 °C at pH = 3.00, to 16.5 °C at pH = 4.11, to 18 °C at pH = 5.07, and 23 °C at pH = 6.00 °C.[63] The CMT curve of the triblock copolymer in 0.02 wt % aqueous solutions exhibited a trend similar to the $T_{sol\text{-}gel}$ curve but there was a shift. It is understandable that at a particular pH the $T_{sol\text{-}gel}$ is higher than the CMT because the gelation requires the formation of a 3-dimensional network with a sufficient mechanical strength, while the CMT is the temperature at which the thermosensitive P(DEGEA-*co*-AA) blocks begins to self-assemble to form micelles in a dilute aqueous solution. The wider gap between CMT and $T_{sol\text{-}gel}$ curves at high pH values can be attributed to the different effects of charges, formed from the ionization of carboxylic acid groups, on CMT and $T_{sol\text{-}gel}$. Although these results were similar to our

previous report, the increase of CMT with pH (from 15 °C at pH = 3.00 to 23 °C at pH = 6.00) was slower compared with a similar thermo- and pH-sensitive ABA triblock copolymer, P(DEGMMA-*co*-MAA)-*b*-PEO-*b*-P(DEGMMA-*co*-MAA),[28] where the CMT jumped by 14 °C from pH = 3.2 to 6.0. We speculate that this is because PDEGEA (cloud point: 9 °C) is less hydrophilic than PDEGMMA (cloud point: 25 °C); the ionization of a small amount of carboxylic acid groups (3.5 carboxylic acid groups per thermosensitive block) did not increase the hydrophilicity of thermosensitive blocks as much as for P(DEGMMA-*co*-MAA).

In the examination of heating ramps for different pH values, we noticed that the sol-to-gel transition became broader with the increase of pH. This can be better seen from the curves of G' normalized by the maximum value of G' versus absolute temperature normalized by $T_{sol\text{-}gel}$ and the curves of tanδ (= G"/G') versus normalized temperature ($T/T_{sol\text{-}gel}$) for four selected pH values (3.00, 4.11, 5.23, and 6.13) in Figure 2.8. The graphs illustrate how sharply the solution is transformed into a gel and how closely it approaches the elastic limit. From both plots in Figure 2.8, the sample at the original pH (3.00) exhibited the sharpest liquid-to-solid transition and the sol-to-gel transition at pH = 6.13 was significantly broader. This phenomenon stems from the weaker and broader LCST transition of thermosensitive P(DEGEA-*co*-AA) blocks at a higher pH, which can be seen from DSC thermograms in Figure 2.3. With the increase of pH, the maximum peak position shifted to a higher temperature and the peak became significantly broader, similar to the observation reported in the literature.[64] As discussed by Urry,[64] the introduction of charges onto a thermosensitive polymer disrupts the structured water, weakening the LCST transition. In addition, the random distribution of a small amount of

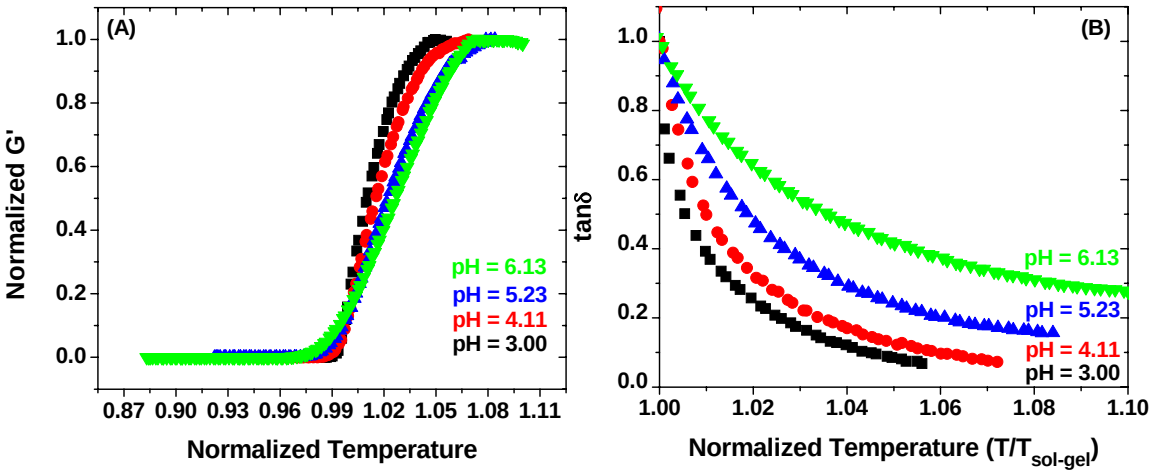

Figure 2.8. Plot of (A) normalized dynamic storage modulus G'/G'_{max}, where G'_{max} is the maximum value of G' observed in the heating ramp experiment, and (B) tanδ (= G"/G') versus normalized temperature $T/T_{sol\text{-}gel}$, where T and $T_{sol\text{-}gel}$ are absolute temperatures, for the 10.0 wt% aqueous solution of P(DEGEA-*co*-AA)-*b*-PEO-*b*-P(DEGEA-*co*-AA) with pH values of 3.00 (■), 4.11 (●), 5.23 (▲), and 6.13 (▼).

charges along the polymer chain also contributes to the broader LCST transition (on average there were only 3.5 carboxylic acid groups per P(DEGEA-*co*-AA) block).

2.3.4 pH Effect on Gel Property of 10.0 wt% Aqueous Solution of P(DEGEA-*co*-AA)-*b*-PEO-*b*-P(DEGEA-*co*-AA)

Three normalized temperatures, $T/T_{sol\text{-}gel}$ = 1.025, 1.032, and 1.039, where T and $T_{sol\text{-}gel}$ were absolute temperatures, were chosen to conduct frequency sweeps to compare the gel properties at a series of pH values in the processes of both increasing and decreasing pH.[63] Because the sol-gel transition became broader with the increase of pH, we found that above pH 5.40 the minimum value of G" was not observed in the studied frequency range for all three normalized temperatures and thus the plateau value of G' could not be determined by the aforementioned method for the original pH. In the examination of frequency sweeps from pH 3.00 to 5.23, we noticed that most of plateau values of G' appeared at ~ 10 Hz. To make the comparison easier, we used the value of G' at f = 10 Hz as G_N for all pH values and made a plot of G_N versus pH for each normalized temperature (Figure 2.9). In addition, a plot of the maximum G' obtained from the heating ramp versus pH was included.

As can be seen from Figure 2.9, the highest moduli appeared at pH = 3.00, which were ~ 5×10^3 Pa. At a particular pH, the G_N value either remained about the same or increased slightly with the increase of normalized temperature $T/T_{sol\text{-}gel}$ from 1.025 to 1.039. For example, the G_N at pH = 4.40 was 3.0×10^3 Pa at $T/T_{sol\text{-}gel}$ = 1.025, 3.2×10^3 Pa at $T/T_{sol\text{-}gel}$ = 1.032, 3.2×10^3 Pa at $T/T_{sol\text{-}gel}$ = 1.039. These G_N values were close to the maximum G' from the heating ramp (2.9×10^3 Pa) at this pH. With the increase of pH from 3.00 to ~ 5.40, the values of G_N at three normalized temperatures evaluated from

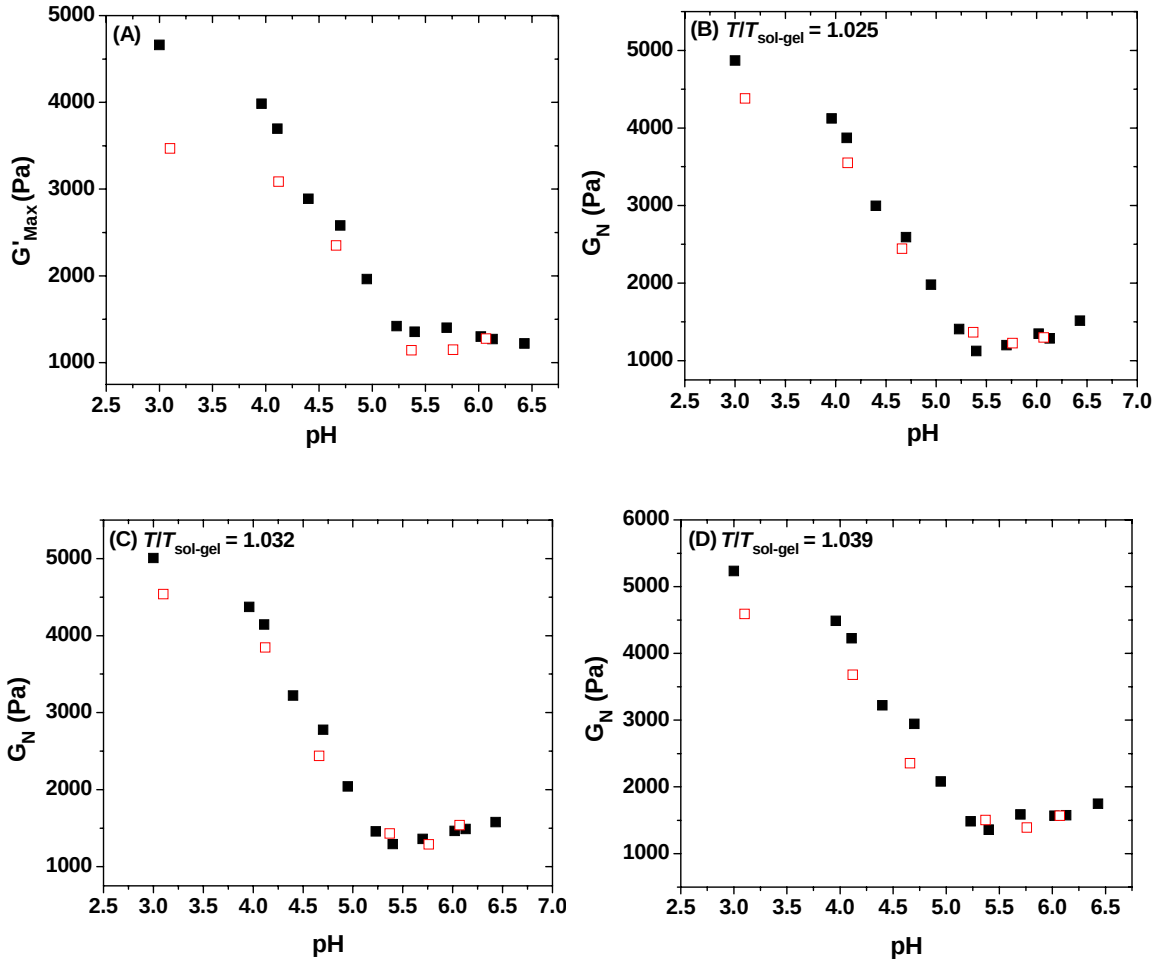

Figure 2.9. The maximum G' from heating ramp (A) and plateau moduli G_N at three normalized temperatures, $T/T_{sol\text{-}gel}$ = 1.025 (B), 1.032 (C), and 1.039 (D), obtained from frequency sweeps as a function of pH obtained from the processes of gradually increasing pH (up to 6.43, ■) by the addition of 1.0 M KOH solution and then gradually decreasing pH (□) by the addition of 1.0 M HCl. T and $T_{sol\text{-}gel}$ are absolute temperatures.

frequency sweeps and the maximum G' obtained from the heating ramp all decreased and the sharpest drop occurred at pH of ~ 4.7. For example, the G_N at $T/T_{sol\text{-}gel}$ = 1.025 was only 1.1×10^3 Pa at pH = 5.40, significantly lower than that at pH = 3.00 (4.9×10^3 Pa). Clearly, at all three normalized temperatures, the gel became weaker with the increase of pH. When the pH was above 5.5, the dynamic moduli appeared to level off. This is somewhat different from the pH effect on $T_{sol\text{-}gel}$, which continued to increase (Figure 2.7). For the process of decreasing pH by the addition of HCl, the moduli exhibited a pH dependence similar to that in the process of increasing pH, but appeared to be slightly lower, especially in the low pH region (e.g., at pH = 4.12 and 3.10).

As mentioned earlier, the G_N of a 3-dimensional physical network gel is a measure of the number density of elastically active polymer chains ($G_N = \upsilon k_B T$). The decrease in G_N means the reduction of the number of bridging polymer chains in the gel. To better view how pH affected the gel property, we calculated the percentages of PEO blocks that were elastically active at three normalized temperatures (Figure 2.10). The percentage of effective network strands decreased with the increase of pH for all three normalized temperatures in the pH range of 3.00 to 5.40. Below pH = 4.0, the change was moderate. For example, for $T/T_{sol\text{-}gel}$ = 1.025, the fraction decreased from 90% at pH 3.00 to 71% at pH = 4.11. With the increase of pH from 4.11 to 5.40, a dramatic drop in the fraction of bridging chains was observed, e.g., from 71% at pH 4.11 to 21% at pH 5.70 at the normalized temperature of $T/T_{sol\text{-}gel}$ = 1.025. Above pH 5.4, the apparent number of bridging polymer chains changed little with pH.

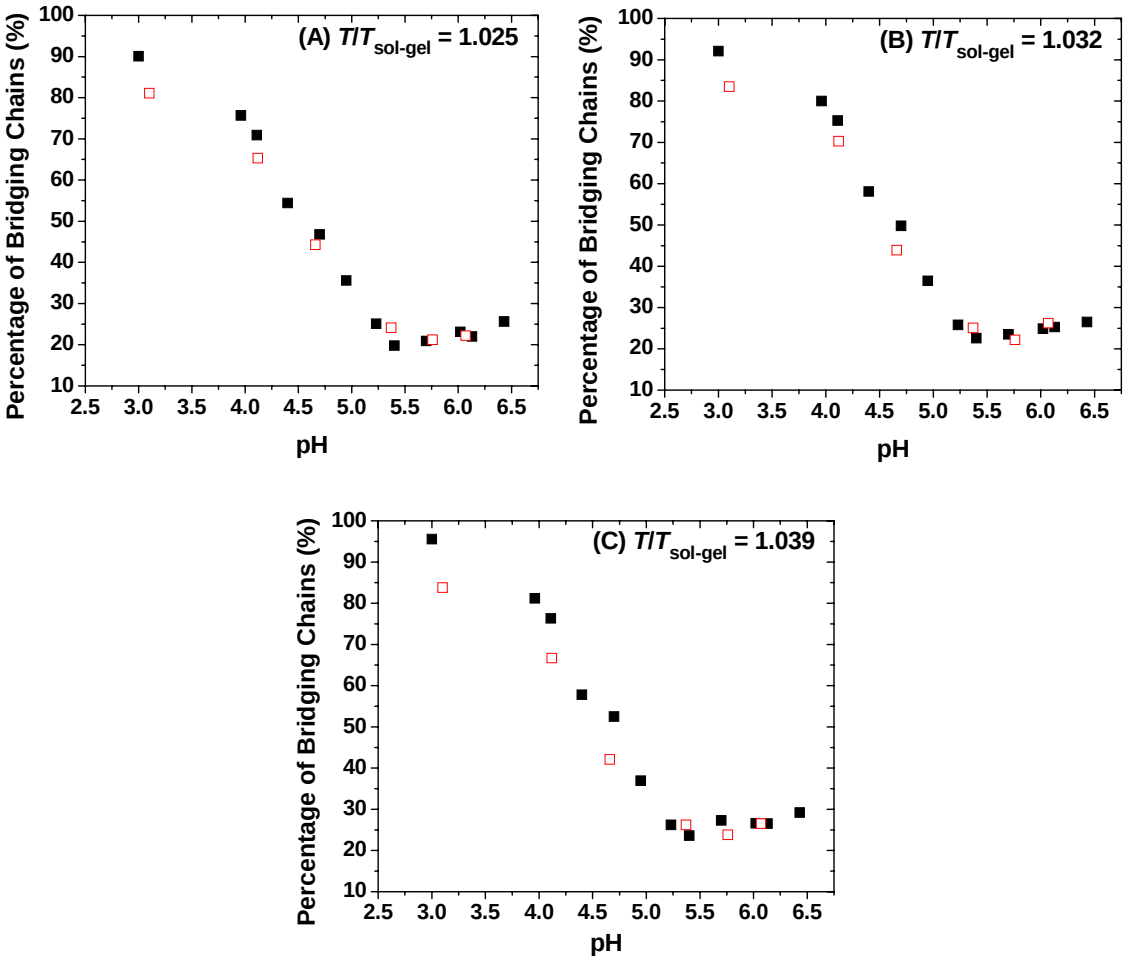

Figure 2.10. Percentage of PEO blocks that were elastically active in the gels at normalized temperature $T/T_{sol\text{-}gel}$ = 1.025 (A), 1.032 (B), and 1.039 (C), respectively, in the processes of increasing (■) and decreasing pH (□).

Decreasing the solution pH from 6.43 to 3.10 gave essentially the same pH dependence as in the process of increasing pH. However, just like the G_N, the fraction of elastically active polymer chains at a particular pH (below 5.0) in the process of decreasing pH appeared to be slightly lower than those at the same pH in the process of increasing pH. We speculate that two factors could be responsible for this observation. (1) The addition of 1.0 M KOH and later 1.0 M HCl aqueous solution to change the pH diluted the polymer solution. Calculations show that the polymer concentration decreased from 10.0% to 9.7% if the carboxylic acid groups were fully ionized by KOH and then fully protonated by HCl. Everything being equal, the value of G_N would decrease by 3 %. This means that at pH = 3.00, the G_N would be 4869 Pa × 97% = 4722 Pa. (2) KCl, an inorganic salt, was produced when 1.0 M HCl was added to decrease the solution pH to 3.10. The presence of a salt could affect sol-to-gel transition and gel characteristics. To look into the possible salt effect, we conducted a study by gradually adding 1.0 M KCl solution into a polymer solution with pH = 4.64. This polymer solution was obtained by changing the pH value of the original 10.0 wt% aqueous solution of P(DEGEA-*co*-AA)-*b*-PEO-*b*-P(DEGEA-*co*-AA) to 6.43 by the addition of 1.0 M KOH solution and then to 3.10 by the addition of 1.0 M HCl solution, followed by the injection of 1.0 M KOH until the solution pH reached 4.64.

As shown in Figure 2.11A, there was very little change in the $T_{sol\text{-}gel}$ even after the addition of KCl twice the amount of COOH/COOK in the solution (the $T_{sol\text{-}gel}$ decrease ≤ 0.6 °C). Similarly, the values of G_N only decreased slightly with the addition of KCl at three normalized temperatures except for [KCl]/[AA] = 200%, where noticeable decreases were observed. Nevertheless, there seemed to be a trend that the G_N decreased

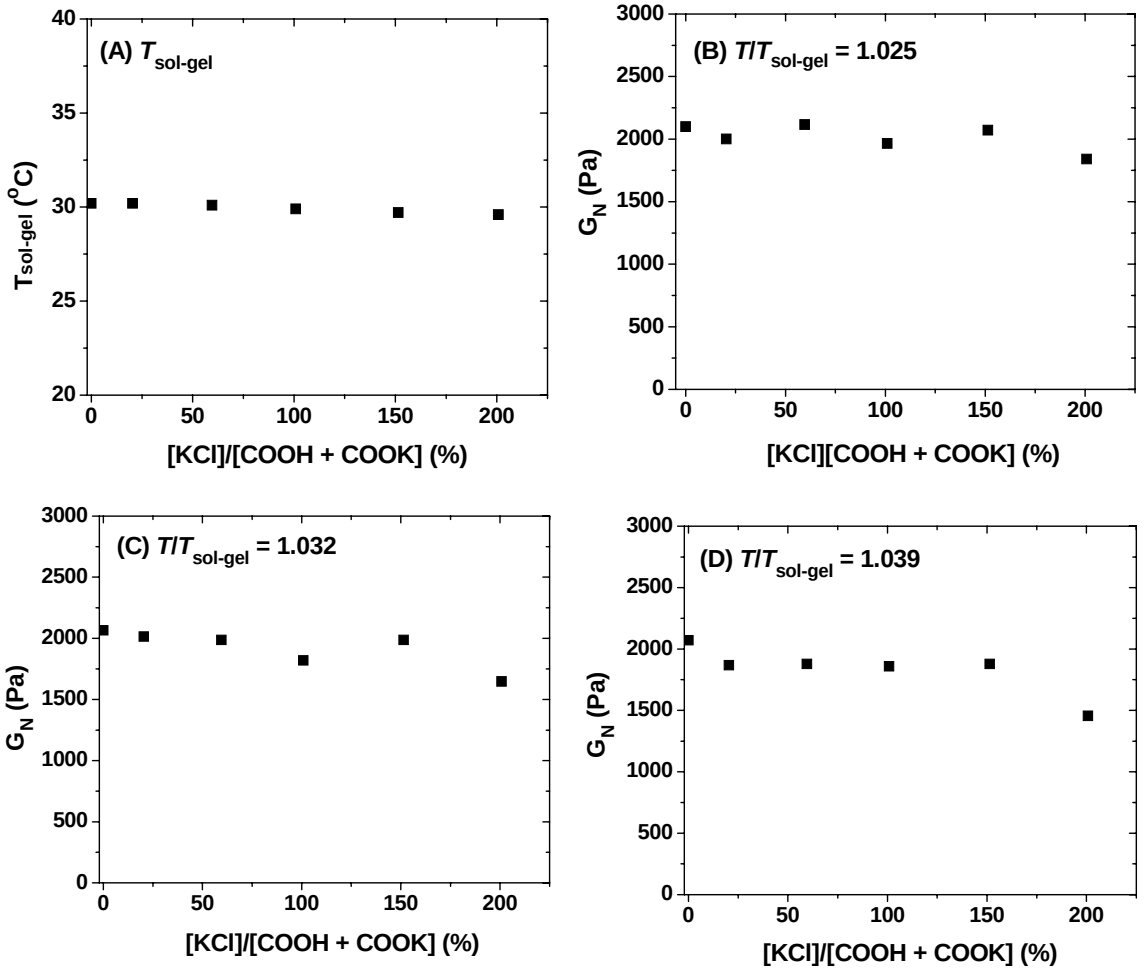

Figure 2.11. Effect of the amount of added KCl relative to the calculated amount of COOH/COOK on the ABA triblock copolymer chains on (A) $T_{sol-gel}$ and plateau moduli G_N at three normalized temperatures, $T/T_{sol-gel}$ = 1.025 (B), 1.032 (C), and 1.039 (D).

with the increase of the amount of added KCl, though quite small. Again, the situation was complicated by the dilution; the polymer concentration decreased by 3 % after the addition of KCl twice the amount of COOH/COOK. From this control experiment, it appeared that both the dilution and the formation of KCl from the injection of 1.0 M KOH and HCl contributed to the difference in the values of G_N at a particular pH in the processes of increasing and decreasing pH and likely the dilution was the main factor.

The decrease of the fraction of bridging polymer chains with the increase of pH was undoubtedly accompanied by the increase in the numbers of loops (the two outer blocks of an ABA triblock copolymer located in the same micelle core) and dangling chains (one outer block staying in bulk water rather than in a micellar core) (see Scheme 2.2 for the schematic illustration of the gel structures of the ABA triblock copolymer at a low pH and a high pH value). Despite that the DLS studies showed that there were no significant differences in micelle sizes at pH of 3.00 (apparent D_h = ~ 64 nm, Figure 2.4B), 4.11 (apparent D_h = ~ 64 nm), 5.07 (apparent D_h = ~ 69 nm), and 6.00 (apparent D_h = ~ 60 nm) at the concentration of 0.02 wt%,[63] we speculated that in the 10.0 wt% polymer solution the size of micellar cores formed by the dehydrated P(DEGEA-*co*-AA) blocks increased slightly at higher pH values because of the charge-charge interaction inside the micellar core. A larger micellar core would facilitate the formation of loops because the larger core size lowers the entropy penalty for polymer chains to loop back to the same core. On the other hand, the ionization of carboxylic acid groups increases the overall hydrophilicity of polymer chains, which may increase the number of dangling polymer chains in water. To look into this possibility, we measured the critical micellization concentrations (CMC) of P(DEGEA-*co*-AA)-*b*-PEO-*b*-P(DEGEA-*co*-AA) at four pH

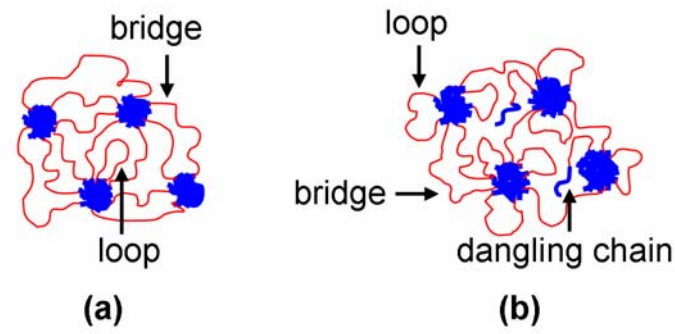

Scheme 2.2. Schematic illustration of the gel structures of 10.0 wt% aqueous solution of P(DEGEA-*co*-AA)-*b*-PEO-*b*-P(DEGEA-*co*-AA) at a low pH (a) and a high pH (b) value. The increased formation of loops and dangling chains contribute to the decrease in the gel strength at high pH values.

values (pH = 3.00, 4.01, 5.00, and 6.02) and at temperatures corresponding to the sol-gel transition temperatures of the 10.0 wt% polymer solution by fluorescence spectroscopy using Nile Red as fluorescence probe. The fluorescence spectra and the plot of fluorescence intensity versus polymer concentration for each pH are shown in Figure 2.12. Figure 2.13 displays the plot of CMC versus pH. The CMC of the triblock copolymer was 0.019 mg/mL at pH = 3.00 (23 °C), 0.020 mg/mL at pH = 4.01 (26 °C), 0.023 mg/mL at pH = 5.00 (32 °C), and 0.024 mg/mL at pH 6.02 (47 °C). Although the increase of the CMC with the increase of pH was small, the trend was discernable, indicating that the polymer chains became more hydrophilic at higher pH values and likely more thermosensitive end blocks were located in bulk water as dangling chains.

It is believed that both the loop formation and the increased presence of dangling chains contribute to the observed decreases of G_N and the percentage of elastically active polymer chains with the increase of pH from 3.00 to 5.40. Above pH = 5.4, it appeared that the ionization of the remaining carboxylic acid groups on the thermosensitive blocks had a negligible effect on the gel characteristics.

2.4 Conclusions

We synthesized a well-defined thermo- and pH-sensitive ABA triblock copolymer, P(DEGEA-*co*-AA)-*b*-PEO-*b*-P(DEGEA-*co*-AA), and conducted a systematic study on thermo-induced sol-gel transitions and gel properties of 10.0 wt% aqueous solution of this block copolymer at various pH values. The $T_{sol\text{-}gel}$ can be continuously and reversibly tuned in a large temperature range by changing the solution pH. The sol-gel transition became broader with the increase of pH, which was caused by the weaker and broader

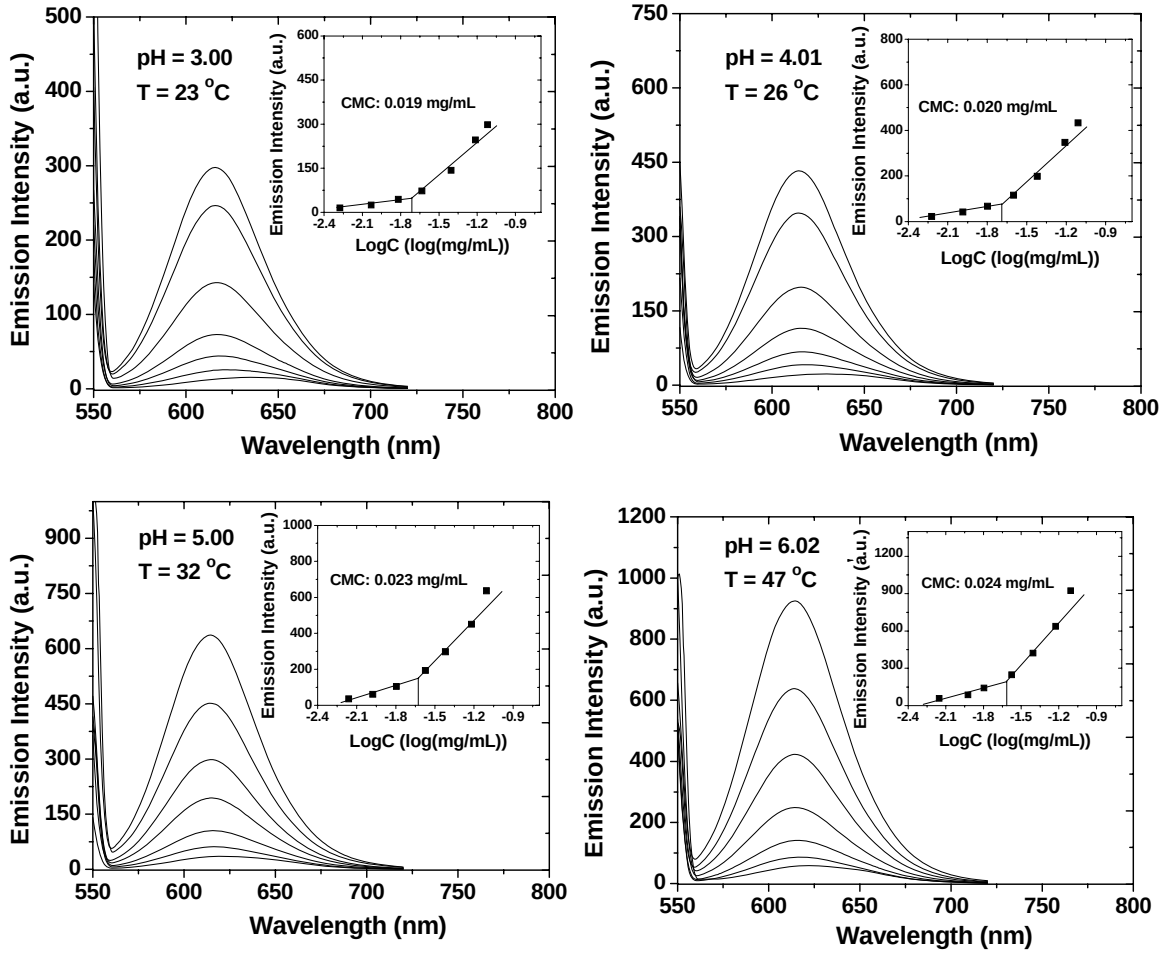

Figure 2.12. Fluorescence spectra of Nile Red and plot of maximum fluorescence emission intensity of Nile Red in aqueous solutions of P(DEGEA-*co*-AA)-*b*-PEO-*b*-P(DEGEA-*co*-AA) versus logarithm of polymer concentration (inset in each plot) at (A) pH = 3.00 and 23 °C, (B) pH 4.01 and 26 °C, (C) pH = 5.00 and 32 °C, and (D) pH = 6.02 and 47 °C.

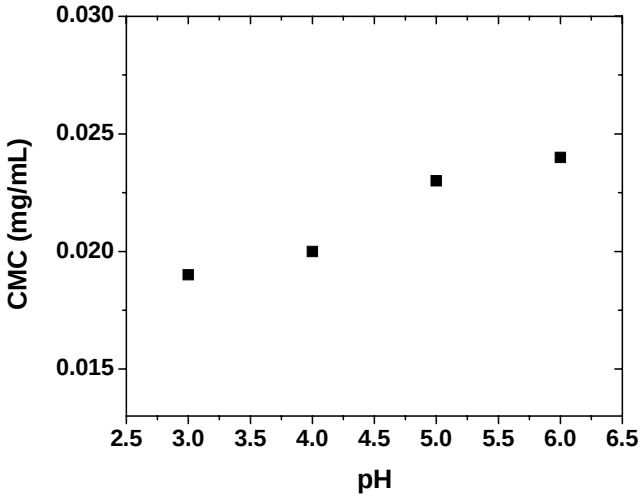

Figure 2.13. The plot of critical micelle concentration (CMC) of P(DEGEA-*co*-AA)-*b*-PEO-*b*-P(DEGEA-*co*-AA) at the sol-gel transition temperature of 10.0 wt% polymer solution versus pH.

LCST transition of P(DEGEA-*co*-AA) blocks at higher pH values. The plateau moduli G_N of the gels at three normalized temperature ($T/T_{sol\text{-}gel}$ = 1.025, 1.032, and 1.039) decreased with the increase of pH with the largest changes observed at pH = ~ 4.7; accordingly, the percentages of elastically active polymer chains, calculated from G_N through $G_N = \upsilon k_B T$, dropped from ~ 90% at pH 3.00 to ~ 25% at pH of 5.23. Above pH5.4, the G_N and the fraction of bridging polymer chains leveled off. Decreasing the pH gave a pH dependence of G_N similar to that in the process of increasing pH, but the value of G_N at a particular pH appeared to be slightly lower. This is believed to result from the dilution of the polymer solution and the formation of KCl in the process of changing the solution pH. The reduction of the number density of bridging polymer chains at a higher pH was undoubtedly accompanied by the increase of number of non-bridging chains (loops and dangling polymer chains). With the increase of pH, the carboxylic acid groups on the polymer chains were ionized and the polymer became more hydrophilic. The charge-charge interaction in the micellar core could cause the core to be larger, which could facilitate the loop formation. The increase in the number of dangling polymer chains with the increase of pH was supported by the results from fluorescence spectroscopy studies, which showed that the CMC of P(DEGEA-*co*-AA)-*b*-PEO-*b*-P(DEGEA-*co*-AA) at a temperature corresponding to $T_{sol\text{-}gel}$ increased with the increase of pH. The results reported in this article showed that both the sol-gel transition temperature and gel strength can be tuned by varying the solution pH.[65] Consider that the type and amount of weak acid or base groups on thermosensitive end blocks can be easily changed, this type of doubly responsive ABA triblock copolymers could offer greater design flexibility for many potential applications.

References

1. Hamley, I. W. *Block Copolymers in Solution: Fundamentals and Applications*, John Wiley & Sons: Chichester, 2005.
2. Hamley, I. W. *Phil. Trans. R. Soc. Lond. A* **2001**, *359*, 1017-1044.
3. Hamley, I. W. *The Physics of Block Copolymers*, Oxford University Press: Oxford, 1998.
4. (a) Hvidt, S.; Jørgensen, E. B.; Schillén, K.; Brown, W. *J. Phys. Chem.* **1994**, *98*, 12320-12328. (b) Mortensen, K.; Brown, W.; Norden, B. *Phys. Rev. Lett.* **1992**, *68*, 2340-2343. (c) Mortensen, K. *Europhys. Lett.* **1992**, *19*, 599-604. (d) Alexandridis, P.; Hatton, T. A. *Colloids and Surfaces A: Physicochem. Eng. Aspects* **1995**, *96*, 1-46. (e) Wanka, G.; Hoffmann, H.; Ulbricht, W. *Macromolecules* **1994**, *27*, 4145-4159. (f) Zhou, Z; Chu, B. *Macromolecules* **1994**, *27*, 2025-2033. (g) Mortensen, K.; Brown, W.; Jørgensen, E. *Macromolecules* **1994**, *27*, 5654. (h) Kirkland-York, S.; Gallow, K.; Loo, Y.-L.; McCormick, C. *Soft Matter* **2009**, *5*, 2179-2182.
5. (a) Li, C.; Tang, Y.; Armes, S. P.; Morris, C. J.; Rose, S. F.; Lloyd, A. W.; Lewis, A. L. *Biomacromolecules* **2005**, *6*, 994-999. (b) Li, C.; Buurma, N. J.; Haq, I.; Turner, C.; Armes, S. P. *Langmuir* **2005**, *21*, 11026-11033.
6. (a) Mortensen, K.; Brown, W.; Jørgensen, E. *Macromolecules* **1994**, *27*, 5654-5666. (b) Hietala, S.; Nuopponen, M.; Kalliomäki, K.; Tenhu, H. *Macromolecules* **2008**, *41*, 2627-2631.
7. Kirkland, S. E.; Hensarling, R. M.; McConaught, S. D.; Guo, Y.; Jarrett, W. L.; McCormick, C. L. *Biomacromolecules* **2008**, *9*, 481-486.
8. Gil, E. S.; Hudson, S. M. *Prog. Polym. Sci.* **2004**, *29*, 1173-1222.

9. He, C. L.; Kim, S. W.; Lee, D. S. *J. Controlled Release* **2008**, *127*, 189-207.

10. Jeong, B.; Kim, S. W.; Bae, Y. H. *Adv. Drug Delivery Rev.* **2002**, *54*, 37-51.

11. Joo, M. K.; Park, M. H.; Choi, B. G.; Jeong, B. *J. Mater. Chem.* **2009**, *19*, 5891-5905.

12. Jiang, X. G.; Jin, S.; Zhong, Q. X.; Dadmun, M. D.; Zhao, B. *Macromolecules* **2009**, *42*, 8648-9476.

13. Woodcock, J. W.; Roger, R. A. E.; Jiang, X. G.; O'Lenick, T. G.; Zhao, B. *Soft Matter* **2010**, *6*, 3325-3336.

14. Sun, K. H.; Sohn, Y. S.; Jeong, B. *Biomacromolecules* **2006**, *7*, 2871-2848.

15. Li, C.; Madsen, J.; Armes, S. P.; Lewis, A. L. *Angew. Chem. Int. Ed.* **2006**, *45*, 3510-3513.

16. Vogt, A. P.; Sumerlin, B. S. *Soft Mater* **2009**, *5*, 2347-2351.

17. Anderson, B. C.; Cox, S. M.; Bloom, P. D.; Sheares, V. V.; Mallapragada, S. K. *Macromolecules* **2003**, *36*, 1670-1676.

18. Determan, M. D.; Cox, J. P.; Seifert, S.; Thiyagarajan, P.; Mallapragada, S. K. *Polymer* **2005**, *46*, 6933-6946.

19. Determan, M. D.; Guo, L.; Thiyagarajan, P.; Mallapragada, S. K. *Langmuir* **2006**, *22*, 1469-1473.

20. Shim, W. S.; Yoo, J. S.; Bae, Y. H.; Lee, D. S. *Biomacromolecules* **2005**, *6*, 2930-2934.

21. Shim, W. S.; Kim, S. W.; Lee, D. S. *Biomacromolecules* **2006**, *7*, 1935-1941.

22. Shim, W.S.; Kim, J. H.; Park, H.; Kim, K.; Kwon, I. C.; Lee, D. S. *Biomaterials* **2006**, *27*, 5178-5185.

23. Dayananda, K.; Pi, B. S.; Kim, B. S.; Park, T. G.; Lee, D. S. *Polymer* **2007**, *48*, 758-762.

24. Park, S. Y.; Lee, Y.; Bae, K. H.; Ahn, C. H.; Park, T. G. *Macromol. Rapid Commun.* **2007**, *28*, 1172-1176.

25. Suh, J. M.; Bae, S. J.; Jeong, B. *Adv. Mater.* **2005**, *17*, 118-120.

26. Dayananda, K.; He, C. L.; Park, D. K.; Park, T. G.; Lee, D. S. *Polymer* **2008**, *49*, 4968-4973.

27. Huynh, D. P.; Nguyen, M. K.; Kim, B. S.; Lee, D. S. *Polymer* **2009**, *50*, 2565-2571.

28. O'Lenick, T. G.; Jiang, X. G.; Zhao, B. *Langmuir* **2010**, *26*, 8787-8796.

29. Jiang, X. G.; Zhao, B. *Macromolecules* **2008**, *41*, 9366-9375.

30. Aoshima, S.; Kanaoka, S. *Adv. Polym. Sci.* **2008**, *210*, 169-208.

31. (a) Han, S.; Hagiwara, M.; Ishizone, T. *Macromolecules* **2003**, *36*, 8312-8319. (b) Ishizone, T.; Seki, A.; Hagiwara, M.; Han, S.; Yokoyama, H.; Oyane, A.; Deffieux, A.; Carlotti, S. *Macromolecules* **2008**, *41*, 2963-2967.

32. Lutz, J.-F.; Hoth, A. *Macromolecules* **2006**, *39*, 893-896.

33. Lutz, J. F.; Weichenhan, K.; Akdemir, O.; Hoth, A. *Macromolecules* **2007**, *40*, 2503-2508.

34. Lutz, J. F.; Andrieu, J.; Üzgün, S.; Rudolph, C.; Agarwal, S. *Macromolecules* **2007**, *40*, 8540-8543.

35. O'Lenick, T. G.; Jiang, X. M.; Zhao, B. *Polymer* **2009**, *50*, 4363-4371.

36. Allcock, H. R.; Dudley, G. K. *Macromolecules* **1996**, *29*, 1313-1319.

37. Chang, Y.; Powell, E. S.; Allcock, H. R.; Park, S. M.; Kim, C. *Macromolecules* **2003**, *36*, 2568-2570.

38. (a) Zhao, B.; Li, D. J.; Hua, F. J.; Green, D. R. *Macromolecules* **2005**, *38*, 9509-9517. (b) Hua, F. J.; Jiang, X. G.; Li, D. J.; Zhao, B. *J. Polym. Sci. Part A: Polym. Chem.* **2006**, *44*, 2454-2467. (c) Hua, F. J.; Jiang, X. G.; Zhao, B. *Macromolecules* **2006,** *39,* 3476-3479. (d) Jiang, X. G., Lavender, C. A.; Woodcock, J. W.; Zhao, B. *Macromolecules* **2008**, *41*, 2632-2643.

39. Aathimanikandan, S. V.; Savariar, E. N.; Thayumanavan, S. *J. Am. Chem. Soc.* **2005**, *127*, 14922-14929.

40. Li, D. J.; Jones, G. L.; Dunlap, J. R.; Hua, F. J.; Zhao, B. *Langmuir* **2006**, 22, 3344-3351.

41. Li, D. J.; Zhao, B. *Langmuir* **2007**, *23*, 2208-2217.

42. Jiang, X. G.; Zhao, B. *J. Polym. Sci. Part A: Polym. Chem.* **2007**, *45*, 3707-3721.

43. Li, D. J.; Dunlap, J. R.; Zhao, B. *Langmuir* **2008**, 24, 5911-5918.

44. Yamamoto, S.-I.; Pietrasik, J.; Matyjaszewski, K. *J. Polym. Sci. Part A: Polym. Chem.* **2008**, *46*, 194-202.

45. Wang, N.; Dong, A.; Radosz, M.; Shen, Y. Q. *J. Biomed. Mater. Res. Part A*. **2008**, *84A*, 148-157.

46. Jiang, X. M.; Wang, B. B.; Li, C. Y.; Zhao, B. *J. Polym. Sci. Part A: Polym. Chem.*, **2009**, *47*, 2853-2870.

47. Fechler, N.; Badi, N.; Schade, K.; Pfeifer, S.; Lutz, J.-F. *Macromolecules* **2009**, *42*, 33-36.

48. Badi, N.; Lutz, J.-F. *J. Controlled Release* **2009**, *140*, 224-229.

49. Qiao, Z.-Y.; Du, F.-S.; Zhang, R.; Liang, D.-H.; Li, Z.-C. *Macromolecules* **2010**, *43*, 6485-6494.

50. Yin, X.; Hoffman, A. S.; Stayton, P. S. *Biomacromolecules* **2006**, *7*, 1381-1385.

51. Feil, H.; Bae, Y. H.; Feijen, J.; Kim, S. W. *Macromolecules* **1992**, *25*, 5528-5530.

52. Feil, H.; Bae, Y. H.; Feijen, J.; Kim, S. W. *Macromolecules* **1993**, *26*, 2496-2500.

53. Bulmus, V.; Ding, Z.; Long, C. J.; Stayton, P. S.; Hoffman, A. S. *Bioconjugate Chem.* **2000**, *11*, 78-83.

54. Olea, A. F.; Thomas, J. K. *Macromolecules* **1989**, *22*, 1165-1169.

55. Zhou, S. Q.; Chu, B. *J. Phys. Chem. B.* **1998**, *102*, 1364-1371.

56. Lokitz, B. S.; York, A. W.; Stempka, J. E.; Treat, N. D.; Li, Y.; Jarrett, W. L.; McCormick, C. L. *Macromolecules* **2007**, *40*, 6473-6480.

57. Yamamoto, S.-I.; Pietrasik, J.; Matyjaszewski, K. *Macromolecules* **2008**, *41*, 7013-7020.

58. Jones, J. A.; Novo, N.; Flagler, K.; Pagnucco, C. D.; Carew, S.; Cheong, C.; Kong, X. Z.; Burke, N. A. D.; Stöver, H. D. H. *J. Polym. Sci. Part A: Polym. Chem.* **2005**, *43*, 6095-6104.

59. Luo, C. H.; Liu, Y.; Li, Z. B. *Macromolecules* **2010**, *43*, 8101-8108.

60. Noro, A.; Matshushita, Y.; Lodge, T. P. *Macromolecules* **2009**, *42*, 5802-5810.

61. (a) He. Y. Y.; Lodge, T. P. *Chem. Commun.* **2007**, 2732-2734. (b) He, Y. Y.; Boswell, P. G.; Bühlmann, P.; Lodge, T. P. *J. Phys. Chem. B.* **2007**, *111*, 4645-4652. (c) He, Y. Y.; Lodge, T. P. *Macromolecules* **2008**, *41*, 167-174.

62. (a) Ferry, J. D. *Viscoelastic Properties of Polymers*, 3rd ed., Wiley: New York, 1980. (b) Larson, R. G.; Sridhar, T.; Leal, L. G.; McKinley, G. H.; Likhtman, A. E.; McLeish, T. C. B. *J. Pheol.* **2003**, *47*, 809-818. (c) Yoshida, T.; Kanaoka, S.;

Watanabe, H.; Aoshima, A. *J. Polym. Sci. Part A: Polym. Chem.* **2005**, *43*, 2712-2722.

63. The data are included in Appendix B.

64. Urry, D. W. *J. Phys. Chem. B* **1997**, *101*, 11007-11028.

65. The work presented in this Chapter has been accepted for publication in *J. Phys. Chem. B.* as an article (manuscript ID: jp-2011-001332).

Chapter 3. Catalytic Activity of a Thermosensitive Hydrophilic Diblock Copolymer-Supported 4-*N*,*N*-Dialkylaminopyridine in Hydrolysis of *p*-Nitrophenyl Acetate in Aqueous Buffers

Abstract

This chapter presents the synthesis of a thermosensitive hydrophilic diblock copolymer with the thermosensitive block containing a catalytic 4-*N*,*N*-dialkylaminopyridine and the study of the effect of thermo-induced micellization on its catalytic activity in the hydrolysis of *p*-nitrophenyl acetate (NPA). The block copolymer, poly(ethylene oxide)-*b*-poly(methoxydi(ethylene glycol) methacrylate-*co*-2-(*N*-methyl-*N*-(4-pyridyl)amino)ethyl methacrylate), was synthesized by ATRP. The critical micellization temperatures (CMTs) of this block copolymer in the pH 7.06 and 7.56 buffers were 40 and 37 ^{o}C, respectively. The polymer was used as the catalyst for the hydrolysis of NPA. We found that below CMT, the logarithm of initial hydrolysis rate changed linearly with inverse temperature. With the increase of temperature above CMT, the plot of logarithm of reaction rate versus 1/T leveled off, i.e., the hydrolysis rate did not increase as much as anticipated from the Arrhenius equation. This is likely because the reaction rate at temperatures above CMT was controlled by mass transport of NPA from bulk water phase to the core of micelles where the catalytic sites were located.

3.1 Introduction

Polymer-supported organic catalysts have been a subject of intensive research in the past decades.[1-3] In addition to offering the advantages of facile recovery and reuse of the catalysts, polymers create a distinct microenviroment, which can be tailored by varying polymer structures, allowing the tuning of catalytic activities of supported catalysts and the control of the compatibility between different types of catalytic groups.[1-22] Of great interest are stimuli-responsive polymer catalysts, which exhibit tunable or switchable catalytic activities in response to environmental stimuli.[23-25] These catalysts are highly desired for many applications as the reaction rates can be conveniently controlled by environmental stimuli. Up to date, there are only a few examples of such polymer organocatalysts in the literature. Tanaka and coworkers reported an imidazole-containing polymer gel consisting of *N*-isopropylacrylamide (NIPAm), 4(5)-vinylimidazole, and a crosslinker.[23] The gel can undergo reversible swelling and shrinking in response to the composition changes of the mixed solvent of water and methanol. They observed that when the gel collapsed, the catalytic activity for esterolysis was dramatically enhanced, which was believed to result from the increased affinity of the substrate to the collapsed hydrophobic network. Khokhlov et al. synthesized thermosensitive random copolymers of 1-vinylimidazole and *N*-vinylcaprolactam or NIPAm, and found that above the lower critical solution temperatures (LCSTs) of the copolymers, the hydrolysis rates of an activated ester were higher than predicted from the Arrhenius equation, presumably because both the substrate and the catalytic imidazole units were enriched at the interface of polymer aggregates.[24]. The observed effect was larger for the copolymer of NIPAm and 1-vinylimidazole than for the copolymer of *N*-vinylcaprolactam and 1-

vinylimidazole. With further increasing temperature, the aggregates became unstable and the activities decreased appreciably.

Compared with thermosensitive catalyst-containing random copolymers, which form unstable large aggregates at temperatures above the LCSTs, block copolymers are more advantageous for developing polymer catalysts with tunable or switchable activities as they can self-assemble into well-defined stable micelles upon application of external stimuli. Patrickios et al. synthesized poly(2-(*N*,*N*-dimethylamino)ethyl methacrylate)-*b*-poly(2-(1-imidazolyl)ethyl methacrylate) (PMAEMA-*b*-PImEMA) by group transfer polymerization.[26-28] Different from their original speculation that the micellization of block copolymers with PImEMA forming the core would accelerate the reaction, they did not observe enhanced catalytic activities of the block copolymers compared with the random copolymers, likely because the hydrophobicity of short PImEMA blocks was not sufficient for extensive micellization. Using reversible addition-fragmentation chain transfer polymerization, Liu et al. synthesized doubly hydrophilic thermosensitive diblock copolymers, PNIPAm-*b*-poly(*N*-vinylimidazole), which self-assembled into micelles with the PNIPAm block forming the core and the catalytic block forming the corona at elevated temperatures.[25] They found that the esterolysis rates were enhanced pronouncedly at temperatures above the critical micellization temperatures (CMTs).

Despite these efforts, the issue, how the micellization affects the catalytic activity of a stimulus-responsive block copolymer with an organic catalyst being incorporated into the core-forming block, has not been elucidated. Understanding this issue will enable a rational design of stimuli-responsive polymeric catalysts. One can envision that if the partition coefficient of the substrate between micelles and bulk water phase is sufficiently

high, it could be concentrated in the core of micelles, resulting in a higher reaction rate. On the other hand, the formation of micelles with the catalyst buried inside the core could impose a mass transport limitation, which might suppress the reaction rate. In the present work, we synthesized a thermosensitive hydrophilic diblock copolymer with the thermosensitive block containing catalytic 4-*N*,*N*-dialkylaminopyridine (DAAP) units and studied the effect of thermo-induced micellization of the block copolymer on the hydrolysis rate of *p*-nitrophenyl acetate (NPA), an activated ester, in aqueous buffers. DAAPs are highly efficient nucleophilic catalysts for many organic reactions, including acylation of sterically hindered alcohols, hydrolysis of activated esters, and Baylis-Hillman reaction.[6-22,29-32] Scheme 3.1 illustrates the synthesis of block copolymer poly(ethylene oxide)-*b*-poly(methoxydi(ethylene glycol) methacrylate-*co*-2-(*N*-methyl-*N*-(4-pyridyl)amino)ethyl methacrylate) (PEO-*b*-P(DEGMMA-*co*-MAPMA) from a PEO macroinitiator by atom transfer radical polymerization (ATRP). PDEGMMA is a thermosensitive water-soluble polymer with a LCST of 25 ^{o}C in water; it belongs to a new family of thermosensitive hydrophilic polymers that contain a short oligo(ethylene glycol) pendant in each monomer unit.[33-42] The thermo-induced micellization of the block copolymer in aqueous buffers (Scheme 3.2) was studied by dynamic light scattering. The block copolymer was then used as catalyst for the hydrolysis of NPA at various temperatures from below to above the CMT and the hydrolysis rates of NPA were measured by UV-vis spectrometry.

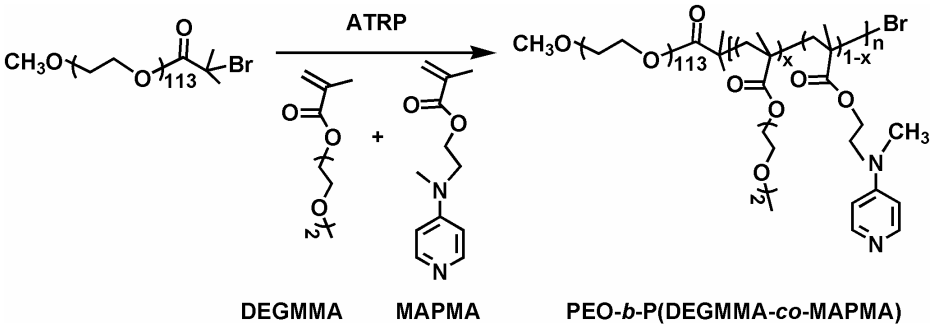

Scheme 3.1. Synthesis of Thermosensitive Block Copolymer PEO-*b*-P(DEGMMA-*co*-MAPMA) with the Thermosensitive Block Containing a Catalytic 4-*N*,*N*-Dialkylaminopyridine by Atom Transfer Radical Polymerization.

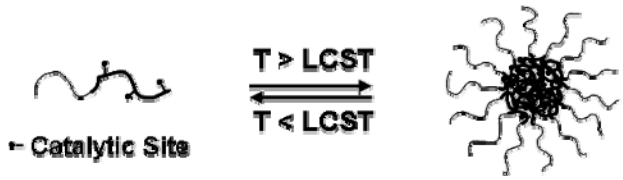

Scheme 3.2. Thermo-Induced Micellization of PEO-*b*-P(DEGMMA-*co*-MAPMA) in an Aqueous Buffer.

3.2. Experimental Section

3.2.1 Materials

Methoxydi(ethylene glycol) methacrylate (DEGMMA, or di(ethylene glycol) methyl ether methacrylate, 95%, Aldrich) was dried with calcium hydride, distilled under a reduced pressure, and stored in a refrigerator prior to use. CuCl (99.995%, Aldrich) was purified according to the procedure described in the literature[43-45] and stored in a desiccator. $CuCl_2$ (anhydrous, 99%), *p*-nitrophenyl acetate (NPA, 97%), acetonitrile (99.5%), *N*,*N*-dimethylformamide (extra dry, with molecular sieves), and sodium tetraborate decahydrate were purchased from Acros and used as received. Potassium dihydrogen phosphate (≥ 99%) and 1,1,4,7,10,10-hexamethyltriethylenetetramine (97%) were obtained from Aldrich-Sigma and used as received. Ethyl 2-bromoisobutyrate (98%, Aldrich) was dried over calcium hydride, distilled under a reduced pressure, and stored in a desiccator prior to use. The synthesis and characterization of 4-(*N*-methyl-*N*-(2-hydroxyethyl)amino)pyridine, 2-(*N*-methyl-*N*-(4-pyridyl)amino)ethyl methacrylate (MAPMA), and macroinitiator PEO-Br (PEO with molecular weight of 5000 Da and one end functionalized with an ATRP initiator) can be found in previous publications.[31,32,46,47]

3.2.2 Characterization

Size exclusion chromatography (SEC) was carried out at ambient temperature using PL-GPC 50 Plus (an integrated GPC/SEC system from Polymer Laboratories, Inc) with a differential refractive index detector, one PSS GRAL guard column (50 × 8 mm, 10 micron particles, Polymer Standards Service-USA, Inc.), and two PSS GRAL linear columns (each 300 × 8 mm, 10 micron, molecular weight range from 500 to 1,000,000 according to Polymer Standards Service-USA, Inc.). The data were processed using

Cirrus™ GPC/SEC software (Polymer Laboratories, Inc.). *N,N*-Dimethylformamide (DMF) was used as the carrier solvent at a flow rate of 1.0 mL/min. Standard monodisperse polystyrenes (Polymer Laboratories, Inc.) were used for calibration. ^{1}H NMR (300 MHz) spectra were recorded on a Varian Mercury 300 NMR spectrometer and the residual solvent proton signal was used as the internal standard.

The cloud points of poly(methoxydi(ethylene glycol) methacrylate-*co*-2-(*N*-methyl-*N*-(4-pyridyl)amino)ethyl methacrylate) (P(DEGMMA-*co*-MAPMA)) in 10 mM aqueous phosphate buffers with pH values of 7.06 and 7.56 at a concentration of 0.020 wt% were measured by turbidimetry. The optical transmittances of polymer solutions at various temperatures were recorded at wavelength of 500 nm with a UV-vis spectrometer (Biomate 5 from Thermospectronic, Inc.). The sample cell was thermostated with an external water bath of a Fisher Scientific Isotemp refrigerated circulator. At each temperature, the solutions were equilibrated for 5 min.

3.2.3. Synthesis of PEO-*b*-P(DEGMMA-*co*-MAPMA)

Copper (I) chloride (4.9 mg, 4.9×10^{-5} mol), copper (II) chloride (2.9 mg, 2.2×10^{-5} mol), macroinitiator PEO-Br (223.6 mg, 4.34×10^{-5} mol), DEGMMA (1.005 g, 5.34 mmol), MAPMA (82.7 mg of a 53.0 wt % solution of MAPMA in DMF, 43.8 mg MAPMA, 1.99×10^{-4} mol), and DMF (1.004 g) were added into a two-necked flask. The reaction mixture was stirred under a dry nitrogen atmosphere. 1,1,4,7,10,10-Hexamethyltriethylenetetramine (HMTETA, 16.2 mg, 7.03×10^{-5} mol) was injected via a microsyringe; the solution turned light green immediately. After the reaction mixture was degassed by three freeze-pump-thaw cycles, the flask was placed in a 75 ^{o}C oil bath. The polymerization was stopped after 156 min by removing the flask from the oil bath and

opening it to air. The mixture was diluted with THF and passed through a short neutral aluminum oxide/silica gel column to remove the copper catalyst. The polymer was precipitated in hexanes three times from its THF solution. The polymer was then dissolved in THF and the solution was stored in a refrigerator (temperature: ~ 4 ^{o}C). The precipitate was removed by filtration. The solution was then concentrated and precipitated in a mixture of hexanes/diethyl either (v/v : 50/50). After being dried in high vacuum, the block copolymer was obtained as a very viscous liquid (0.696 g). SEC analysis results (polystyrene standards): $M_{n,SEC}$ = 26600 Da, polydispersity index (PDI) = 1.12. The numbers of DEGMMA and MAPMA units in the block copolymer were calculated from the ^{1}H NMR spectrum using the integral values of the peak at 8.2 ppm (N(C*H*CH)$_2$ of MAPMA units), the peaks from 3.9 to 4.5 ppm (C*H*$_2$OCO of DEGMMA and MAPMA units), and the peaks from 3.0 to 3.9 ppm (OC*H*$_2$ from the PEO block and DEGMMA units plus CH_2OCH_3 of DEGMMA units and the C-N(C*H*$_3$)C*H*$_2$ of MAPMA units). The numbers of DEGMMA (n_{DEGMMA}) and MAPMA units (n_{MAPMA}) in the block copolymer were 117 and 3, respectively. A random copolymer P(DEGMMA-*co*-MAPMA) was prepared by ATRP using ethyl 2-bromoisobutyrate as initiator under the same conditions for the synthesis of PEO-*b*-P(DEGMMA-*co*-MAPMA). $M_{n,SEC}$ = 19100 Da, PDI = 1.11, n_{DEGMMA} = 92 and n_{MAPMA} = 3.

3.2.4 Determination of pK_a of the MAPMA Units in PEO-*b*-P(DEGMMA-*co*-MAPMA)

A series of 10 mM aqueous buffer solutions were made by dissolving sodium tetraborate decahydrate (borax) or potassium dihydrogen phosphate in deionized water. The pH values of buffer solutions were adjusted by the addition of a 1.0 M NaOH or a

1.0 M HCl solution and measured by a pH meter. To determine the pK_a of the MAPMA units in PEO-*b*-P(DEGMMA-*co*-MAPMA) at room temperature, the UV-vis spectra of the block copolymer in these buffer solutions were recorded at room temperature with a UV-vis spectrometer (Biomate 5 from Thermospectronic, Inc.). A typical UV-vis experiment is described below. A phosphate buffer (pH = 7.14, 1.069 g) was added into a quartz cuvette, followed by the injection of an aqueous polymer solution (24.8 mg, 0.95 wt %) via a microsyringe. The solution was then agitated with a glass pipette. The cuvette was placed into the cell holder of the instrument and the UV-vis spectrum of the block copolymer was recorded. DAAPs are known to exhibit a 20 nm shift in λ_{max} when the basic (B, nonporotonated) and conjugated acid forms (BH^+, protonated) are compared. The absorbances at 280 nm (from protonated MAPMA, BH^+) and 260 nm (from nonprotonated MAPMA, B) were used for the calculation of pK_a.[9] The absorbances of PEO-*b*-P(DEGMMA-*co*-MAPMA) at pH = 1 and 13 were measured from 0.1 N aqueous HCl and 0.1 N NaOH solutions, respectively. A similar procedure was used to measure the pK_a of MAPMA units in PEO-*b*-P(DEGMMA-*co*-MAPMA) at 44 ^oC.

3.2.5 Dynamic Light Scattering Study of Thermo-Induced Micellization of PEO-*b*-P(DEGMMA-*co*-MAPMA) in Aqueous Buffer Solutions

The thermo-induced micellization of PEO-*b*-P(DEGMMA-*co*-MAPMA) in aqueous buffers was studied by dynamic light scattering (DLS). The block copolymer PEO-*b*-P(DEGMMA-*co*-MAPMA) was dried in high vacuum for > 3 h. Aqueous solutions of PEO-*b*-P(DEGMMA-*co*-MAPMA) with a concentration of 0.020 wt % were prepared by use of 10 mM phosphate buffers with pH of 7.06 and 7.56. The polymer solutions were sonicated in an ultrasonic ice/water bath for 5 min to ensure complete dissolution. Note

that in the hydrolysis experiments, a solution of NPA in acetonitrile was injected into the polymer solution via a microsyringe; the concentration of acetonitrile in the final solution was 1.6 wt%. Considering that the LCST transition of the thermosensitive block of PEO-*b*-P(DEGMMA-*co*-MAPMA) could be affected by the presence of a small amount of acetonitrile, we injected a calculated amount of acetonitrile into the polymer solutions for DLS study to ensure that the concentration of acetonitrile was the same as that in the hydrolysis experiments.

DLS measurements were conducted with a Brookhaven Instruments BI-200SM goniometer equipped with a PCI BI-9000AT digital correlator, a temperature controller, and a solid-state laser (model 25-LHP-928-249, λ = 633 nm) at a scattering angle of 90^{o}. The polymer solutions, containing 1.6 wt% acetonitrile, were filtered into borosilicate glass tubes with an inner diameter of 7.5 mm by the use of 0.2 μm filters. The glass tubes were then sealed with a PE stopper. The solutions were gradually heated from room temperature to 50 ^{o}C. At each temperature, the solutions were equilibrated for 30 min prior to data recording. The time correlation functions were analyzed with a Laplace inversion program (CONTIN).

3.2.6 Kinetics Studies of the Hydrolysis of *p*-Nitrophenyl Acetate in Aqueous Buffers Using PEO-*b*-P(DEGMMA-*co*-MAPMA) as Catalyst

The hydrolysis reactions of NPA were performed in 10 mM aqueous phosphate buffer solutions with pH of 7.06 and 7.56. The buffers were made by dissolving KH_2PO_4 in deionized water and the pH values were adjusted by addition of an aqueous NaOH solution and measured with a pH meter (Accumet AB 15 pH meter from Fisher Scientific, calibrated with pH = 4.01, 7.00, and 10.01 standard buffer solutions).

The kinetics studies of the hydrolysis of NPA were conducted in a quartz cuvette using a Hewlett Packard 8542A Diode Array UV-vis spectrophotometer equipped with a Hewlett Packard 89090A Peltier temperature controller. In all hydrolysis experiments, the concentrations of NPA and the MAPMA units of the block copolymer in the reaction medium were 2.9×10^{-4} M and 2.2×10^{-5} M, respectively. The absorbance of the ionized form of the hydrolysis product *p*-nitrophenol at 400 nm was recorded as a function of time by a computer program. A typical procedure for the NPA hydrolysis experiment is described below. A 0.020 wt % solution of PEO-*b*-P(DEGMMA-*co*-MAPMA) in a 10 mM phosphate buffer with pH of 7.06 (1.100 g) was added into a quartz cuvette equipped with a small magnetic stir bar. The cuvette was then placed into the cell holder of the UV-vis spectrometer with a preset temperature. After the solution was equilibrated for 25 min, a background scan was performed to record the absorbance of the polymer solution. A solution of NPA in acetonitrile (17.5 mg, 0.34 wt %) was injected into the cuvette via a microsyringe and the reaction mixture was immediately agitated with a glass pipette for 5 sec. The UV-vis spectra of the reaction mixture were recorded as a function of time by a computer program. The time at which the NPA solution was injected was taken as $t = 0$ sec. The absorbance at 400 nm was plotted vs. time and the initial slope was obtained by linear regression of the first five points. The initial rates of the hydrolysis of NPA were calculated by using equation 1.[24,32]

$$V = \frac{\mathrm{d}A_{400}}{\mathrm{d}t} \frac{1}{\varepsilon b} \frac{1}{f} \qquad (1)$$

where $\mathrm{d}A_{400}/\mathrm{d}t$ is the initial slope of the variation of the absorbance at 400 nm (A_{400}) with time, ε is the extinction coefficient of ionized *p*-nitrophenol, b is the optical path length

(1 cm), and f is the fraction of ionized *p*-nitrophenol in the buffer used in the hydrolysis experiment. The product of extinction coefficient ε and fraction of ionized *p*-nitrophenol f is equal to the apparent coefficient ε' of *p*-nitrophenol in a buffer with a specific pH, which can be obtained by using the concentration of *p*-nitrophenol instead of the concentration of ionized *p*-nitrophenol in the calculations. The apparent extinction coefficients ε' (= εf) of *p*-nitrophenol in the pH 7.06 and 7.56 buffers were 9446 and 12025 $Lmol^{-1}cm^{-1}$, respectively, obtained by a method described below. A series of solutions of *p*-nitrophenol with different concentrations were made by the use of a buffer with pH of either 7.06 or 7.56, and their absorbances at 400 nm were recorded with a UV-vis spectrometer. The apparent extinction coefficient was obtained by linear regression of the plot of the absorbance at 400 nm versus nominal concentration of *p*-nitrophenol.

3.3 Results and Discussion

3.3.1 Synthesis of Thermosensitive Hydrophilic Block Copolymer PEO-*b*-P(DEGMMA-*co*-MAPMA) with the Thermosensitive Block Containing a DAAP Catalyst

This work is intended to study the effect of thermo-induced micellization of a hydrophilic block copolymer in aqueous buffers on the catalytic activity of a DAAP catalyst that is incorporated into the thermosensitive block. DAAPs are highly efficient nucleophilic catalysts widely used in many organic reactions including hydrolysis of activated esters.[6-22,29-32] We chose the hydrolysis of *p*-nitrophenyl acetate, an activated ester, in aqueous buffers for studying the catalytic activity of a thermosensitive block

copolymer-supported DAAP catalyst because this reaction proceeds cleanly to yield *p*-nitrophenol via a known pathway (Scheme 3.3) and the reaction can be conveniently followed by UV-vis spectrometry due to the absorbance of ionized *p*-nitrophenol at 400 nm.[9,24,32]

The thermosensitive hydrophilic block copolymer, PEO-*b*-P(DEGMMA-*co*-MAPMA), was synthesized from macroinitiator PEO-Br by ATRP of a mixture of DEGMMA and MAPMA with a molar ratio of 100 : 3.7 at 75 ^{o}C using CuCl/$CuCl_2$/HMTETA as catalytic system in DMF. We used a small amount of MAPMA in the copolymerization for two reasons: (i) it is known that DAAPs are superior nucleophilic organocatalysts for the hydrolysis of *p*-nitrophenyl esters;[6-9] (ii) the incorporation of a small amount of MAPMA into the thermosensitive block will not change the thermosensitive property too much.[32] Size exclusion chromatography analysis of the purified block copolymer showed a monomodal peak with a number average molecular weight $M_{n,SEC}$ of 26600 Da (relative to polystyrene standards) and a polydispersity index of 1.12 (Figure 3.1a). On the basis of the degree of polymerization of the PEO block (DP of PEO block = 113), the numbers of DEGMMA and MAPMA units in the thermosensitive block were calculated from the ^{1}H NMR spectrum (Figure 3.1b) and they were 117 and 3, respectively. The molar ratio of DEGMMA to MAPMA units in the block copolymer (100 : 2.6) is close to the feed ratio in the polymerization mixture (100 : 3.7). For comparison of thermoresponsive properties, a random copolymer of DEGMMA and MAPMA, P(DEGMMA-*co*-MAPMA), was synthesized by ATRP using a small molecule initiator, ethyl 2-bromoisobutyrate, under the same conditions for the synthesis of the block copolymer. The $M_{n,SEC}$ determined by SEC using polystyrene

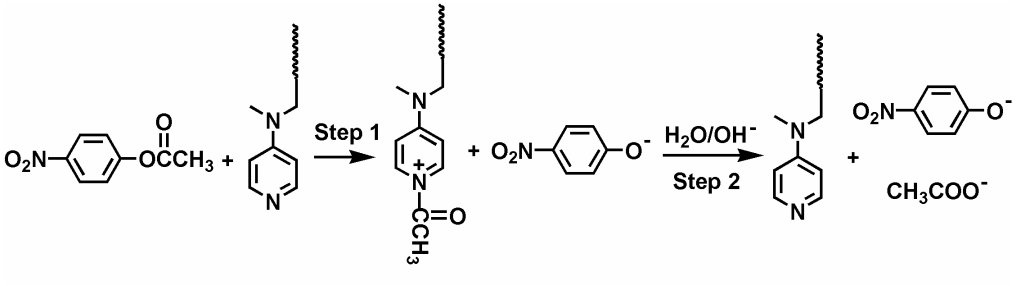

Scheme 3.3. Hydrolysis of *p*-Nitrophenyl Acetate Catalyzed by a *N,N*-Dialkylaminopyridine.

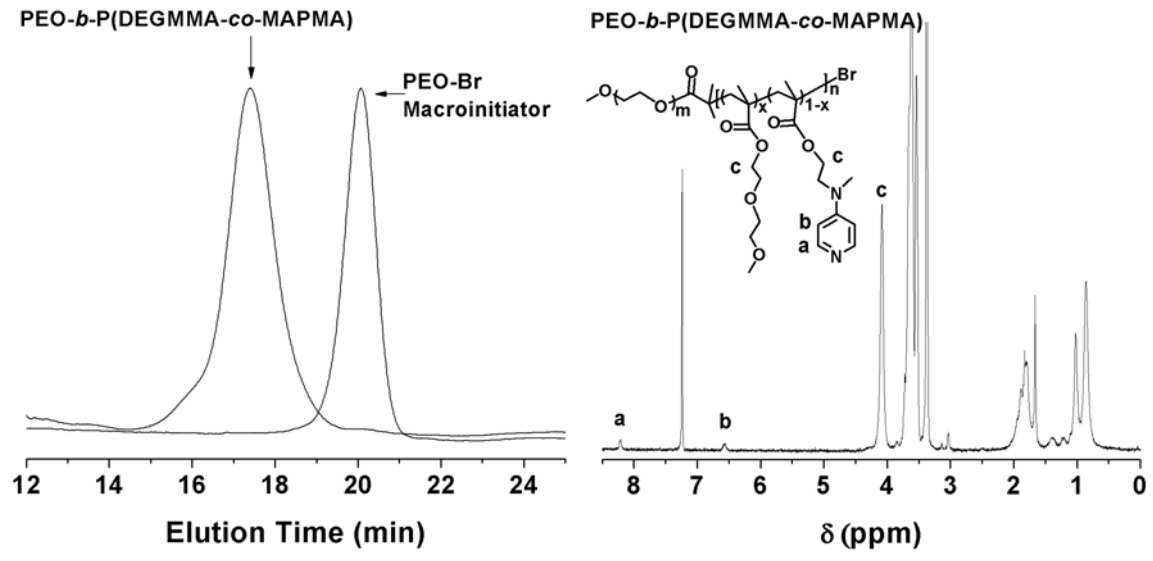

(a) (b)

Figure 3.1. (a) Size exclusion chromatography analysis of macroinitiator PEO-Br and the block copolymer PEO-*b*-P(DEGMMA-*co*-MAPMA), and (b) ^{1}H NMR spectrum of PEO-*b*-P(DEGMMA-*co*-MAPMA) in $CDCl_3$.

calibration is 19100 Da and the PDI is 1.11. The numbers of DEGMMA and MAPMA units in the random copolymer are 92 and 3, respectively.

3.3.2. pK_a of the MAPMA units in Block Copolymer PEO-*b*-P(DEGMMA-*co*-MAPMA)

The hydrolysis rate of an activated ester in an aqueous solution with a DAAP as catalyst is heavily dependent on the concentration of nonprotonated DAAP, which is in turn dependent on the solution pH.[6-9,32] Thus, it is necessary to study its pK_a. The pK_a value of the MAPMA units in PEO-*b*-P(DEGMMA-*co*-MAPMA) was determined spectrophotometrically following a method described in the literature.[9] DAAPs are known to exhibit a 20 nm shift in λ_{max} when the basic (B, nonporotonated) and conjugated acid forms (BH^+, protonated) are compared, the peaks appearing typically at 260 and 280 nm, respectively.[6-9,32] The following equation was used to calculate the molar fraction of nonprotonated DAAP units, x(B), at pH = *p*:[9]

$$x(B) = \frac{[A_{280}/A_{260}]_{pH\ 1} - [A_{280}/A_{260}]_{pH\ p}}{[A_{280}/A_{260}]_{pH\ 1} - [A_{280}/A_{260}]_{pH\ 13}} \qquad (2)$$

where A_{280} and A_{260} are the absorbances at 280 and 260 nm, respectively. The absorbances at pH = 1 and 13 were obtained from the UV-vis spectra of the block copolymer in a 0.1 N aqueous HCl solution and a 0.1 N NaOH solution, respectively. A series of aqueous buffers with salt concentrations of 10 mM and various pH values were prepared and used to make solutions of PEO-*b*-P(DEGMMA-*co*-MAPMA) for UV-vis measurements. The ratio of [B]/[BH^+] at each pH was calculated, and the pK_a value was then determined by the use of Henderson-Hasselbalck equation:

$$pH = pK_a + n \log([B]/[BH^+]) \qquad (3)$$

where n is a measure of deviation from ideal titration behavior.[9,32]

Figure 3.2 shows the plot of log([B]/[BH^+]) versus pH for PEO-*b*-P(DEGMMA-*co*-MAPMA) in aqueous buffers at room temperature. The pK_a of the MAPMA units in the block copolymer, obtained by linear regression (R = 0.999, n = 1.29, Figure 3.2), was 7.91. Our group previously reported that the pK_a of small molecule 4-(*N*-methyl-*N*-(2-hydroxyethyl)amino)pyridine (EGMAP) was 9.31.[32] Note that EGMAP is the precursor for the synthesis of monomer MAPMA. Thus, the pK_a value of the MAPMA units in the block copolymer is 1.40 pH units lower than that of EGMAP, indicating that the incorporation of a DAAP into a polymer has a significant effect on its pK_a value. This observation is consistent with the results reported in the literature for the polymer-supported DAAPs.[6-9,32] Since the molar content of MAPMA units in the thermosensitive block was very small, only 2.5 % (approximately one MAPMA unit every 40 monomer units in the P(DEGMMA-*co*-MAPMA) block), the electrostatic repulsive interaction among protonated DAAP units, which has been used to explain the lower pK_a values of polymer-supported DAAPs,[8] is unlikely the predominant cause of the decreased pK_a value of PEO-*b*-P(DEGMMA-*co*-MAPMA). We believe that the main reason, as discussed by Urry,[48] is that the introduction of charges (protonation of DAAP) onto a thermosensitive water-soluble polymer chain disrupts the "ordered" water structures around the hydrophobic moieties of the thermosensitive block and the charges on the MAPMA units compete with the hydrophobic groups for water molecules for hydration. Thus, to achieve the same degree of protonation of MAPMA units on a thermosensitive polymer chain, a lower solution pH, compared with small molecule EGMAP, is required. Since the nonprotonated DAAP is the actual nucleophilic catalyst, a

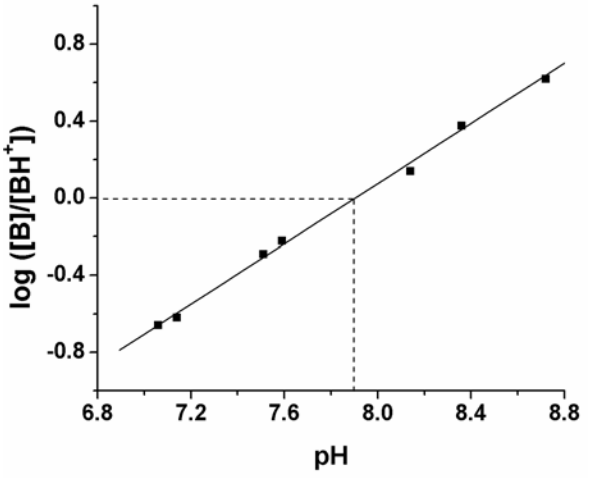

Figure 3.2. Plot of log([B]/[BH^+]) versus pH for the MAPMA units in the block copolymer PEO-*b*-P(DEGMMA-*co*-MAPMA) in aqueous buffers with various pH values at room temperature, where [B] and [BH^+] are the concentrations of nonprotonated and protonated MAPMA units, respectively.

lower pK_a makes the polymer catalyst more attractive than small molecule DAAPs because the reaction can be carried out at a milder pH at a reaction rate that can only be obtained at a higher pH with a small molecule DAAP as catalyst. For the same reason, we chose phosphate buffers with pH of 7.06 and 7.56, which are close to the pK_a of PEO-*b*-P(DEGMMA-*co*-MAPMA), as reaction media for the hydrolysis of NPA with the block copolymer as catalysts.

3.3.3. Cloud Points of Random Copolymer P(DEGMMA-*co*-MAPMA) in Aqueous Phosphate Buffers with pH of 7.06 and 7.56

We first studied the thermosensitive property of a random copolymer of DEGMMA and MAPMA with a similar molar ratio as in the block copolymer. The cloud points (CPs) of P(DEGMMA-*co*-MAPMA) in aqueous phosphate buffers with pH of 7.06 and 7.56 were determined by turbidimetry. Figure 3.3 shows the optical transmittances of 0.020 wt% solutions of P(DEGMMA-*co*-MAPMA) in the two buffers at wavelength of 500 nm as a function of temperature in both heating and cooling processes. The optical transmittance began to decrease at 30 ^{o}C for the pH 7.56 polymer solution and 32.5 ^{o}C for the pH 7.06 solution upon increasing temperature. If 50 % of the transmittance change is used for the determination of CP, the CP of the random copolymer was 34 ^{o}C in the pH 7.06 buffer and 31 ^{o}C in the pH 7.56 aqueous buffer. The cloud point of P(DEGMMA-*co*-MAPMA) in the pH 7.06 buffer is 3 ^{o}C higher than that at pH = 7.56. This is reasonable because at pH = 7.06 more MAPMA units are protonated, making the polymer more hydrophilic, and thus the coil-to-globule transition occurs at a higher temperature. From Figure 3.3, one can also find that for both solutions there was

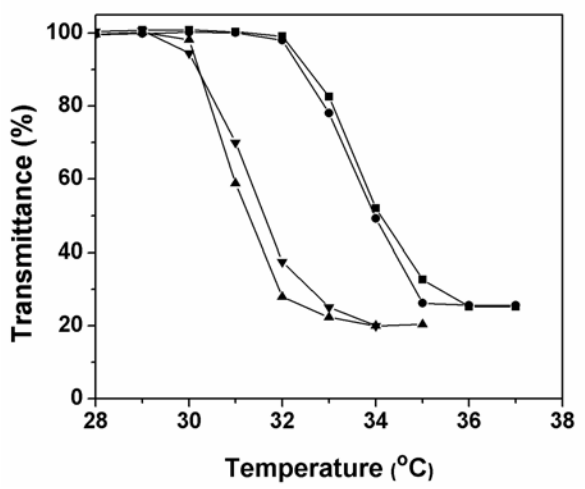

Figure 3.3. Optical transmittance of 0.020 wt% solutions of P(DEGMMA-*co*-MAPMA) in 10 mM phosphate buffers with pH of 7.56 (▲ heating and ▼ cooling) and 7.06 (● heating and ■ cooling) as a function of temperature. The transmittances were recorded at wavelength of 500 nm with a UV-vis spectrometer.

essentially no hysteresis between the heating and cooling processes. The thermo-induced LCST transitions of this random copolymer in the two buffers were reversible.

3.3.4. Thermo-Induced Micellization of PEO-*b*-P(DEGMMA-*co*-MAPMA) in Aqueous Buffer Solutions with pH of 7.06 and 7.56

Dynamic light scattering was employed to study the thermo-induced micellization of PEO-*b*-P(DEGMMA-*co*-MAPMA) in 10 mM phosphate buffers with pH of 7.06 and 7.56, the solutions used as reaction media for the hydrolysis of NPA. The block copolymer concentration in both buffers was 0.020 wt%, same as that in the hydrolysis experiments. It should be noted that in the hydrolysis experiments, NPA was added in the form of its solution in acetonitrile; the final solution contained 1.6 wt% acetonitrile. Since the presence of a small amount of acetonitrile could affect the thermoresponsive properties of the thermosensitive block and thus the CMT of the block copolymer in the aqueous buffers, we added a predetermined amount of acetontrile into the polymer solutions for the DLS experiments such that the acetonitrile concentration was the same as that in the hydrolysis experiments.

Figure 3.4 shows the results from a DLS study of a 0.020 wt% solution of PEO-*b*-P(DEGMMA-*co*-MAPMA) in the pH 7.06 phosphate buffer. When the temperature was below 39 ^{o}C, the scattering intensity was very low and the hydrodynamic size of the block copolymer was small, < 8 nm, suggesting that the block copolymer was molecularly dissolved in the aqueous buffer solution. When the temperature reached 40 ^{o}C, the scattering intensity began to increase and the hydrodynamic size jumped to ~ 80 nm, indicating that the thermosensitive block was undergoing a temperature-induced hydration-dehydration transition. With further increasing the temperature to 41 ^{o}C and

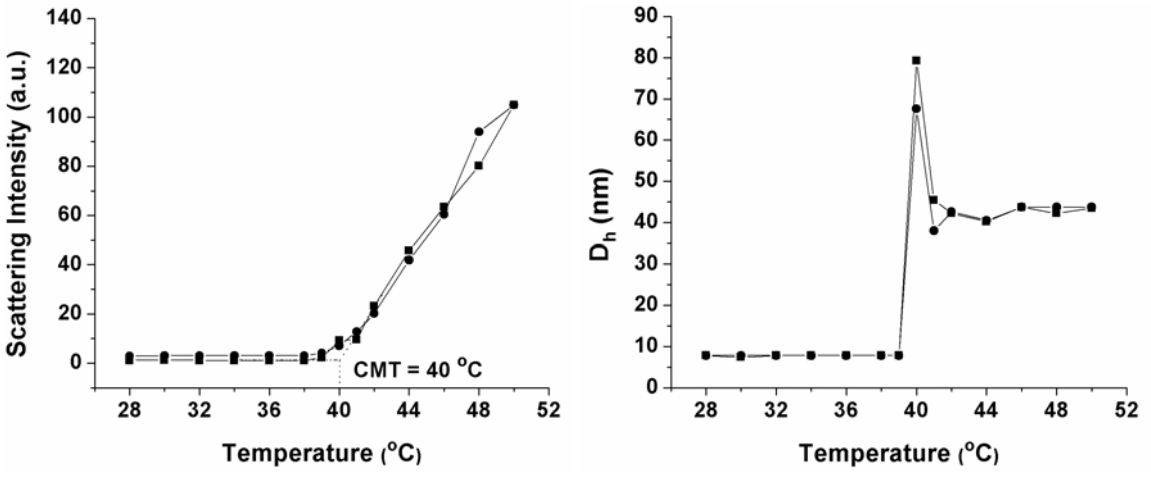

(a) (b)

Figure 3.4. (a) Scattering intensity at the scattering angle of 90° and (b) apparent hydrodynamic diameter, D_h, as a function of temperature, obtained from a dynamic light scattering study of a 0.020 wt% solution of PEO-*b*-P(DEGMMA-*co*-MAPMA) in the pH = 7.06 aqueous phosphate buffer (■ heating; ● cooling).

beyond, the value of D_h became stabilized around 43 nm. The CMT determined from the plot of scattering intensity versus temperature in the heating process is 40 ^oC (Figure 3.4a). The data from the cooling process essentially superimposed the heating curve. When the temperature was decreased to 39 ^oC, the block copolymer micelles dissociated into the unimers.

Figure 3.5 shows the data from a DLS study of a 0.020 wt % solution of PEO-*b*-P(DEGMMA-*co*-MAPMA) in the pH 7.56 buffer. Similar to the observations for the pH 7.06 buffer, the block copolymer self-assembled into micelles with an apparent hydrodynamic diameter of ~ 43 nm when the temperature was higher than 40 ^oC. This thermo-induced micellization was reversible. Decreasing the temperature caused the micelles to dissociate into the unimers (Figure 3.5). The CMT, determined from the heating curve in Figure 3.5a, was 37 ^oC, which is 3 ^oC lower than that in the pH 7.06 buffer, consistent with our observations of the cloud points of random copolymer P(DEGMMA-*co*-MAPMA) in the two buffers. At a lower pH, more MAPMA monomer units were protonated, rendering the thermosensitive block more hydrophilic and thus a higher LCST transition temperature. Calculations show that 82 % of MAPMA units were protonated at pH = 7.06, while 65 % MAPMA units were protonated in the pH 7.56 buffer. Note that the CMT of PEO-*b*-P(DEGMMA-*co*-MAPMA) in each buffer was 6 ^oC higher than the CP of the corresponding random copolymer solution. This is consistent with the observations previously reported by our group.[46,47] It is known that the LCST transition temperature is slightly higher when a thermosensitive polymer is attached to a hydrophilic block.[49-51]

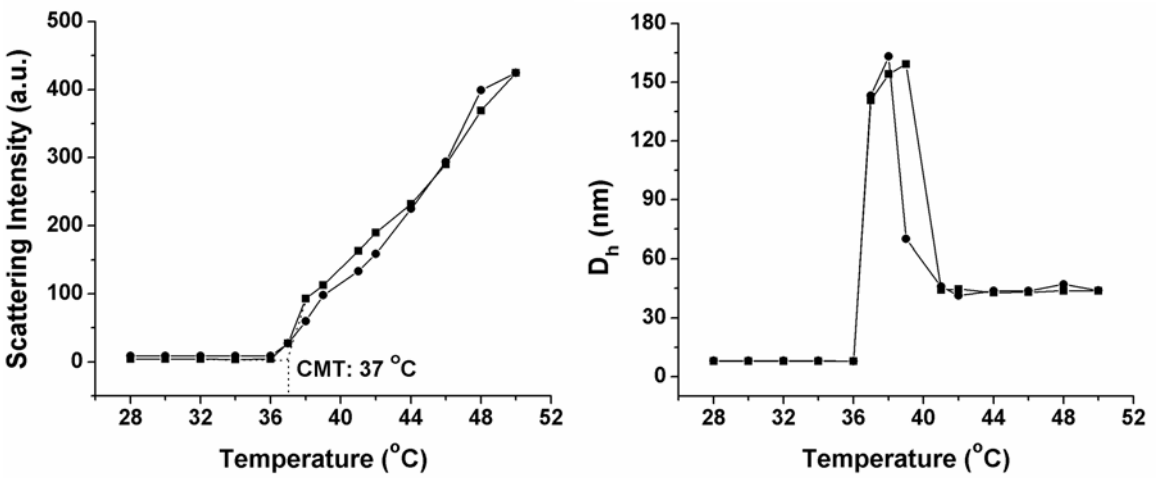

(a) (b)

Figure 3.5. (a) Scattering intensity at the scattering angle of 90° and (b) apparent hydrodynamic diameter, D_h, as a function of temperature, obtained from a dynamic light scattering study of a 0.020 wt% solution of PEO-*b*-P(DEGMMA-*co*-MAPMA) in a pH = 7.56 aqueous buffer solution (■ heating; ● cooling).

3.3.5. Hydrolysis of *p*-Nitrophenyl Acetate with PEO-*b*-P(DEGMMA-*co*-MAPMA) as Catalyst in the pH 7.06 and 7.56 Buffer solutions at Various Temperatures

The hydrolysis reactions of *p*-nitrophenyl acetate with PEO-*b*-P(DEGMMA-*co*-MAPMA) as catalyst were carried out in 10 mM aqueous phosphate buffers with pH of 7.06 and 7.56 under the stirring condition in the temperature range of 30-48 ^{o}C. The reactions were monitored by recording the absorbance at 400 nm (A_{400nm}) as a function of time by a UV-vis spectrometer via a computer program. For all hydrolysis experiments, [NPA] = 2.9×10^{-4} M and [MAPMA] = 2.2×10^{-5} M. Figure 3.6 shows A_{400nm} as a function of time for the hydrolysis of NPA in the pH 7.56 buffer at (a) 30 ^{o}C, which was below the CMT, and (b) 44 ^{o}C, which was above the CMT. Clearly, the absorbance A_{400nm} increased smoothly and, in the beginning, linearly with the increase of time at both temperatures. The initial hydrolysis rate was derived by a linear regression of the first five points and the use of equation (1) as described in the experimental section. Since the buffer might also contribute to the initial rate of the hydrolysis of NPA, we also measured the background rates by performing the reactions at the same conditions except without addition of any DAAP catalyst. We found that the background rate accounted for a small fraction of the total rate, e.g., 5.3 % of the total rate catalyzed by the block copolymer in the pH 7.56 buffer at 30 ^{o}C and 16.5 % at 48 ^{o}C. To better understand the catalytic activity of the block copolymer-supported DAAP catalyst before and after the thermo-induced micellization, we derived the net initial rates of the hydrolysis of NPA by subtracting the corresponding background rates from the overall rates for all temperatures.

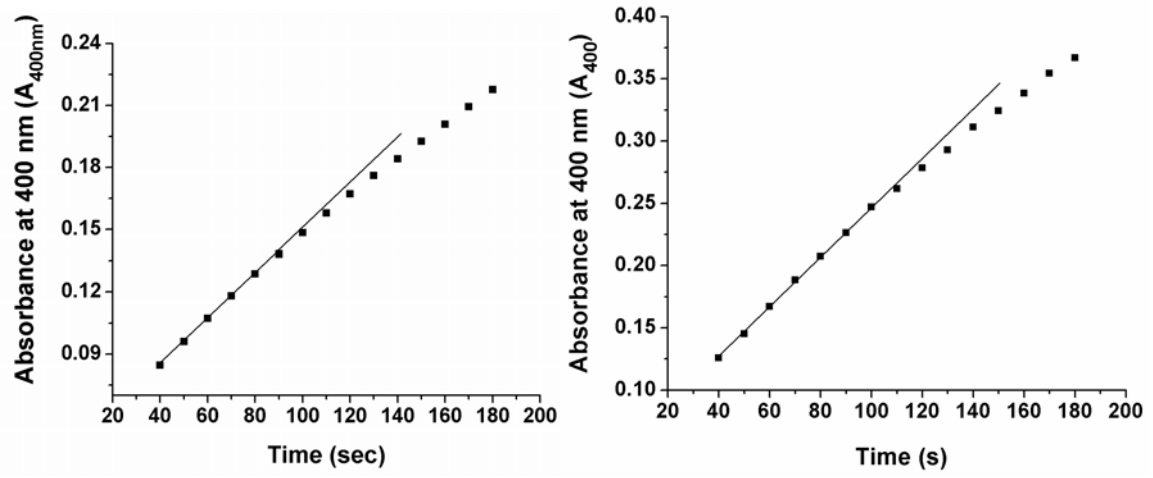

(a) (b)

Figure 3.6. Absorbance at 400 nm (A_{400}) recorded with a UV-vis spectrometer by a computer program as a function of time for the hydrolysis of *p*-nitrophenyl acetate using PEO-*b*-P(DEGMMA-*co*-MAPMA) as catalyst in the pH = 7.56 buffer at (a) 30 ^{o}C, which was below CMT, and (b) 44 ^{o}C, which was above CMT.

The effect of temperature on reaction rate constant is usually expressed by Arrhenius equation, that is, ln*k* changes linearly with inverse temperature 1/T.[24,25,32] Figure 3.7 shows the plots of logarithm of net initial rate (logV) versus 1/T for the hydrolysis of NPA using PEO-*b*-P(DEGMMA-*co*-MAPMA) as catalyst. A linear relationship between logV and 1/T was observed in the range of 30-38 ^{o}C for the reactions in the pH 7.56 buffer and 30-40 ^{o}C for the reactions in the pH 7.06 buffer, indicating that the hydrolysis of NPA with PEO-*b*-P(DEGMMA-*co*-MAPMA) as catalyst in these temperature ranges followed the Arrhenius behavior. The two curves in these ranges were essentially in parallel. From DLS studies, the CMT of PEO-*b*-P(DEGMMA-*co*-MAPMA) was 37 ^{o}C in the pH 7.56 buffer and 40 ^{o}C in the pH 7.06 buffer. Thus, the block copolymer was in the unimer state at these temperatures except 38 ^{o}C in the pH 7.56 buffer.

From Figure 3.7, one can also find that the reaction at any temperature in the pH = 7.56 buffer was consistently faster than that at pH = 7.06. For example, the net initial hydrolysis rate in the pH 7.56 buffer at 30 ^{o}C was 8.4×10^{-8} molL^{-1}sec^{-1}, which was ~ 1.6 times the initial rate in the pH 7.06 buffer at the same temperature (5.1×10^{-8} molL^{-1}sec^{-1}). This is because the concentration of the nonprotonated MAPMA units of the block copolymer in the pH 7.56 buffer was higher than that in the 7.06 buffer. Calculations show that about 35 % of the MAPMA units were in the nonprotonated state in the pH 7.56 buffer while 18 % of the MAPMA units were nonprotonated in the pH 7.06 buffer.

For the reactions in both buffers, the plot of logV versus 1/T did not follow the Arrhenius equation in the entire studied temperature range but leveled off with the increase of temperature above a certain point, i.e., the reaction rate did not increase as

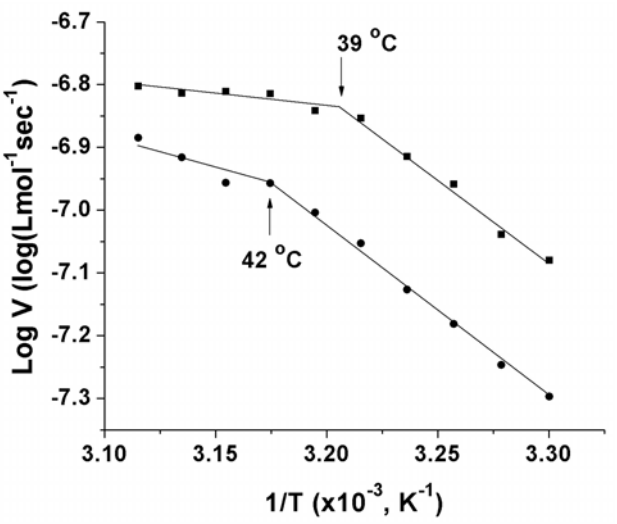

Figure 3.7. Plot of the logarithm of net initial rate (logV) versus 1/T for the hydrolysis of *p*-nitrophenyl acetate catalyzed by PEO-*b*-P(DEGMMA-*co*-MAPMA) in the pH 7.56 buffer (■) and pH 7.06 aqueous buffer (●).

much as anticipated from the Arrhenius equation. For the hydrolysis reactions in the pH 7.56 buffer, the transition temperature was ~ 39 ^{o}C, just above the CMT of the block copolymer in this buffer (37 ^{o}C), while the transition for the reactions in the pH 7.06 buffer occurred at ~ 42 ^{o}C, 2 ^{o}C above the CMT of the block copolymer in this buffer. Clearly, the thermo-induced micellization of PEO-*b*-P(DEGMMA-*co*-MAPMA) exerted an appreciable effect on the hydrolysis rate of NPA; the net initial rate was suppressed by the formation of micelles with the catalyst-containing block P(DEGMMA-*co*-MAPMA) forming the core in the aqueous buffers.

Since the pK_a of MAPMA units in the core of micelles could be different from that in water, we determined its value at 44 ^{o}C by the same method described in the experimental section and found that it was 7.10, slightly lower than that at room temperature (7.91). Thus, the change of the pK_a before and after micellization cannot account for the suppression of the initial hydrolysis rate at temperatures above the CMT because a lower pK_a value means that the fraction of nonprotonated MAPMA units is higher, which should result in a higher reaction rate.

In our hydrolysis experiments, the polymer solution was equilibrated at each temperature for 25 min before the injection of the NPA solution. Thus, at temperatures above the CMT, micelles were already formed and the catalytic MAPMA units were buried inside the core of micelles. Therefore, the initial hydrolysis rate depends on how fast the reactants (NPA and water) can diffuse into the core of micelles. The study by Vaidya and Mathias has established that the first step in the hydrolysis mechanism is the rate-determining step (Scheme 3.3), which involves only NPA and DAAP, and the second step, the deacylation of acylpyridinium species in the presence of water, is the

faster step.[8] In addition, there is a significant amount of water molecules associated with the thermosensitive block even at temperatures above the LCST. Thus, the initial hydrolysis rate or the rate of the formation of *p*-nitrophenoxide is dependent on the diffusion rate of NPA, not water molecules. NPA is an amphiphilic substrate with a partition coefficient of 7.4 between hexane and water (log*P* = 0.87 at 25 ^{o}C) according to the literature.[24] Our thermosensitive block is a polymethacrylate with an oligo(ethylene glycol) pendant from each repeat unit. Considering that its hydrophobicity is much lower than hexane even at temperatures above the LCST, we believe that the partition coefficient of NPA between the core of micelles and bulk water phase should be appreciably lower than 7.4. Thus, NPA is not strongly favored in the core of the micelles compared with the bulk water phase, i.e., the driving force for NPA molecules to diffuse into the core of micelles is not strong. On the other hand, DAAPs are known to be superior nucleophilic organic catalysts for the hydrolysis of activated esters.[6-9] Combining these two factors, it is very likely that the hydrolysis rate of NPA with PEO-*b*-P(DEGMMA-*co*-MAPMA) at temperatures above the CMT is controlled by the diffusion rate of NPA from bulk water phase to the core of micelles. In other words, the reaction rate is determined by the mass transport limitation of NPA from bulk water phase to the core of micelles, which is imposed by the micellization of the block copolymer, resulting in the suppression of reaction rates compared with those predicted from the Arrhenius equation. Thus, the curve of logV versus 1/T leveled off with the increase of temperature.

From Figure 3.7, one can also find that above the transition temperature the magnitude of the slope of the pH 7.56 curve is smaller than that of the pH 7.06 curve, i.e.,

the increase of reaction rate with temperature in the pH 7.56 buffer is more suppressed than that in the pH 7.06 buffer. This is likely because more MAPMA units of the block copolymer are protonated in the pH 7.06 buffer and thus are not active in the catalysis, causing the reaction rate to be more comparable to the diffusion rate of NPA than in the pH 7.56 buffer. In addition, the micelles might not be as tight as those in the pH 7.56 buffer because of more charged MAPMA units in the core; it could be slightly easier for NPA to diffuse into the core of micelles to access the buried catalytic sites.

3.4. Conclusions

A thermosensitive hydrophilic block copolymer with the thermosensitive block containing catalytic DAAP units, PEO-*b*-P(DEGMMA-*co*-MAPMA), was synthesized from macroinitiator PEO-Br by ATRP.[52] The pK_a of the block copolymer at room temperature was 7.91, which was 1.40 pH units lower than that of EGMAP. DLS studies showed that the CMTs of PEO-*b*-P(DEGMMA-*co*-MAPMA) in the pH 7.06 and 7.56 buffers at a concentration of 0.020 wt % were 40 and 37 ^{o}C, respectively. Above 42 ^{o}C, well-defined micelles with the thermosensitive catalytic block forming the core were observed in both buffer solutions. The block copolymer was used as catalyst for the hydrolysis of NPA and the reactions were monitored by a UV-vis spectrometer. We found that the plot of logarithm of net initial hydrolysis rate vs. inverse temperature did not follow the Arrhenius equation in the entire studied temperature range (30-48 ^{o}C), but leveled off with the increase of temperature above the CMT of the block copolymer in the buffer. Considering that NPA molecules must diffuse into the core of micelles and the DAAPs are superior nucleophilic organic catalysts for the hydrolysis of activated esters,

the observed phenomenon is likely because the hydrolysis rate of NPA is controlled by the mass transport limitation of NPA from bulk water phase to the core of micelles. The block copolymer reported in this work represents a new type of stimuli-responsive polymer organocatalysts.

References

1. Benaglia, M.; Puglisi, A.; Cozzi, F. *Chem. Rev.* **2003** *103*, 3401-3429.
2. Bergbreiter, D. E. *Chem. Rev.* **2002**, *102*, 3345-3383.
3. Cozzi, F. *Adv. Synth. Catal.* **2006**, *348*, 1367-1390.
4. Overberger, C. G.; Salamone, J. C. *Acc. Chem. Res.* **1969**, *2*, 217-224.
5. Overberger, C. G.; Stpierre, T.; Vorchhei, N.; Lee, J.; Yaroslav, S. *J. Am. Chem. Soc.* **1965**, *87*, 296-301.
6. Hierl, M. A.; Gamson, E. P.; Klotz, I. M. *J. Am. Chem. Soc.* **1979**, *101*, 6020-6021.
7. Delaney, E. J.; Wood, L. E.; Klotz, I. M. *J. Am. Chem. Soc.* **1982**, *104*, 799-807.
8. Vaidya, R. A.; Mathias, L. J. *J. Am. Chem. Soc.* **1986**, *108*, 5514-5520.
9. Mathias, L. J., Cei, G. *Macromolecules* **1987**, *20*, 2645-2650.
10. Fife, W. K.; Rubinsztajn, S.; Zeldin, M. *J. Am. Chem. Soc.* **1991**, *113*, 8535-8537.
11. Rubinsztajn, S.; Zeldin, M.; Fife, W. K. *Macromolecules* **1991**, *24*, 2682-2688.
12. Wang, G. J.; Ye, D.; Fife, W. K. *J. Am. Chem. Soc.* **1996**, *118*, 12536-12540.
13. Bergbreiter, D. E; Osburn, P. L.; Li, C. M. *Org. Lett.* **2002**, *4*, 737-740.
14. Bergbreiter, D. E.; Li, C. M. *Org. Lett.* **2003**, *5*, 2445-2447.
15. Deratani, A.; Darling, G. D.; Fréchet, J. M. J. *Polymer* **1987**, *28*, 825-830.

16. Deratani, A.; Darling, G. D.; Horak, D.; Fréchet, J. M. J. *Macromolecules* **1987**, *20*, 767-772.

17. Liang, C. O.; Helms, B.; Hawker, C. J.; Fréchet, J. M. J. *Chem. Commun.* **2003**, *20*, 2524-2525.

18. Helms, B.; Liang, C. O.; Hawker, C. J.; Fréchet, J. M. J. *Macromolecules* **2005**, *3*8, 5411-5415.

19. Helms, B.; Guillaudeu, S. J.; Xie, Y.; McMurdo, M.; Hawker, C. J.; Fréchet, J. M. J. *Angew. Chem. Int. Ed.* **2005**, *44*, 6384-6387.

20. Tomoi, M.; Akada, Y.; Kakiuchi, H. *Makromol. Chem. Rapid Commun.* **1982**, *3*, 537-542.

21. Menger, F. M.; McCann, D. J. *J. Org. Chem.* **1985**, *50*, 3928-3930.

22. Huang, J. W.; Shi, M. *Adv. Synth. Catal.* **2003**, *345*, 953-958.

23. Wang, G. Q.; Kuroda, K.; Enoki, T.; Grosberg, A.; Masamune, S.; Oya, T.; Takeoka, Y.; Tanaka, T. *Proc. Natl. Acad. Sci. USA* **2000**, *97*, 9861-9864.

24. Okhapkin, I. M.; Bronstein, L. M.; Makhaeva, E. E.; Matveeva, V. G.; Sulman, E. M.; Sulman, M. G.; Khokhlov, A. R. *Macromolecules* **2004**, *37*, 7879-7883.

25. Ge, Z. S.; Xie, D.; Chen, D. Y.; Jiang, X.; Zhang, Y.; Liu, H.; Liu, S. Y. *Macromolecules* **2007**, *40*, 3538-3546.

26. Simmons, M. R.; Patrickios, C. S. *Macromolecules* **1998**, *31*, 9075-9077.

27. Simmons, M. R.; Patrickios, C. S. *J. Polym. Sci. Part A: Polym. Chem.* **1999**, *37*, 1501-1512.

28. Patrickios, C. S.; Simmons, M. R. *Colloids and Surfaces A: Physiochemical and Engineering Aspects* **2000**, *167*, 61-72.

29. Scriven, E. F. V. *Chem. Soc. Rev.* **1983**, *12*, 129-161.

30. Chen, H. T.; Huh, S.; Wiench, J. W.; Pruski, M.; Lin, V. S. Y. *J. Am. Chem. Soc.* **2005**, *127*, 13305-13311.

31. Zhao, B.; Jiang, X. M.; Li, D. J.; Jiang, X. G.; O'Lenick, T. G.; Li, B.; Li, C. Y. *J. Polym. Sci. Part A: Polym. Chem.* **2008**, *46*, 3438-3446.

32. Jiang, X. M.; Wang, B. B.; Li, C. Y.; Zhao, B. *J. Polym. Sci. Part A: Polym. Chem.* **2009**, *47*, 2853-2870.

33. Han, S.; Hagiwara, M.; Ishizone, T. *Macromolecules* **2003**, *36*, 8312-8319.

34. Aoshima, S.; Sugihara, S. *J. Polym. Sci. Part A: Polym. Chem.* **2000**, *38*, 3962-3965.

35. Li, D. J.; Jones, G. L.; Dunlap, J. R.; Hua, F. J.; Zhao, B. *Langmuir* **2006**, *22*, 3344-3351.

36. Li, D. J.; Zhao, B. *Langmuir* **2007**, *23*, 2208-2217.

37. Zhao, B.; Li, D. J.; Hua, F. J.; Green, D. R. *Macromolecules* **2005**, *38*, 9509-9517.

38. Hua, F. J.; Jiang, X. G.; Li, D. J.; Zhao, B. *J. Polym. Sci. Part A: Polym. Chem.* **2006**, *44*, 2454-2467.

39. Hua, F. J.; Jiang, X. G.; Zhao, B. *Macromolecules* **2006**, *39*, 3476-3479.

40. Jiang, X. G.; Zhao, B. *J. Polym. Sci. Part A: Polym. Chem.* **2007**, *45*, 3707-3721.

41. Lutz JF, Weichenhan K, Akdemir O, Hoth A. Macromolecules 2007;40:2503-2508.

42. Li, D. J.; Dunlap, J. R.; Zhao, B. *Langmuir* **2008**, *24*, 5911-5918.

43. Matyjaszewski, K.; Miller, P. J.; Shukla, N.; Immaraporn, B.; Gelman, A.; Luokala, B. B.; Siclovan, T. M.; Kickelbick, G.; Vallant, T.; Hoffmann, H.; Pakula, T. *Macromolecules* **1999**, *32*, 8716-8724.

44. Miller, P. J.; Matyjaszewski, K. *Macromolecules* **1999**, *32*, 8760-8767.

45. Zhao, B.; He, T. *Macromolecules* **2003**, *36*, 8599-8602.

46. Jiang, X. G.; Lavender, C. A.; Woodcock, J. W.; Zhao, B. *Macromolecules* **2008**, *41*, 2632-2643.

47. Jiang, X. G.; Zhao, B. *Macromolecules* **2008**, *41*, 9366-9375.

48. Urry, D. W. *J. Phys. Chem. B.* **1997**, *101*, 11007-11028.

49. Rijcken, C. J. F.; Soga, O.; Hennink, W. E.; van Nostrum, C. F. J. Controlled Release 2007, 120, 131-148.

50. Dimitrov, I.; Trzebicka, B.; Müller, A. H. E.; Dworak, A.; Tsvetanov, C. B. *Prog. Polym. Sci.* **2007**, *32*, 1275-1343.

51. Gil, E. S.; Hudson, S. M. *Prog. Polym. Sci.* **2004**, *29*, 1173-1222.

52. The work presented in this Chapter has been published in *Polymer* (**2009**, *50*, 4363-4371).

Chapter 4. Summary and Future Work

4.1 Summary

Well-defined thermo- and pH-sensitive hydrophilic ABA triblock and AB diblock copolymers were prepared via the incorporation of a small amount of weak acid or base groups into the thermosensitive block(s) of block copolymers in a random/statistical distribution fashion.[1-3] Compared with the methods reported in the literature for the synthesis of thermo- and pH-sensitive block copolymers (e.g., copolymers made of thermosensitive blocks and pH-responsive blocks),[4-6] our approach allowed the lower critical solution temperature (LCST) of thermosensitive block(s) of block copolymers to be tuned and thus micellization to be precisely controlled by solution pH.

The carboxylic acid-containing ABA triblock copolymers were made by copolymerization of methoxydi(ethylene glycol) methacrylate (DEGMMA) and *tert*-butyl methacrylate (*t*BMA) or ethoxydi(ethylene glycol) acrylate (DEGEA) and *tert*-butyl acrylate (*t*BA) from a difunctional poly(ethylene oxide) (PEO) macroinitiator with a molecular weight of 20000 g/mol via atom transfer radical polymerization and subsequent removal of *tert*-butyl groups using trifluoroacetic acid (TFA).[1,2] The sol-gel transition temperatures ($T_{sol\text{-}gel}$) of moderately concentrated aqueous solutions of these ABA triblock copolymers can be precisely controlled and reversibly tuned over a wide temperature range by changing the solution pH. The tunability of sol-gel transition temperature stemmed from the pH dependence of the LCST of thermosensitive outer blocks of triblock copolymers. The critical micellization temperature (CMT), determined by dynamic light scattering, versus pH curve exhibited the same trend as the $T_{sol\text{-}gel}$ versus pH curve, though there was a shift. We showed that a 12.0 wt % aqueous solution of P(DEGMMA-*co*-methacrylic acid)-*b*-PEO-*b*-P(DEGMMA-*co*-methacrylic acid)

underwent multiple sol-gel-sol transitions in response to environmental variations, demonstrating the possibility of achieving on-demand sol-gel-sol transitions using two external stimuli.

To look into how sol-gel transition and gel property were affected by solution pH, we conducted an in-depth rheological study from which the following conclusions were drawn. (i) The gel was a 3-dimensional micellar network as dynamic strain amplitude sweep tests showed that the gel exhibited a linear response up to at least 15 % strain. (ii) The gel was a physically crosslinked thermoreversible gel with a finite relaxation time. (iii) The sol-gel transition became broader with the increase of pH, which originated from the broader and weaker LCST transitions of thermosensitive blocks at higher pH values. (iv) The gel strength decreased with the increase of pH with the sharpest drop observed at pH = ~ 4.7; accordingly, the percentage of elastically active polymer chains decreased from ~ 90% at pH 3.00 to ~ 25% at pH of 5.23. Above pH 5.4, the gel strength and the fraction of bridging polymer chains leveled off. The decrease of the fraction of bridging polymer chains with the increase of pH was accompanied by the increase in the numbers of loops and dangling chains. This study provides insights into how the gel properties are affected by solution pH, which can be useful for the design of multi-responsive injectable micellar hydrogels for biomedical applications.

In the AB diblock copolymer work,[3] we incorporated a small amount of *N*, *N*-dialkylaminopyridine (DAAP), a weak base and also an organic catalyst, into the thermosensitive block of a PEO-based diblock copolymer and studied how the thermo-induced micellization at two different pH values affected the catalytic activity of DAAP in the hydrolysis of *p*-nitrophenyl acetate (NPA), an activated ester. DLS studies showed

that the CMT of the diblock copolymer was lower when the pH value was higher. The block copolymer was used as catalyst for the hydrolysis of NPA at two different pH values and the reactions were monitored by a UV-vis spectrometer. We found that the plot of logarithm of net initial hydrolysis rate vs. inverse temperature did not follow the Arrhenius equation in the entire studied temperature range (30-48 °C), but leveled off with the increase of temperature above the CMT of the block copolymer in the buffer. This is the first time that the effect of micellization on the catalytic activity of a stimulus-responsive block copolymer with an organic catalyst incorporated into the core-forming block was elucidated, which could be valuable for the design of stimuli-responsive block copolymer catalysts.

A characteristic feature of thermo- and pH-sensitive hydrophilic block copolymers presented in this dissertation is that the LCST of the thermosensitive block(s) is determined by solution pH, allowing us to actively and precisely control the self-assembly of block copolymers in water. The ionization and protonation of weak acid or weak base groups reversibly shifted the hydrophilic-hydrophobic balance of whole thermosensitive blocks, changed the amount of structured water around the hydrophobic moieties of polymer chains, and consequently modified their LCSTs.[7-9] Differential scanning calorimetry analysis of aqueous solutions of a doubly responsive ABA triblock copolymer showed that the LCST transition was an entropically driven process as an endothermic peak appeared in the DSC thermogram.[2] From the results presented in this dissertation, we can conclude that it is a viable approach to design multiresponsive hydrophilic block copolymers by incorporating a small amount of stimuli-sensitive groups into the thermosensitive blocks of block copolymers.

4.2 Future Work

Owing to the in situ sol-gel transitions, stimuli-responsive, especially thermosensitive, block copolymer aqueous micellar gels hold great promise in sustained drug delivery as they can be administered via syringe and needle, a minimally invasive method. Compared with injectable thermosensitive hydrogels that respond to only one external stimulus, thermo- and pH-responsive block copolymer micellar gels offer more advantages and greater design flexibility, e.g., tunable sol-gel transition temperature and gel strength, which are important for controlled release in living systems.

It is known that the diseased tissues exhibited unusual acidic pH values.[10] Thus, to use injectable hydrogels as drug delivery systems to battle certain diseases, we need to employ a weak base with a suitable pK_a for the thermo- and pH-sensitive ABA triblock copolymers, which would allow the drugs loaded into the gels to be released at a greater rate at acidic pH values. Although 2-(*N*-methyl-*N*-(4-pyridyl)amino)ethyl methacrylate, the monomer presented in Chapter 3, can be used for copolymerization with another monomer, it is not commercially available and the synthesis is tedious.[3] Herein, I propose to synthesize thermo- and pH-sensitive hydrophilic ABA triblock copolymers from a difunctional PEO macroinitiator with the thermosensitive outer blocks incorporated with a tertiary amine-containing monomer, either *N*,*N*-diethylaminoethyl methacrylate (DEAEMA) or *N*,*N*-diisopropylaminoethyl methacrylate (DPAEMA). The values of pK_a of poly(DEAEMA) and poly(DPAEMA) in water have been reported to be 7.2 and 6.3.[11] To form aqueous micellar gels at the physiological temperature (37 °C), it is necessary to use a thermosensitive polymer with a relatively lower LCST. Since the cloud points of poly(DEGMMA) and poly(ethoxydi(ethylene glycol) methacrylate) (poly(DEGEMA)) in

water are 25 and 4 °C, respectively,[12] the copolymerization of DEGMMA and DEGEMA might be a good choice. Therefore, the targeted thermo- and pH-responsive ABA triblock copolymers are poly(DEGMMA-*co*-DEGEMA-*co*-DEAEMA)-*b*-PEO-*b*-poly(DEGMMA-*co*-DEGEMA-*co*-DEAEMA) and poly(DEGMMA-*co*-DEGEMA-*co*-DPAEMA)-*b*-PEO-*b*-poly(DEGMMA-*co*-DEGEMA-*co*-DPAEMA) with various compositions for the thermosensitive blocks. It is expected that the sol-gel transition temperatures of moderately concentrated aqueous solutions of these two thermo- and pH-sensitive ABA triblock copolymers increase with the decrease of solution pH. These micellar gels might be more suitable for biomedical applications.

References:

1. O'Lenick, T. G.; Jiang X. G.; Zhao, B. *Langmuir* **2010**, *26*, 8787–8796.
2. O'Lenick, T. G.; Jin, N. X.; Woodcock, J. W.; Zhao, B. *J. Phys. Chem. B.* **2011**, *115*, 2870-2881.
3. O'Lenick, T. G.; Jiang, X. M.; Zhao, B. *Polymer* **2009**, *50*, 4363-4371.
4. Anderson, B. C.; Cox, S. M.; Bloom, P. D.; Sheares, V. V.; Mallapragada, S. K. *Macromolecules* **2003**, *36*, 1670-1676.
5. Determan, M. D.; Cox, J. P.; Seifert, S.; Thiyagarajan, P.; Mallapragada, S. K. *Polymer* **2005**, *46*, 6933-6946.
6. Determan, M. D.; Guo, L.; Thiyagarajan, P.; Mallapragada, S. K. *Langmuir* **2006**, *22*, 1469-1473.
7. Yin, X.; Hoffman, A. S.; Stayton, P. S. *Biomacromolecules* **2006**, *7*, 1381-1385.
8. Feil, H.; Bae, Y. H.; Feijen, J.; Kim, S. W. *Macromolecules* **1993**, *26*, 2496-2500.

9. Urry, D. W. *J. Phys. Chem. B* **1997**, *101*, 11007-11028.

10. Lee, E. S.; Gao, Z.; Bae, Y. H. *J. Controlled Release* **2008**, *132*, 164-170.

11. Taktak, F. F.; Butun, V. *Polymer*, **2010**, *51*, 3618-3626.

12. Ishizone, T.; Seki, A.; Hagiwara, M.; Han, S.; Yokoyama, H.; Oyane, A.; Deffieux, A.; Carlotti, S. *Macromolecules* **2008**, *41*, 2963-2967.

Appendix A

for

Chapter 1. Thermosensitive Aqueous Gels with Tunable Sol-Gel Transition Temperatures from Thermo- and pH-Responsive Hydrophilic ABA Triblock Copolymer

A.1. Synthesis of Poly(methoxydi(ethylene glycol) methacrylate-*co*-*t*-butyl methacrylate) (P(DEGMMA-*co*-*t*BMA)). Copper (I) bromide (5.7 mg, 4.0×10^{-5} mol), DEGMMA (2.057 g, 10.9 mmol), *t*BMA (0.083 g, 5.85×10^{-4} mol), *N,N,N′,N′,N″*-pentamethyldiethylenetriamine (PMDETA) (6.0 mg, 3.45×10^{-5} mol), and anisole (4.307 g) were added into a two-necked flask and stirred under a dry nitrogen atmosphere. Ethyl 2-bromoisobutyrate (EBiB, 7.5 mg, 3.85×10^{-5} mol) was injected into the flask via an argon-purged microsyringe. After the reaction mixture was degassed by three freeze-pump-thaw cycles, the flask was placed into a 75 °C oil bath. ^{1}H NMR spectroscopy was used to monitor the polymerization. After 110 min, the reaction was stopped by opening the flask to air and diluting the mixture with THF. The copper catalyst was removed by passing the solution through a short basic aluminum oxide/silica gel column. The polymer was purified by precipitation in hexanes (100 mL × 3). The polymer was then dried under vacuum. GPC analysis results (polystyrene standards): $M_{n,GPC}$ = 24,500 Da, polydispersity index (PDI) = 1.15. The numbers of DEGMMA and *t*BMA units in the copolymer were 148 and 7, respectively, which were calculated from the ^{1}H NMR spectrum using the integral values of the peak at 4.1 ppm (COOCH_2CH$_2$ of the DEGMMA units), and the peak at 1.4 ppm (COOC(CH_3)$_3$ of the *t*BMA units, excluding the integral value of the remaining broad peak in the ^{1}H NMR spectrum of P(DEGMMA-*co*-MAA) after the cleavage of *t*-butyl groups).

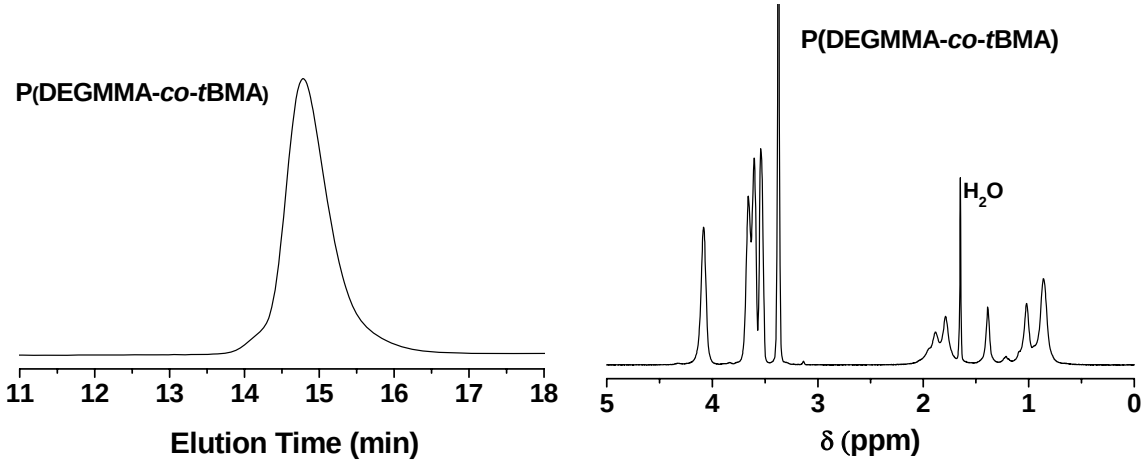

(a) (b)

Figure A.1. (a) Gel permeation chromatography trace of P(DEGMMA-*co*-*t*BMA) and (b) ^{1}H NMR spectrum of P(DEGMMA-*co*-*t*BMA) in $CDCl_3$.

A.2. Synthesis of P(DEGMMA-*co*-MAA). Dry P(DEGMMA-*co*-*t*BMA) (0.698 g) was added into a 25 mL round bottom flask and dissolved with dry dichloromethane (3.5 mL). The mixture was stirred for 45 min to ensure complete dissolution. Triflouroacetic acid (TFA, 1.721 g, 15.1 mmol) was added into the flask. After being stirred at room temperature for 52 h, the reaction mixture was diluted with dichloromethane (100 mL). Most of TFA was removed under a reduced pressure. The polymer was repeatedly precipitated in a mixture of hexanes : diethyl either (10 : 1) to completely remove TFA. The polymer was then dried under vacuum at 70 °C for 5 h.

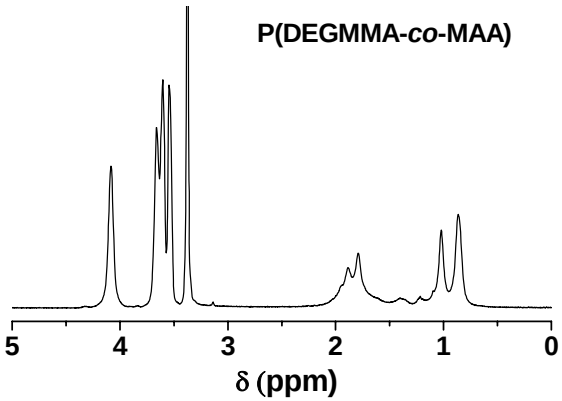

Figure A.2. ^{1}H NMR spectrum of P(DEGMMA-*co*-MAA) in $CDCl_3$.

A.3. Determination of pK_a value of Carboxylic Acid in P(DEGMMA-*co*-MAA). P(DGEMMA-*co*-MAA) (0.221 g) was thoroughly dried in a round bottom flask under high vacuum. Mili-Q water (2.220 g) was added into the round bottom flask and the mixture was sonicated in an ice/water ultrasonic bath to dissolve the polymer in water, yielding an aqueous solution of P(DEGMMA-*co*-MAA) with a concentration of 9.1 wt%. The solution was then transferred into a small vial. The pH of the solution was measured with a pH meter (Accumet AB15 pH meter from Fisher Scientific, calibrated with pH = 4.01, 7.00, and 10.01 standard buffer solutions) equipped with a temperature probe. 5.0 μL of a 1.0 M KOH solution was injected into the vial via a microsyringe. The vial was sonicated in an ice/water ultrasonic bath for 2 min to ensure that the solution was homogeneous and the pH was recorded. This process was repeated until a total of 70.0 μL of a 1.0 M KOH solution was added. A plot of pH versus the number of μmol of KOH was constructed and the pK_a was determined to be 5.59.

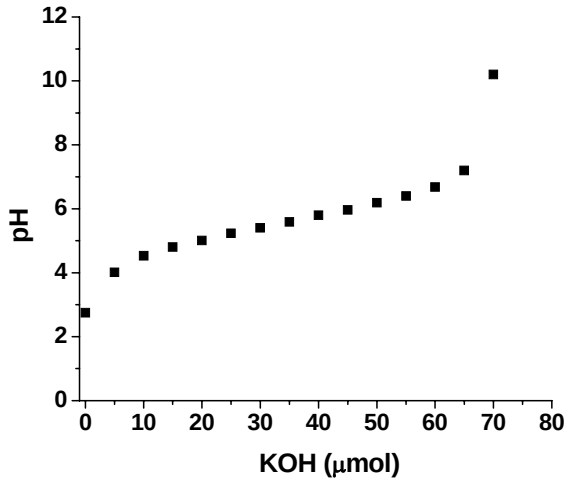

Figure A.3. The plot of solution pH versus number of μmols of KOH injected into a 9.1 wt% aqueous solution of P(DEGMMA-*co*-MAA) (2.441 g). The KOH aqueous solution was added stepwise; each time, 5.0 μL of a 1.0 M aqueous KOH solution was injected via a microsyringe, followed by the measurement of pH with a pH meter.

A.4. Synthesis of PDEGMMA. A procedure similar to that for the synthesis of P(DEGMMA-*co*-*t*BMA) was used to prepare PDEGMMA. GPC analysis showed that $M_{n,GPC}$ was 12,700 Da and polydispersity index (PDI) was 1.14. The GPC trace and ^{1}H NMR spectrum are shown in Figure A.4. A small broad peak at ~ 1.4 ppm can be seen from ^{1}H NMR spectrum.

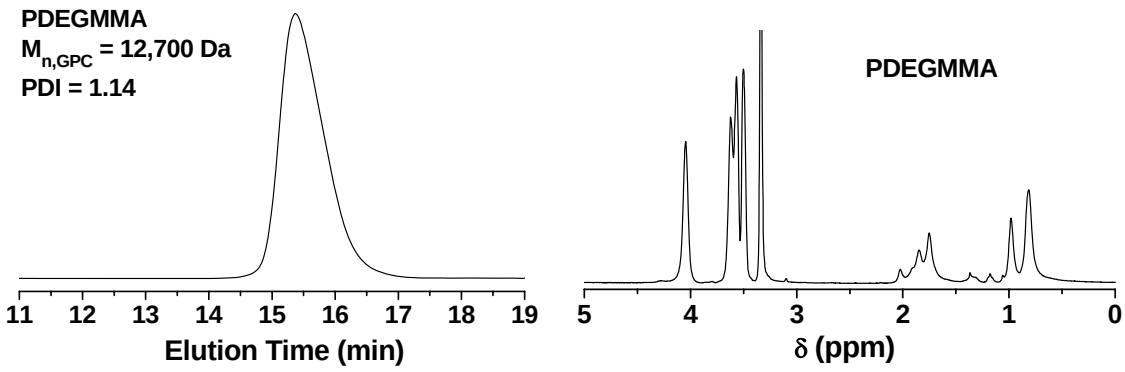

(a) (b)

Figure A.4. (a) Gel permeation chromatography trace and (b) ^{1}H NMR spectrum of PDEGMMA.

A.5. Concentration Effect on the Sol-Gel Transition of Aqueous Solution of P(DEGMMA-*co*-MAA)-*b*-PEO-*b*-P(DEGMMA-*co*-MAA) at pH = 4.0.

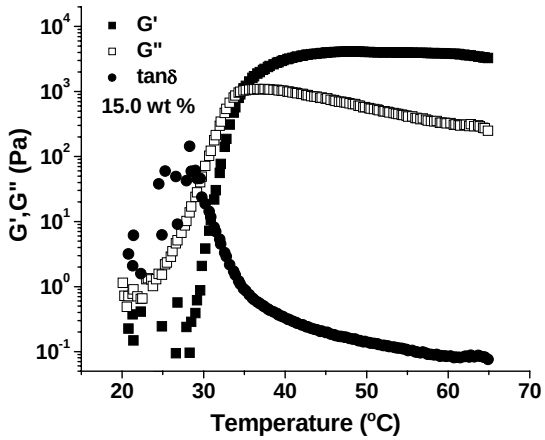

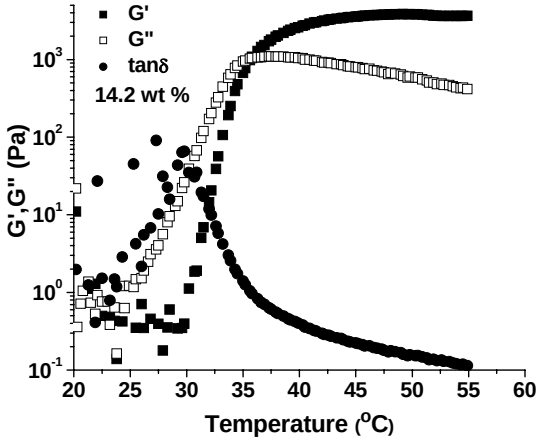

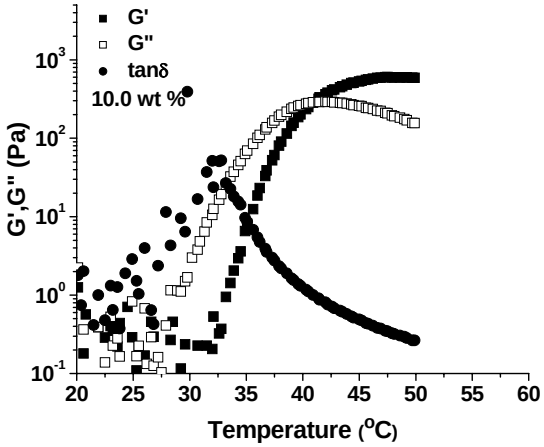

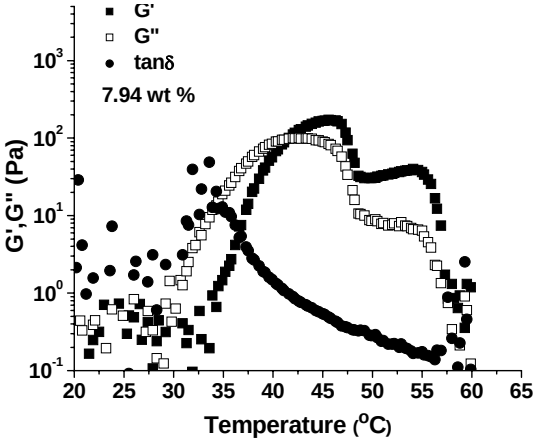

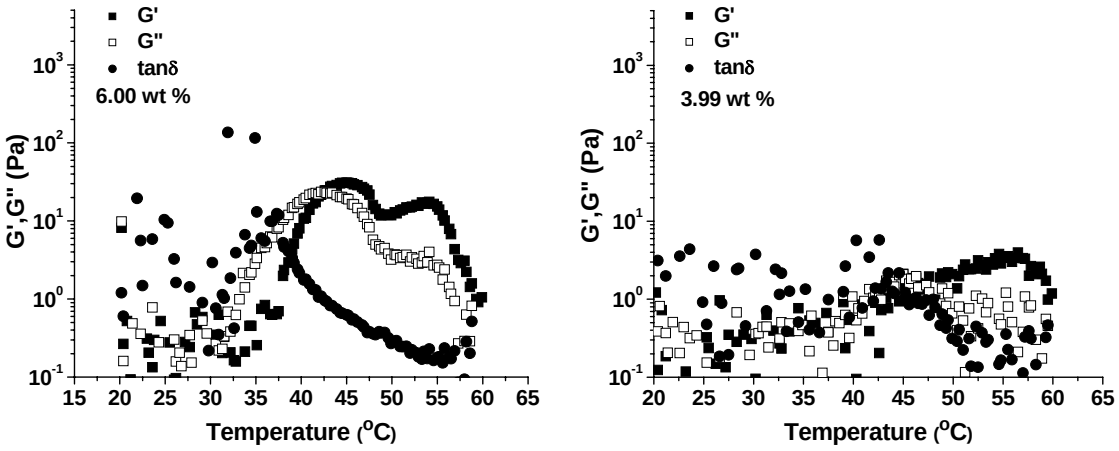

Figure A.5. Temperature ramps for aqueous solutions of P(DEGMMA-*co*-MAA)-*b*-PEO-*b*-P(DEGMMA-*co*-MAA) with various concentrations at pH = 4.0 performed at a constant frequency of 1 Hz, a strain amplitude of 0.2 %, and a heating rate of 2 °C/min.

Appendix B

for

Chapter 2. Rheological Properties of Thermo- and pH-Responsive ABA Triblock Copolymer Aqueous Micellar Gels

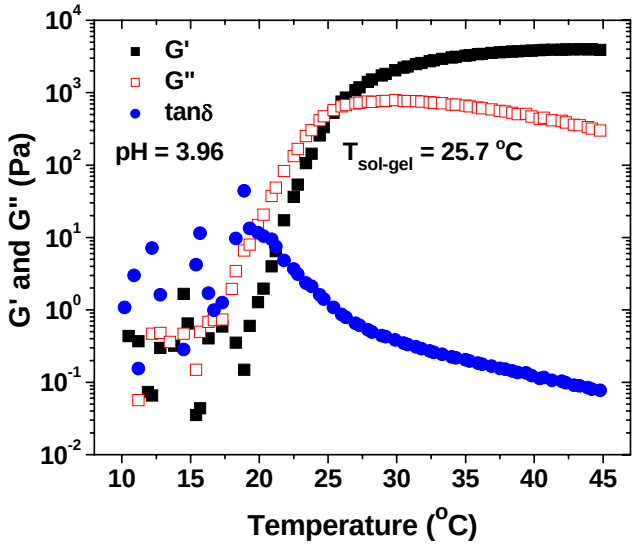

Figure B.1. Plot of dynamic storage modulus G' (■), dynamic loss modulus G" (□), and tanδ (●) versus temperature for a 10.0 wt% aqueous solution of P(DEGEA-*co*-AA)-*b*-PEO-*b*-P(DEGEA-*co*-AA) with a pH value of 3.96. The data were collected from a temperature ramp experiment using a heating rate of 3 °C/min, a strain amplitude of 0.2 %, and an oscillation frequency of 1 Hz.

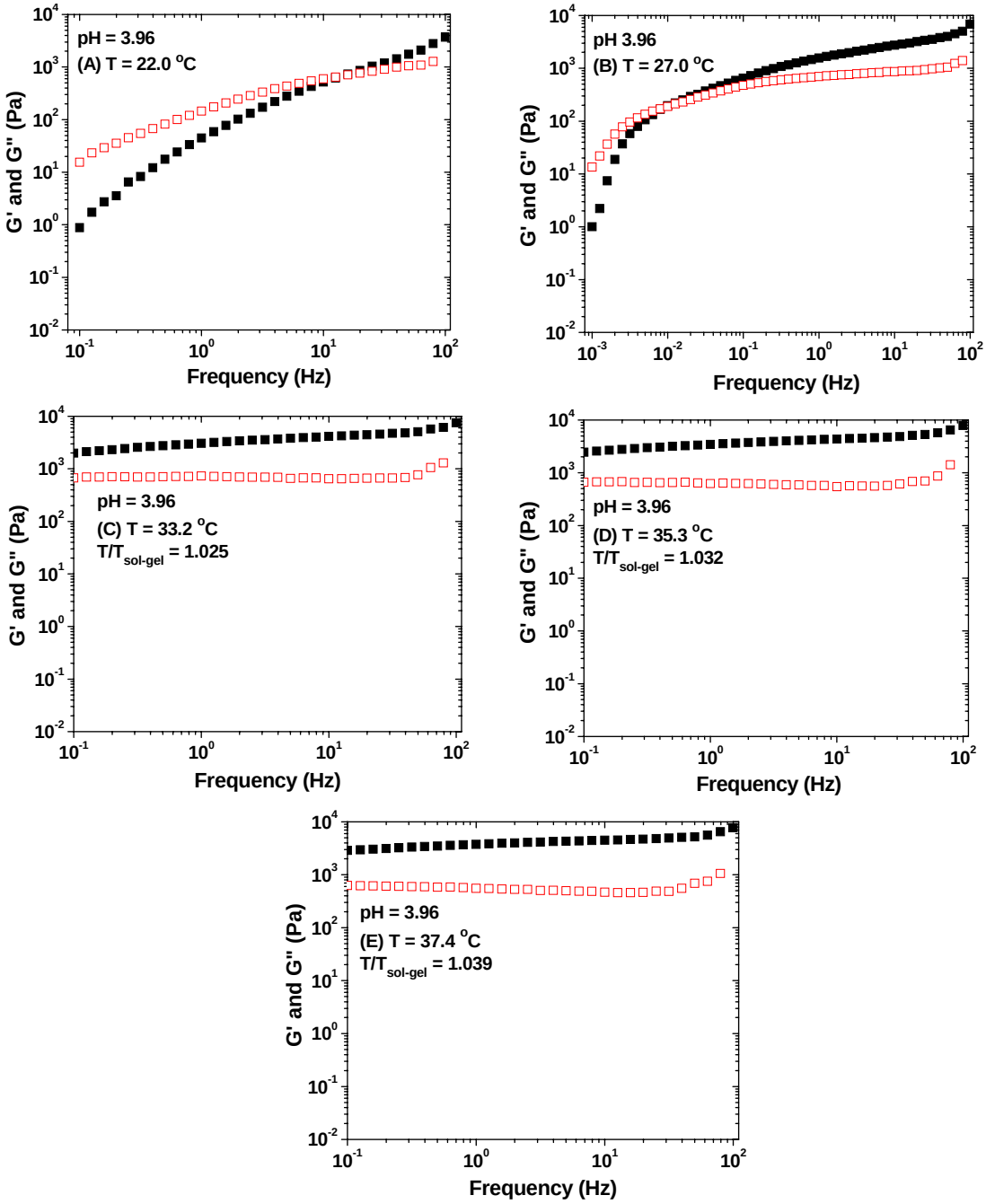

Figure B.2. Frequency dependences of dynamic storage modulus G' (■) and loss modulus G" (□) of the 10.0 wt% aqueous solution of P(DEGEA-*co*-AA)-*b*-PEO-*b*-P(DEGEA-*co*-AA) with a pH of 3.96 at (A) 22.0 °C, (B) 27.0 °C, (C) 33.2 °C ($T/T_{sol\text{-}gel}$ = 1.025), (D) 35.3 °C ($T/T_{sol\text{-}gel}$ = 1.032), and (E) 37.4 °C ($T/T_{sol\text{-}gel}$ = 1.039). A strain amplitude of 0.2 % was used in the frequency sweep experiments.

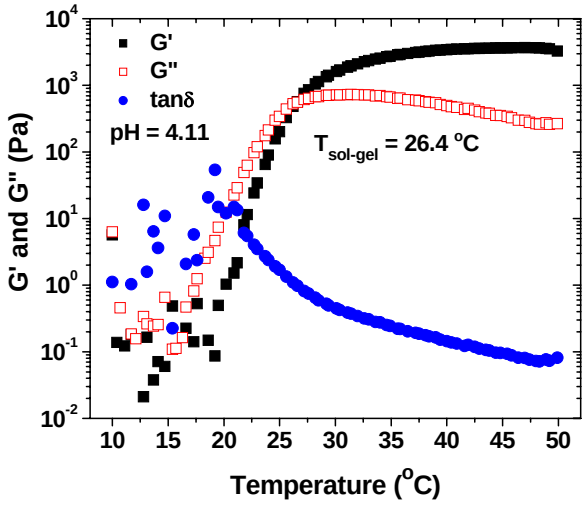

Figure B.3. Plot of dynamic storage modulus G' (■), dynamic loss modulus G" (□), and tanδ (●) versus temperature for a 10.0 wt% aqueous solution of P(DEGEA-*co*-AA)-*b*-PEO-*b*-P(DEGEA-*co*-AA) with a pH value of 4.11. The data were collected from a temperature ramp experiment using a heating rate of 3 °C/min, a strain amplitude of 0.2 %, and an oscillation frequency of 1 Hz.

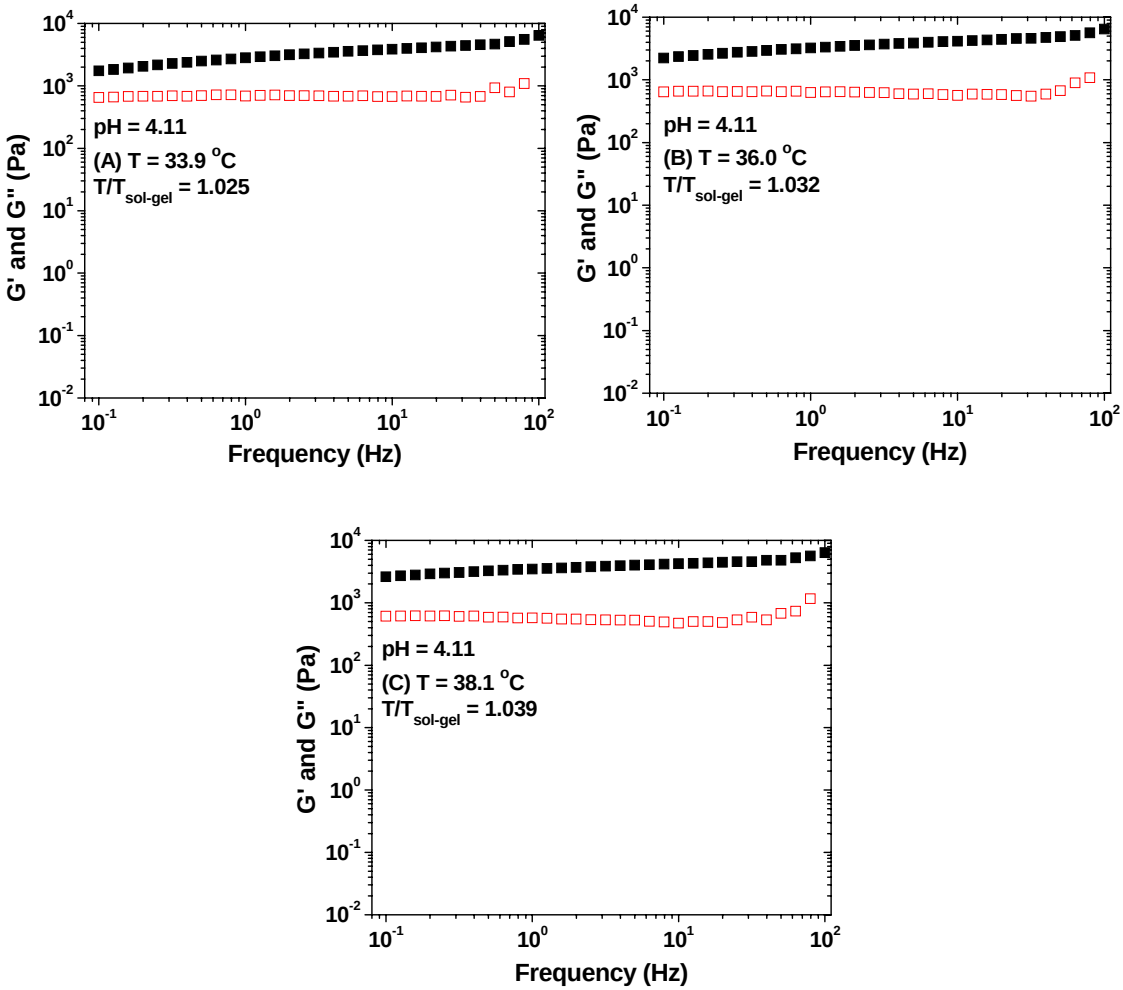

Figure B.4. Frequency dependences of dynamic storage modulus G' (■) and loss modulus G" (□) of a 10.0 wt% aqueous solution of P(DEGEA-*co*-AA)-*b*-PEO-*b*-P(DEGEA-*co*-AA) with pH of 4.11 at (A) 33.9 °C ($T/T_{sol\text{-}gel}$ = 1.025), (B) 36.0 °C ($T/T_{sol\text{-}gel}$ = 1.032), and (C) 38.1 °C ($T/T_{sol\text{-}gel}$ = 1.039). A strain amplitude of 0.2 % was used in the frequency sweep experiments.

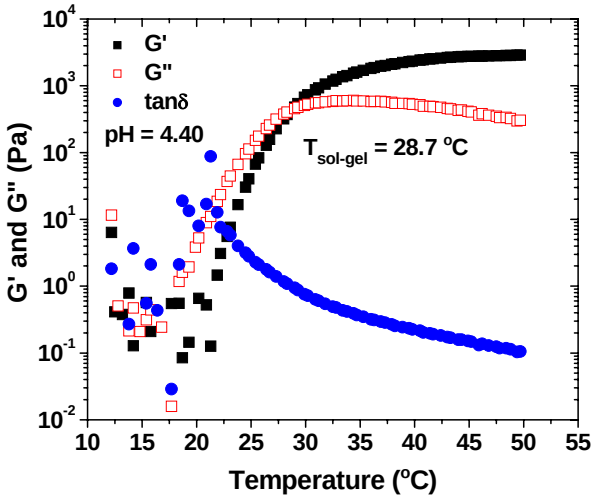

Figure B.5. Plot of dynamic storage modulus G' (■), dynamic loss modulus G" (□), and tanδ (●) versus temperature for a 10.0 wt% aqueous solution of P(DEGEA-*co*-AA)-*b*-PEO-*b*-P(DEGEA-*co*-AA) with a pH value of 4.40. The data were collected from a temperature ramp experiment performed using a heating rate of 3 °C/min, a strain amplitude of 0.2 %, and an oscillation frequency of 1 Hz.

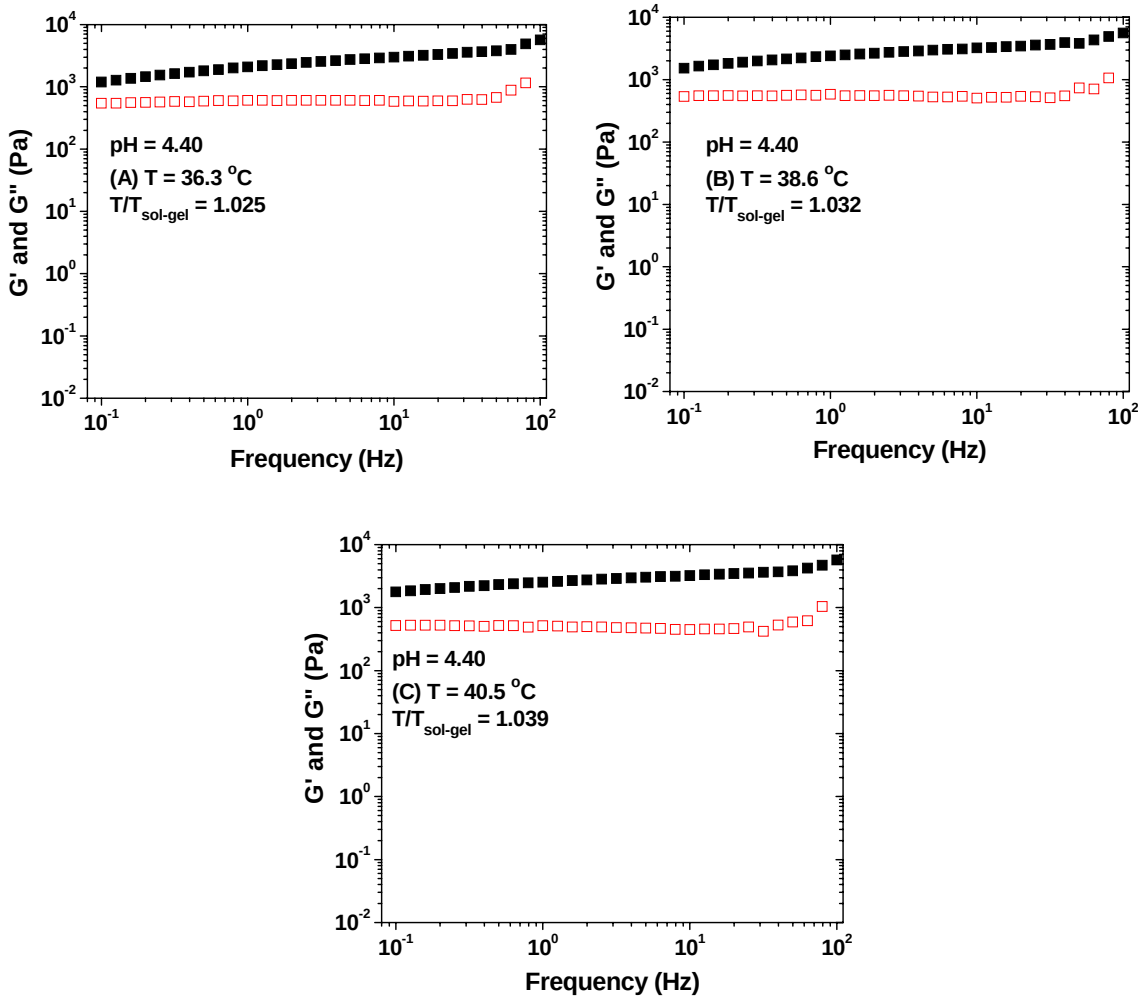

Figure B.6. Frequency dependences of dynamic storage modulus G' (■) and loss modulus G" (□) of a 10.0 wt% aqueous solution of P(DEGEA-*co*-AA)-*b*-PEO-*b*-P(DEGEA-*co*-AA) with pH of 4.40 at (A) 36.3 °C ($T/T_{sol\text{-}gel}$ = 1.025), (B) 38.6 °C ($T/T_{sol\text{-}gel}$ = 1.032), and (C) 40.5 °C ($T/T_{sol\text{-}gel}$ = 1.039). A strain amplitude of 0.2 % was used in the frequency sweep experiments.

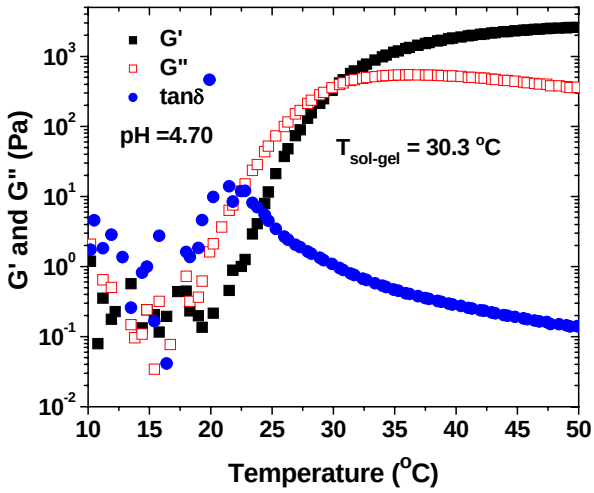

Figure B.7. Plot of dynamic storage modulus G' (■), dynamic loss modulus G" (□), and tanδ (●) versus temperature for a 10.0 wt% aqueous solution of P(DEGEA-*co*-AA)-*b*-PEO-*b*-P(DEGEA-*co*-AA) with a pH value of 4.70. The data were collected from a temperature ramp experiment performed using a heating rate of 3 °C/min, a strain amplitude of 0.2 %, and an oscillation frequency of 1 Hz.

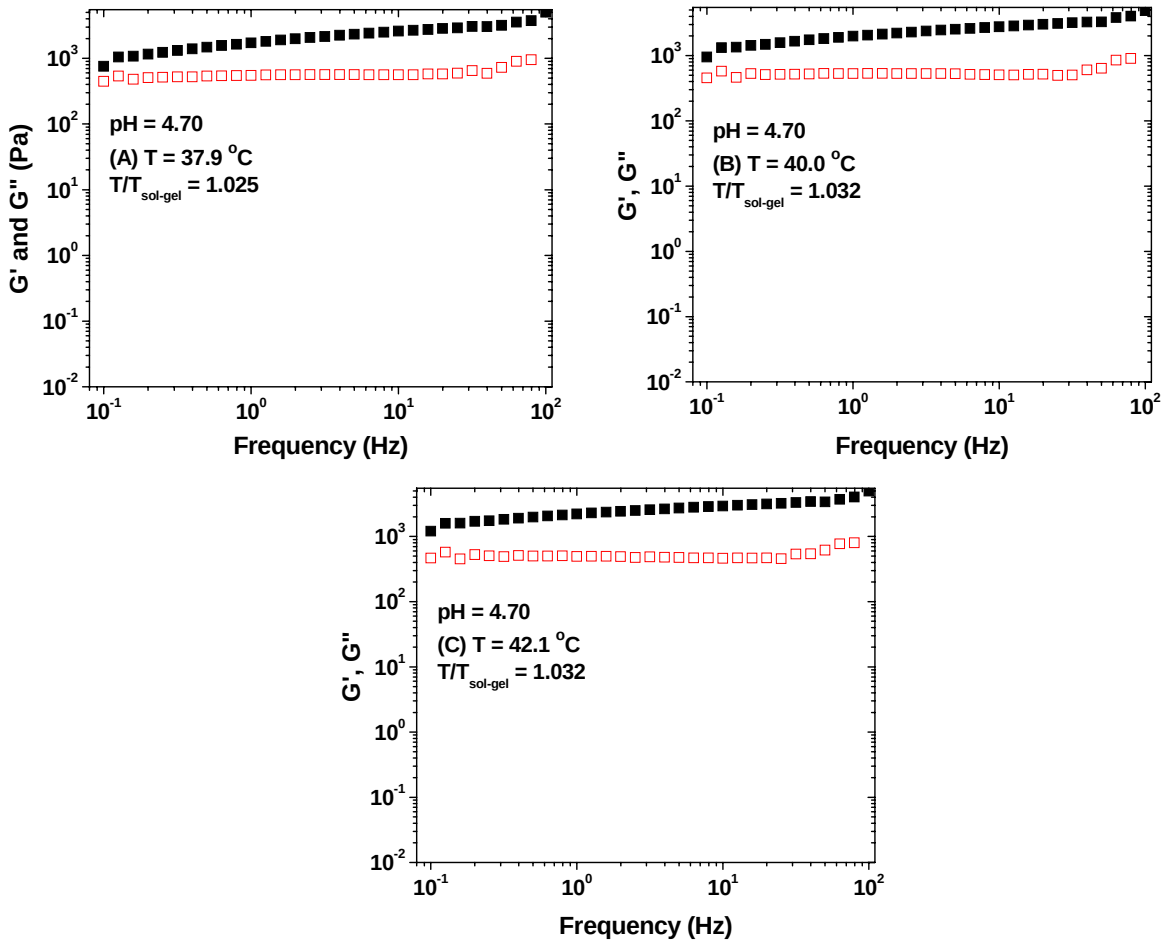

Figure B.8. Frequency dependences of dynamic storage modulus G' (■) and loss modulus G" (□) of the 10.0 wt% aqueous solution of P(DEGEA-*co*-AA)-*b*-PEO-*b*-P(DEGEA-*co*-AA) with pH of 4.70 at (a) 37.9 °C ($T/T_{sol\text{-}gel}$ = 1.025), (b) 40.0 °C ($T/T_{sol\text{-}gel}$ = 1.032), and (c) 42.1 °C ($T/T_{sol\text{-}gel}$ = 1.039). A strain amplitude of 0.2 % was used in the frequency sweep experiments.

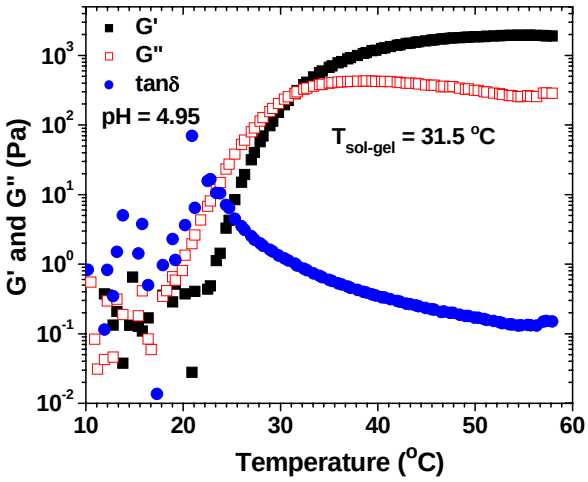

Figure B.9. Plot of dynamic storage modulus G' (■), dynamic loss modulus G" (□), and tanδ (●) versus temperature for a 10.0 wt% aqueous solution of P(DEGEA-*co*-AA)-*b*-PEO-*b*-P(DEGEA-*co*-AA) with a pH value of 4.95. The data were collected from a temperature ramp experiment performed using a heating rate of 3 °C/min, a strain amplitude of 0.2 %, and an oscillation frequency of 1 Hz.

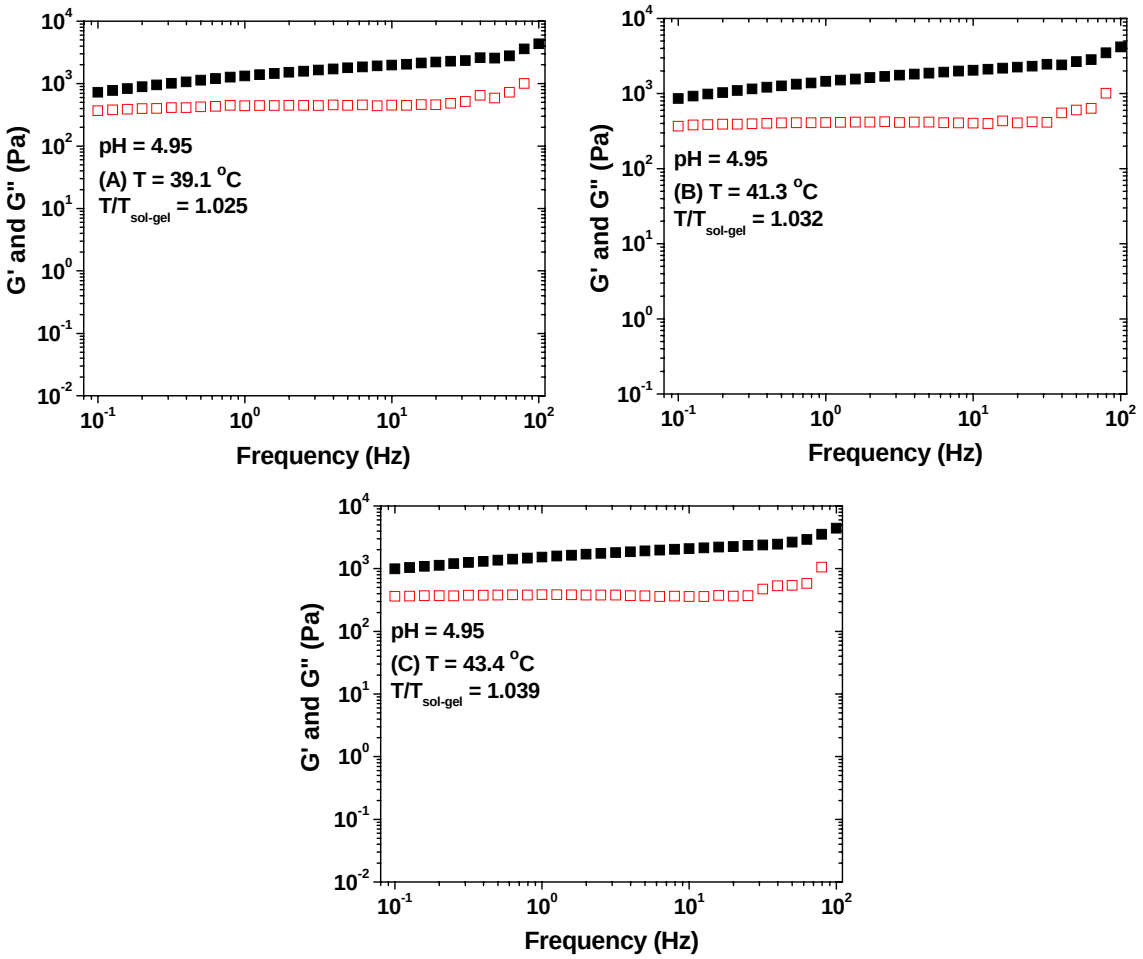

Figure B.10. Frequency dependences of dynamic storage modulus G' (■) and loss modulus G" (□) of a 10.0 wt% aqueous solution of P(DEGEA-*co*-AA)-*b*-PEO-*b*-P(DEGEA-*co*-AA) with pH of 4.95 at (A) 39.1 °C ($T/T_{sol\text{-}gel}$ = 1.025), (B) 41.3 °C ($T/T_{sol\text{-}gel}$ = 1.032), and (C) 43.4 °C ($T/T_{sol\text{-}gel}$ = 1.039). A strain amplitude of 0.2 % was used in the frequency sweep experiments.

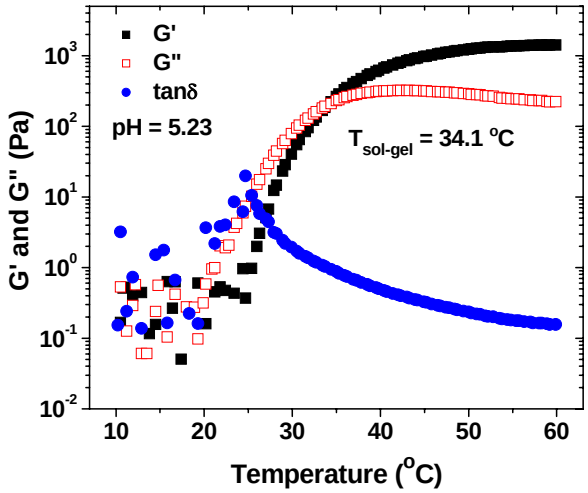

Figure B.11. Plot of dynamic storage modulus G' (■), dynamic loss modulus G" (□), and tanδ (●) versus temperature for a 10.0 wt% aqueous solution of P(DEGEA-*co*-AA)-*b*-PEO-*b*-P(DEGEA-*co*-AA) with pH of 5.23. The data were collected from a temperature ramp experiment performed using a heating rate of 3 °C/min, a strain amplitude of 0.2 %, and an oscillation frequency of 1 Hz.

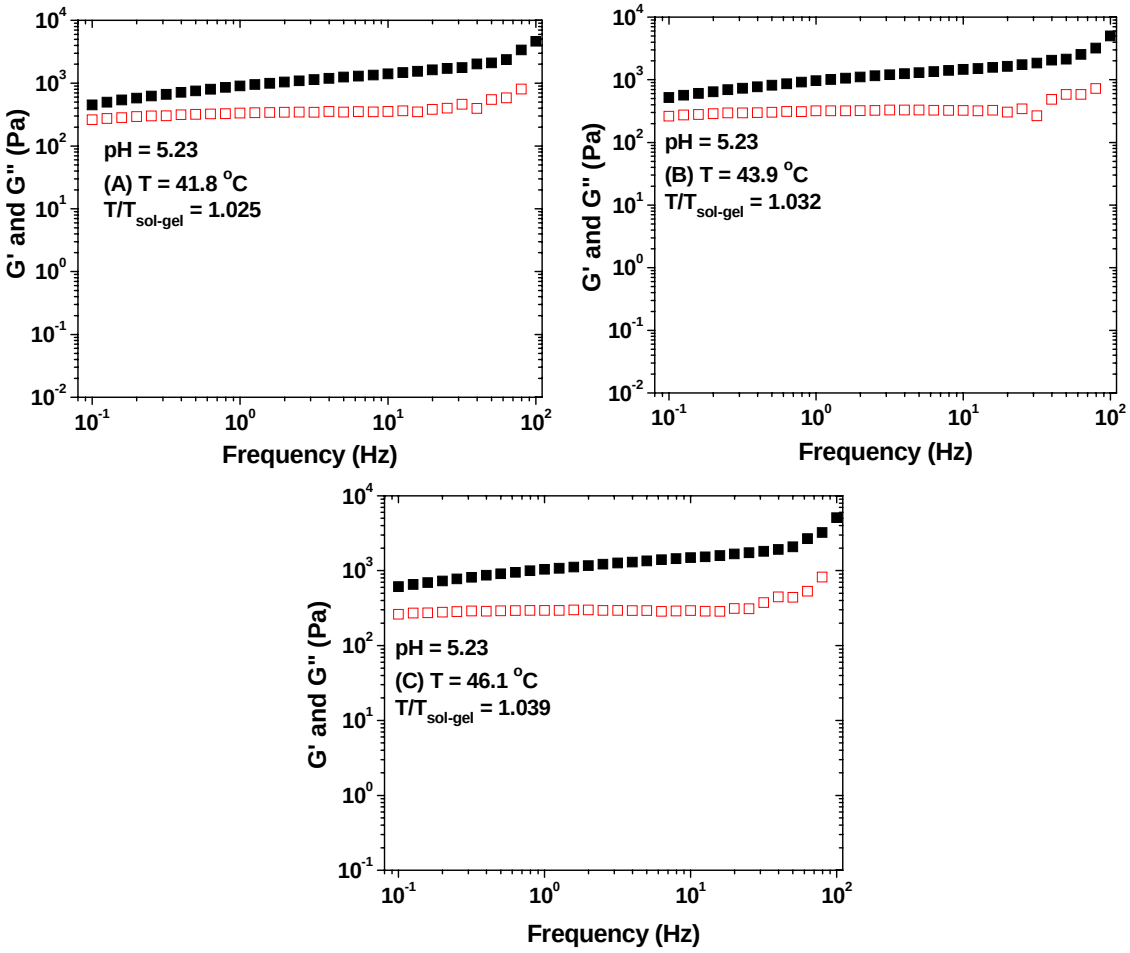

Figure B.12. Frequency dependences of dynamic storage modulus G' (■) and loss modulus G" (□) of a 10.0 wt% aqueous solution of P(DEGEA-*co*-AA)-*b*-PEO-*b*-P(DEGEA-*co*-AA) with pH of 5.23 at (A) 41.8 °C ($T/T_{sol\text{-}gel}$ = 1.025), (B) 43.9 °C ($T/T_{sol\text{-}gel}$ = 1.032), and (C) 46.1 °C ($T/T_{sol\text{-}gel}$ = 1.039). A strain amplitude of 0.2 % was used in the frequency sweep experiments.

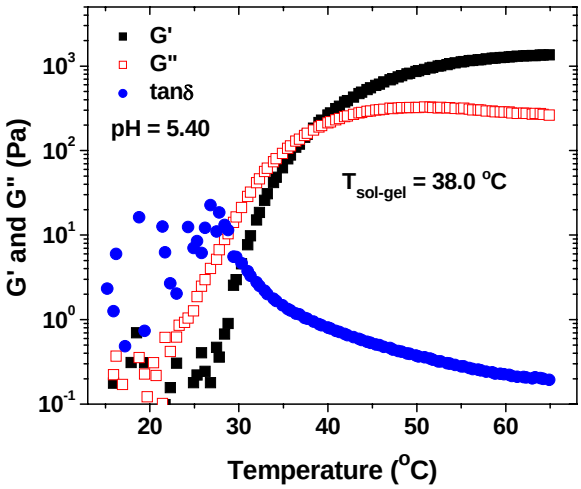

Figure B.13. Plot of dynamic storage modulus G' (■), dynamic loss modulus G" (□), and tanδ (●) versus temperature for a 10.0 wt% aqueous solution of P(DEGEA-*co*-AA)-*b*-PEO-*b*-P(DEGEA-*co*-AA) with a pH value of 5.40. The data were collected from a temperature ramp experiment performed using a heating rate of 3 °C/min, a strain amplitude of 0.2 %, and an oscillation frequency of 1 Hz.

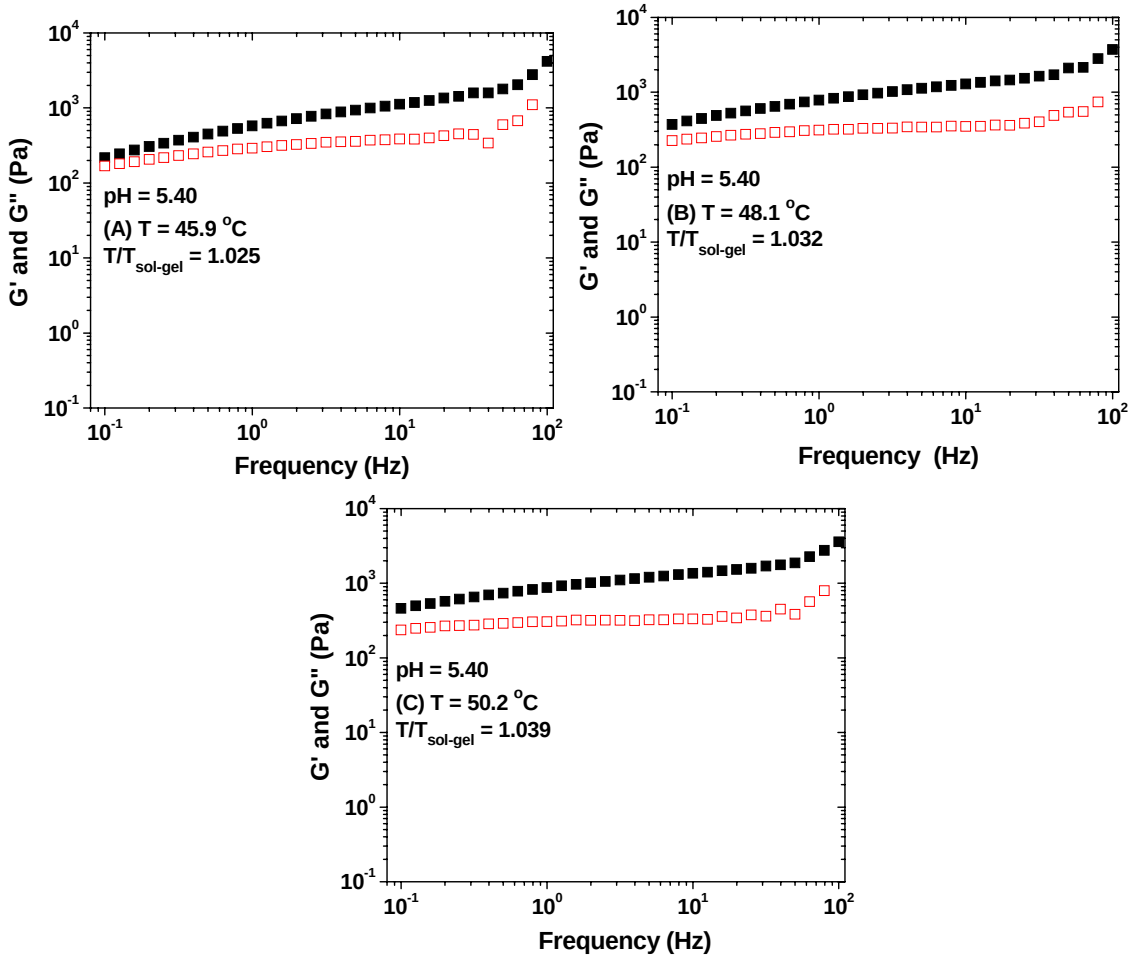

Figure B.14. Frequency dependences of dynamic storage modulus G' (■) and loss modulus G" (□) of a 10.0 wt% aqueous solution of P(DEGEA-*co*-AA)-*b*-PEO-*b*-P(DEGEA-*co*-AA) with pH of 5.40 at (A) 45.9 °C ($T/T_{sol\text{-}gel}$ = 1.025), (B) 48.1 °C ($T/T_{sol\text{-}gel}$ = 1.032), and (C) 50.2 ($T/T_{sol\text{-}gel}$ = 1.039). A strain amplitude of 0.2 % was used in the frequency sweep experiments.

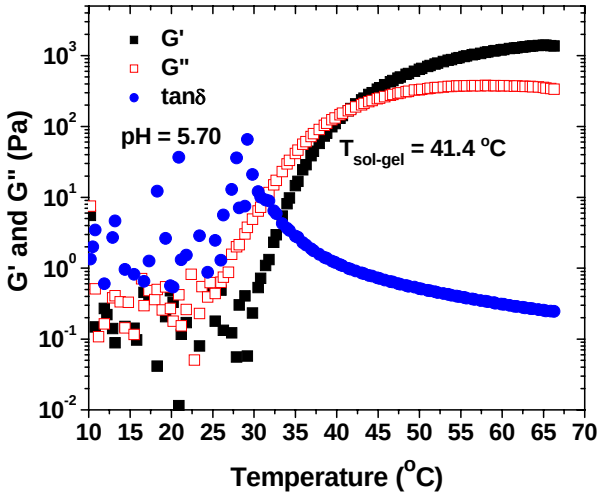

Figure B.15. Plot of dynamic storage modulus G' (■), dynamic loss modulus G" (□), and tanδ (●) versus temperature for a 10.0 wt% aqueous solution of P(DEGEA-*co*-AA)-*b*-PEO-*b*-P(DEGEA-*co*-AA) with a pH value of 5.70. The data were collected from a temperature ramp experiment performed using a heating rate of 3 °C/min, a strain amplitude of 0.2 %, and an oscillation frequency of 1 Hz.

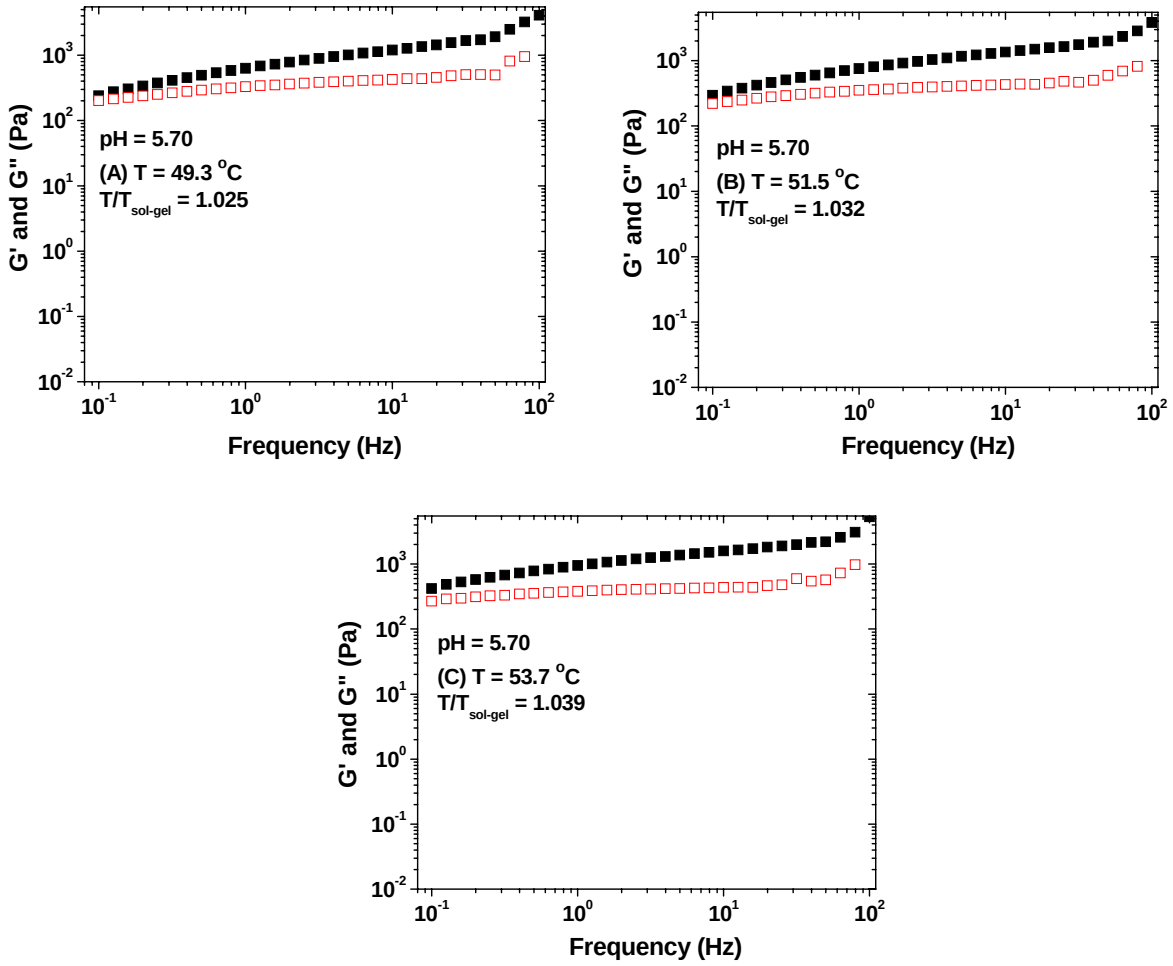

Figure B.16. Frequency dependences of dynamic storage modulus G' (■) and loss modulus G" (□) of a 10.0 wt% aqueous solution of P(DEGEA-*co*-AA)-*b*-PEO-*b*-P(DEGEA-*co*-AA) with pH of 5.70 at (A) 49.3 °C ($T/T_{sol\text{-}gel}$ = 1.025), (B) 51.5 °C ($T/T_{sol\text{-}gel}$ = 1.032), and (C) 53.7 °C ($T/T_{sol\text{-}gel}$ = 1.039). A strain amplitude of 0.2 % was used in the frequency sweep experiments.

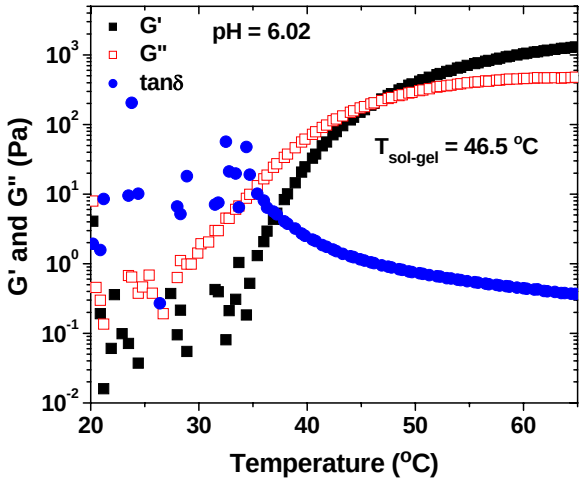

Figure B.17. Plot of dynamic storage modulus G' (■), dynamic loss modulus G" (□), and tanδ (●) versus temperature for a 10.0 wt% aqueous solution of P(DEGEA-*co*-AA)-*b*-PEO-*b*-P(DEGEA-*co*-AA) with a pH value of 6.02. The data were collected from a temperature ramp experiment performed using a heating rate of 3 °C/min, a strain amplitude of 0.2 %, and an oscillation frequency of 1 Hz.

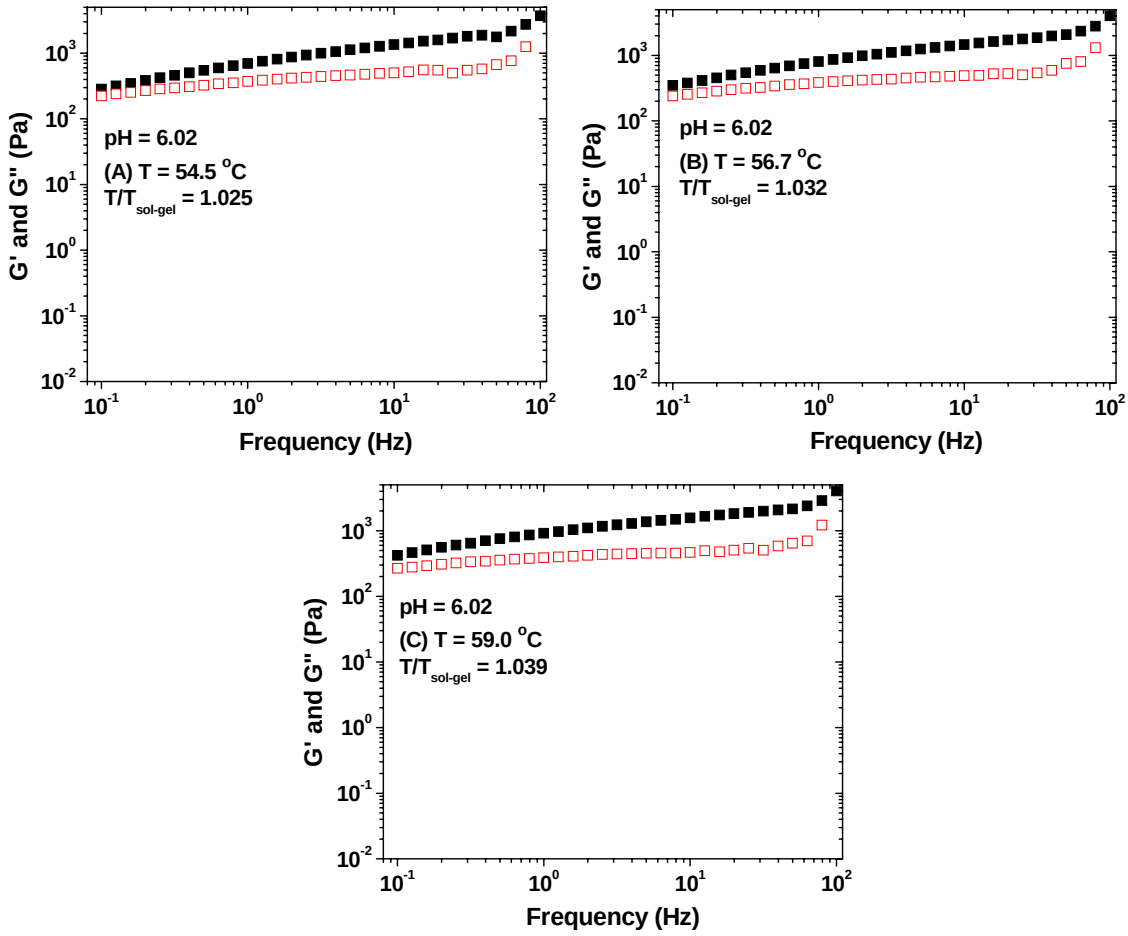

Figure B.18. Frequency dependences of dynamic storage modulus G' (■) and loss modulus G" (□) of a 10.0 wt% aqueous solution of P(DEGEA-*co*-AA)-*b*-PEO-*b*-P(DEGEA-*co*-AA) with pH of 6.02 at (A) 54.5 °C ($T/T_{sol\text{-}gel}$ = 1.025), (B) 56.7 °C ($T/T_{sol\text{-}gel}$ = 1.032), and (C) 59.0 °C ($T/T_{sol\text{-}gel}$ = 1.039). A strain amplitude of 0.2 % was used in the frequency sweep experiments.

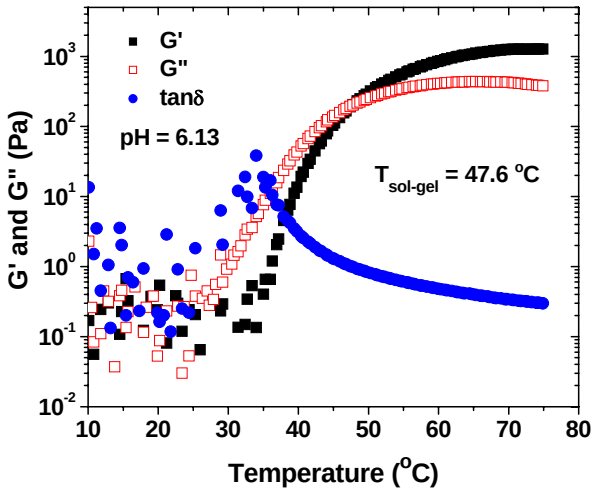

Figure B.19. Plot of dynamic storage modulus G' (■), dynamic loss modulus G" (□), and tanδ (●) versus temperature for a 10.0 wt% aqueous solution of P(DEGEA-*co*-AA)-*b*-PEO-*b*-P(DEGEA-*co*-AA) with a pH value of 6.13. The data were collected from a temperature ramp experiment performed using a heating rate of 3 °C/min, a strain amplitude of 0.2 %, and an oscillation frequency of 1 Hz.

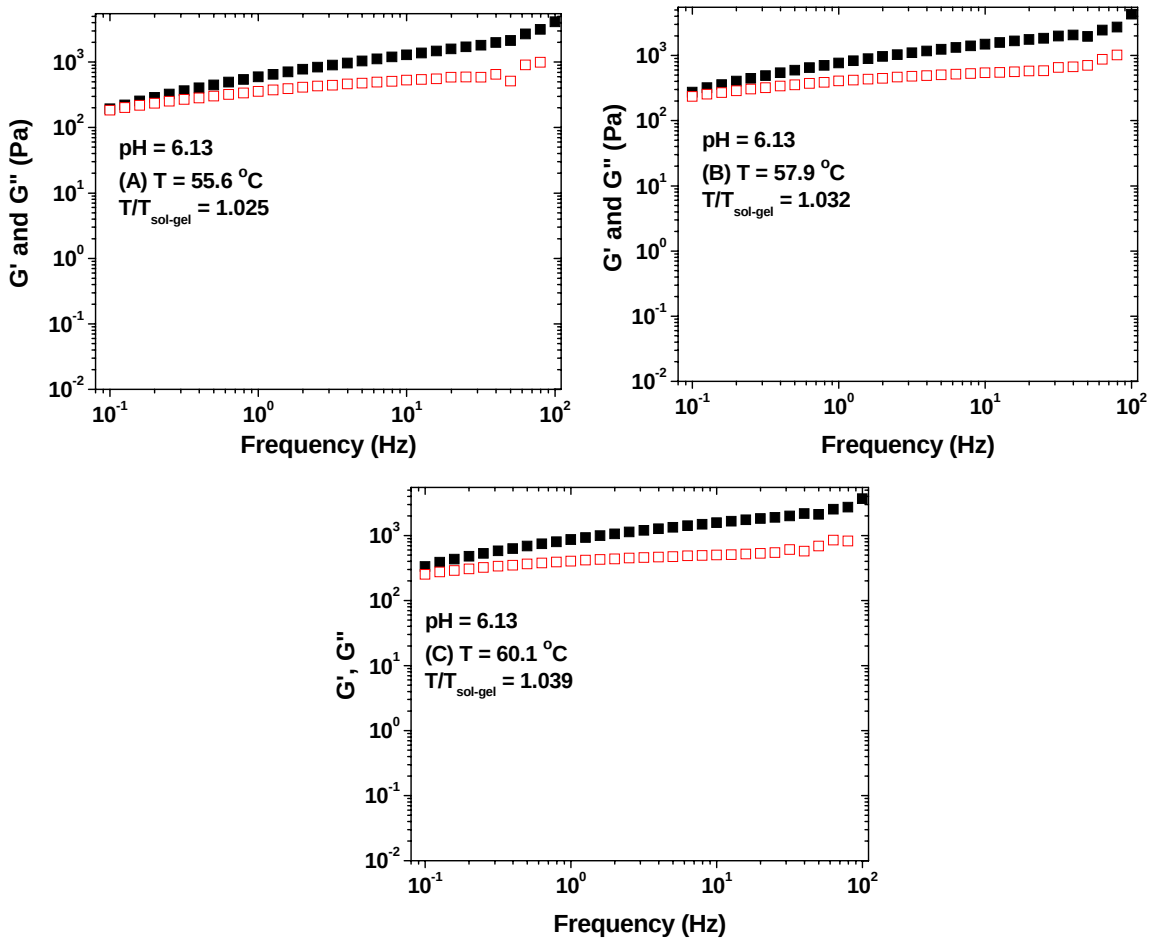

Figure B.20. Frequency dependences of dynamic storage modulus G' (■) and loss modulus G" (□) of a 10.0 wt% aqueous solution of P(DEGEA-*co*-AA)-*b*-PEO-*b*-P(DEGEA-*co*-AA) with pH of 6.13 at (A) 55.6 °C ($T/T_{sol\text{-}gel}$ = 1.025), (B) 57.9 °C ($T/T_{sol\text{-}gel}$ = 1.032), and (C) 60.1 °C ($T/T_{sol\text{-}gel}$ = 1.039). A strain amplitude of 0.2 % was used in the frequency sweep experiments.

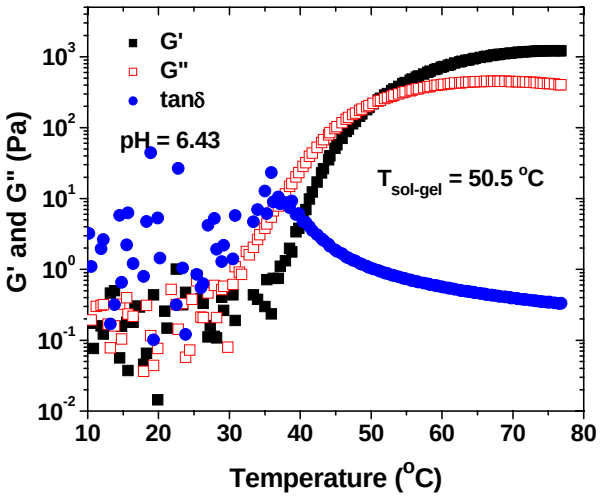

Figure B.21. Plot of dynamic storage modulus G' (■), dynamic loss modulus G" (□), and tanδ (●) versus temperature for a 10.0 wt% aqueous solution of P(DEGEA-*co*-AA)-*b*-PEO-*b*-P(DEGEA-*co*-AA) with a pH value of 6.43. The data were collected from a temperature ramp experiment performed using a heating rate of 3 °C/min, a strain amplitude of 0.2 %, and an oscillation frequency of 1 Hz.

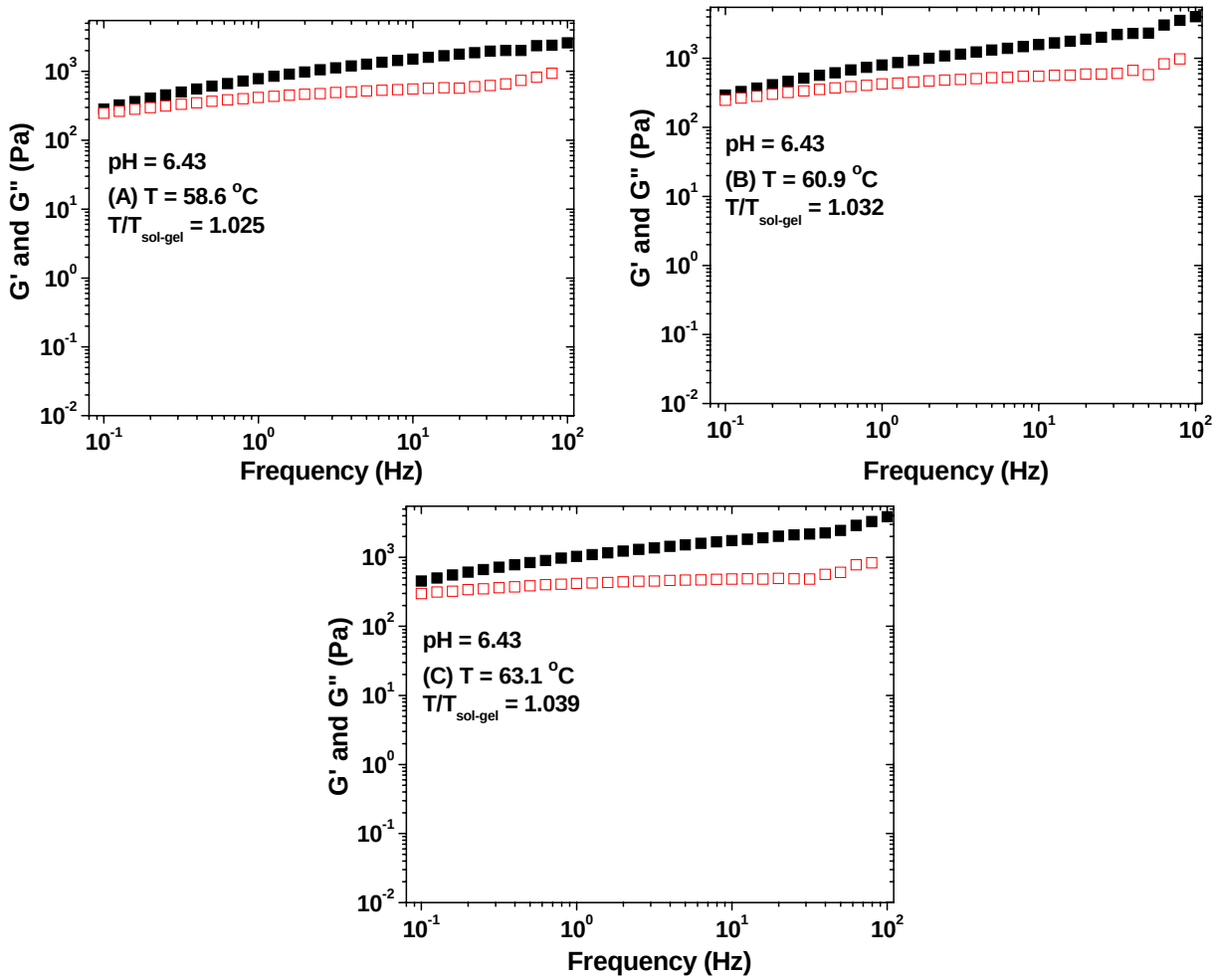

Figure B.22. Frequency dependences of dynamic storage modulus G' (■) and loss modulus G" (□) of a 10.0 wt% aqueous solution of P(DEGEA-*co*-AA)-*b*-PEO-*b*-P(DEGEA-*co*-AA) with pH of 6.43 at (A) 58.6 °C ($T/T_{sol\text{-}gel}$ = 1.025), (B) 60.9 °C ($T/T_{sol\text{-}gel}$ = 1.032), and (C) 63.1 °C ($T/T_{sol\text{-}gel}$ = 1.039). A strain amplitude of 0.2 % was used in the frequency sweep experiments.

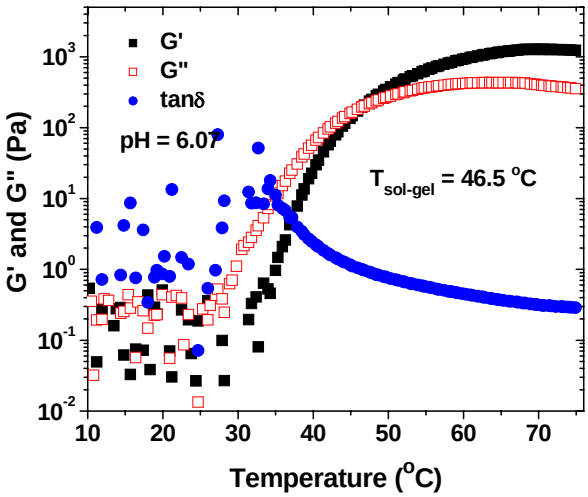

Figure B.23. Plot of dynamic storage modulus G' (■), dynamic loss modulus G" (□), and tanδ (●) versus temperature for a 10.0 wt% aqueous solution of P(DEGEA-*co*-AA)-*b*-PEO-*b*-P(DEGEA-*co*-AA) with a pH value of 6.07, which was obtained by injecting 1.0 M HCl into the 10.0 wt% solution with pH of 6.43. The data were collected from a temperature ramp experiment performed using a heating rate of 3 °C/min, a strain amplitude of 0.2 %, and an oscillation frequency of 1 Hz.

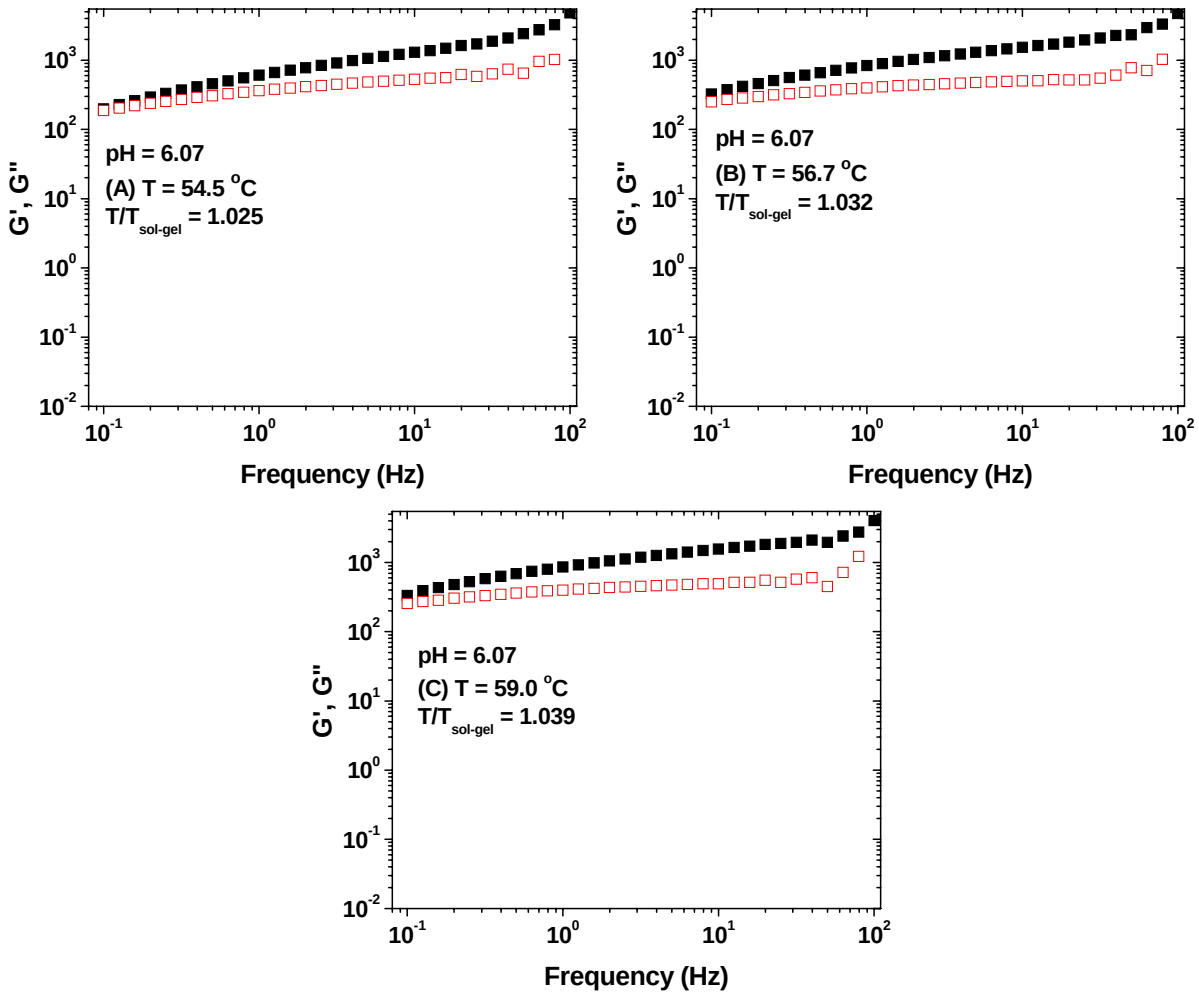

Figure B.24. Frequency dependences of dynamic storage modulus G' (■) and loss modulus G" (□) of a 10.0 wt% aqueous solution of P(DEGEA-*co*-AA)-*b*-PEO-*b*-P(DEGEA-*co*-AA) with pH of 6.07, which was obtained by injecting 1.0 M HCl into the 10.0 wt% solution with pH of 6.43, at (A) 54.5 °C ($T/T_{sol\text{-}gel}$ = 1.025), (B) 56.7 °C ($T/T_{sol\text{-}gel}$ = 1.032), and (C) 59.0 °C ($T/T_{sol\text{-}gel}$ = 1.039). A strain amplitude of 0.2 % was used in the frequency sweep experiments.

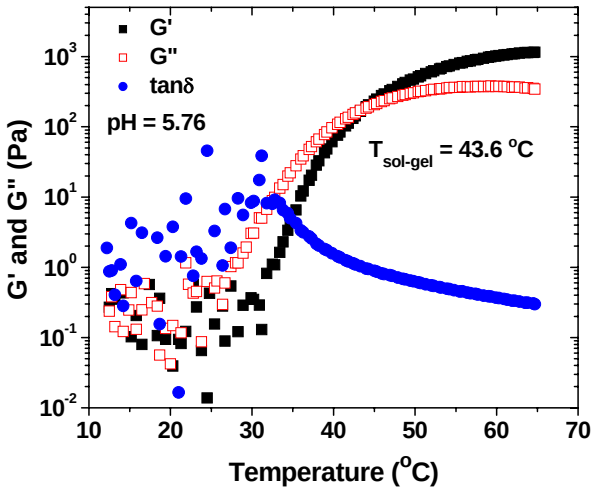

Figure B.25. Plot of dynamic storage modulus G' (■), dynamic loss modulus G" (□), and tanδ (●) versus temperature for a 10.0 wt% aqueous solution of P(DEGEA-*co*-AA)-*b*-PEO-*b*-P(DEGEA-*co*-AA) with a pH value of 5.76 obtained in the process of decreasing pH. The data were collected from a temperature ramp experiment performed using a heating rate of 3 °C/min, a strain amplitude of 0.2 %, and an oscillation frequency of 1 Hz.

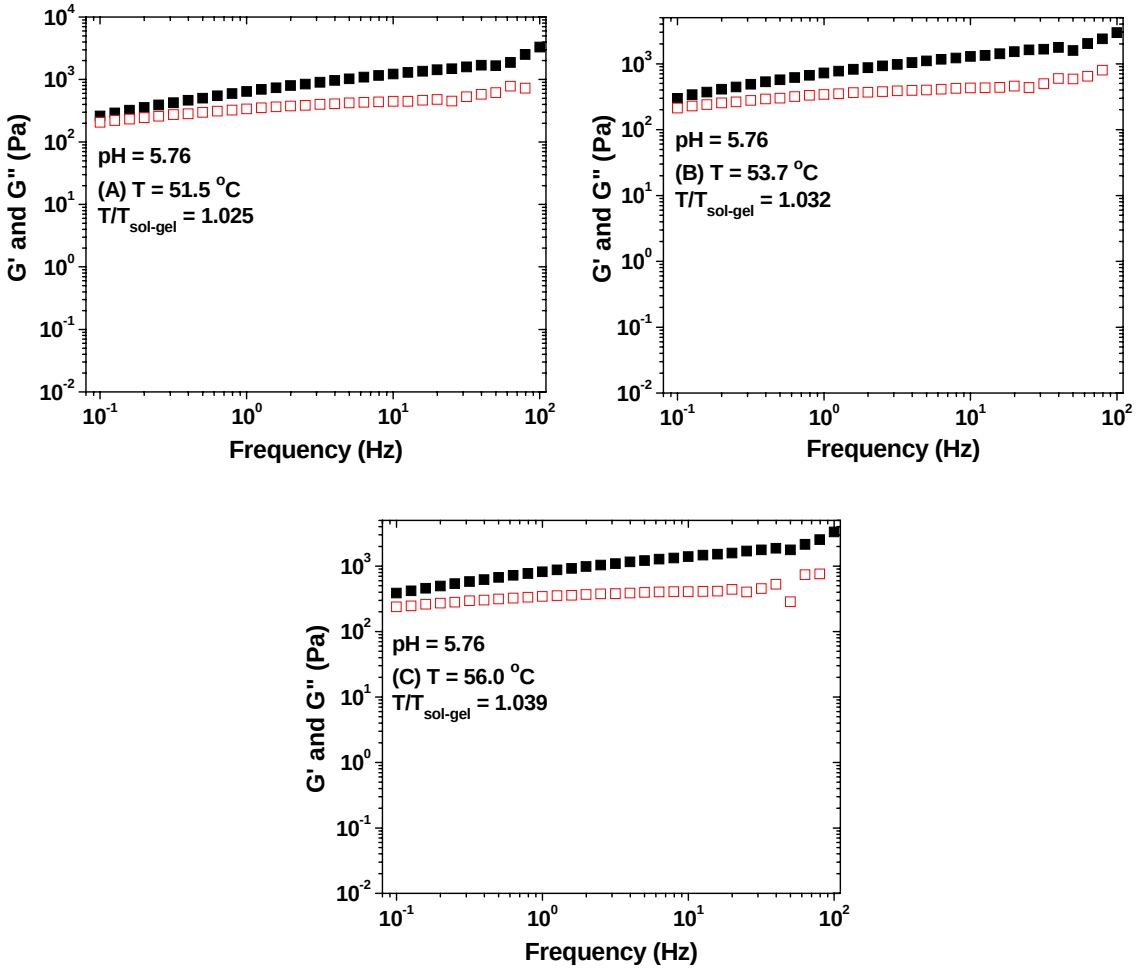

Figure B.26. Frequency dependences of dynamic storage modulus G' (■) and loss modulus G" (□) of a 10.0 wt% aqueous solution of P(DEGEA-*co*-AA)-*b*-PEO-*b*-P(DEGEA-*co*-AA) with pH of 5.76, which was obtained in the process of decreasing pH, at (A) 51.5 °C ($T/T_{sol\text{-}gel}$ = 1.025), (B) 53.7 °C ($T/T_{sol\text{-}gel}$ = 1.032), and (C) 56.0 °C ($T/T_{sol\text{-}gel}$ = 1.039). A strain amplitude of 0.2 % was used in the frequency sweep experiments.

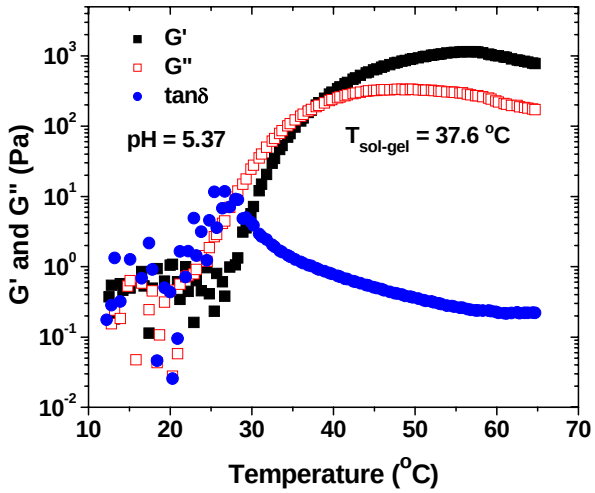

Figure B.27. Plot of dynamic storage modulus G' (■), dynamic loss modulus G" (□), and tanδ (●) versus temperature for a 10.0 wt% aqueous solution of P(DEGEA-*co*-AA)-*b*-PEO-*b*-P(DEGEA-*co*-AA) with a pH value of 5.37, which was obtained in the process of decreasing pH. The data were collected from a temperature ramp experiment performed using a heating rate of 3 °C/min, a strain amplitude of 0.2 %, and an oscillation frequency of 1 Hz.

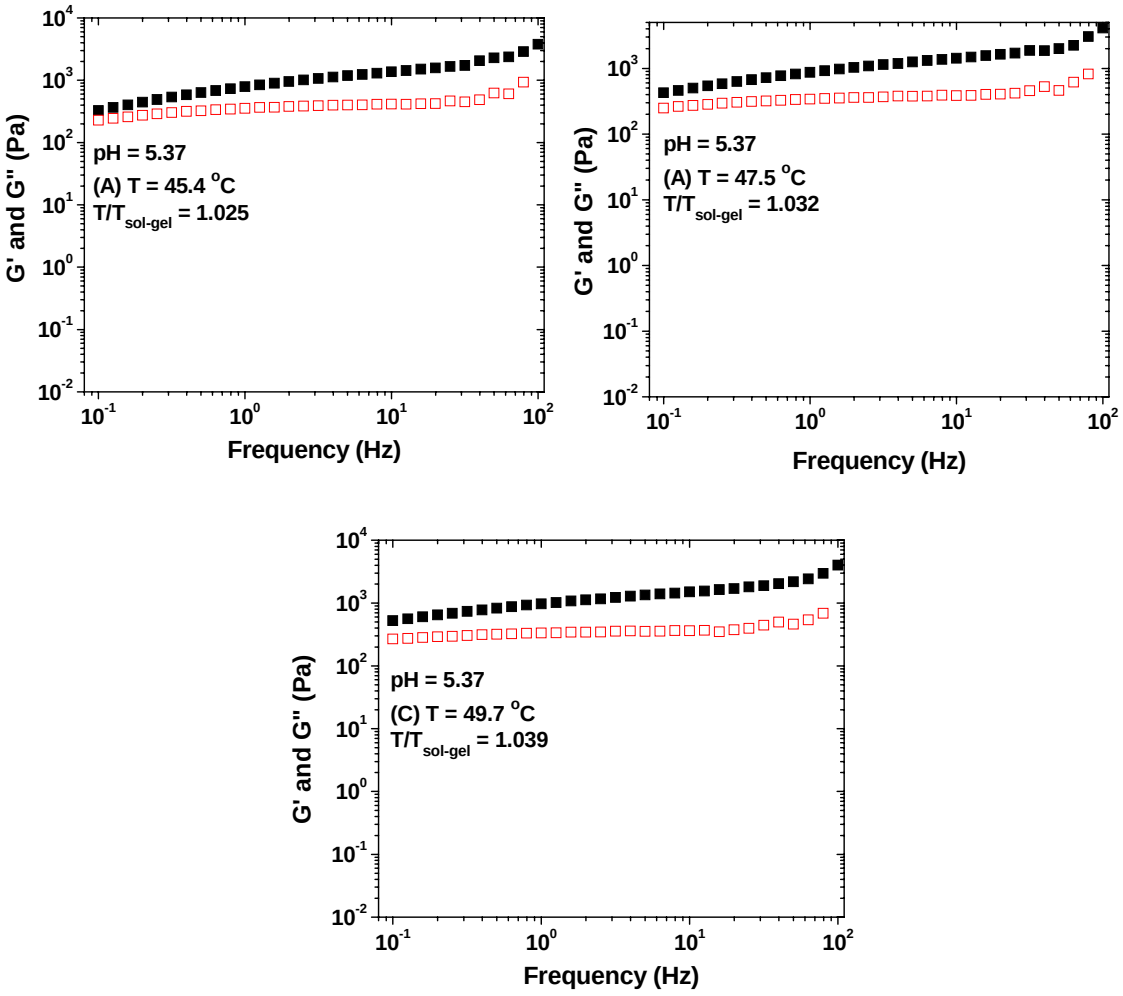

Figure B.28. Frequency dependences of dynamic storage modulus G' (■) and loss modulus G'' (□) of a 10.0 wt% aqueous solution of P(DEGEA-*co*-AA)-*b*-PEO-*b*-P(DEGEA-*co*-AA) with pH of 5.37 obtained in the process of decreasing pH at (A) 45.4 °C ($T/T_{sol\text{-}gel}$ = 1.025), (B) 47.5 °C ($T/T_{sol\text{-}gel}$ = 1.032), and (C) 49.7 °C ($T/T_{sol\text{-}gel}$ = 1.039). A strain amplitude of 0.2 % was used in the frequency sweep experiments.

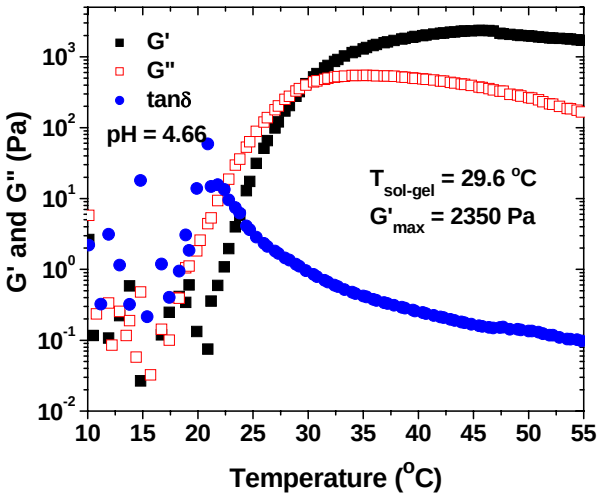

Figure B.29. Plot of dynamic storage modulus G' (■), dynamic loss modulus G" (□), and tanδ (●) versus temperature for a 10.0 wt% aqueous solution of P(DEGEA-*co*-AA)-*b*-PEO-*b*-P(DEGEA-*co*-AA) with a pH value of 4.66 obtained in the process of decreasing pH. The data were collected from a temperature ramp experiment performed using a heating rate of 3 °C/min, a strain amplitude of 0.2 %, and an oscillation frequency of 1 Hz.

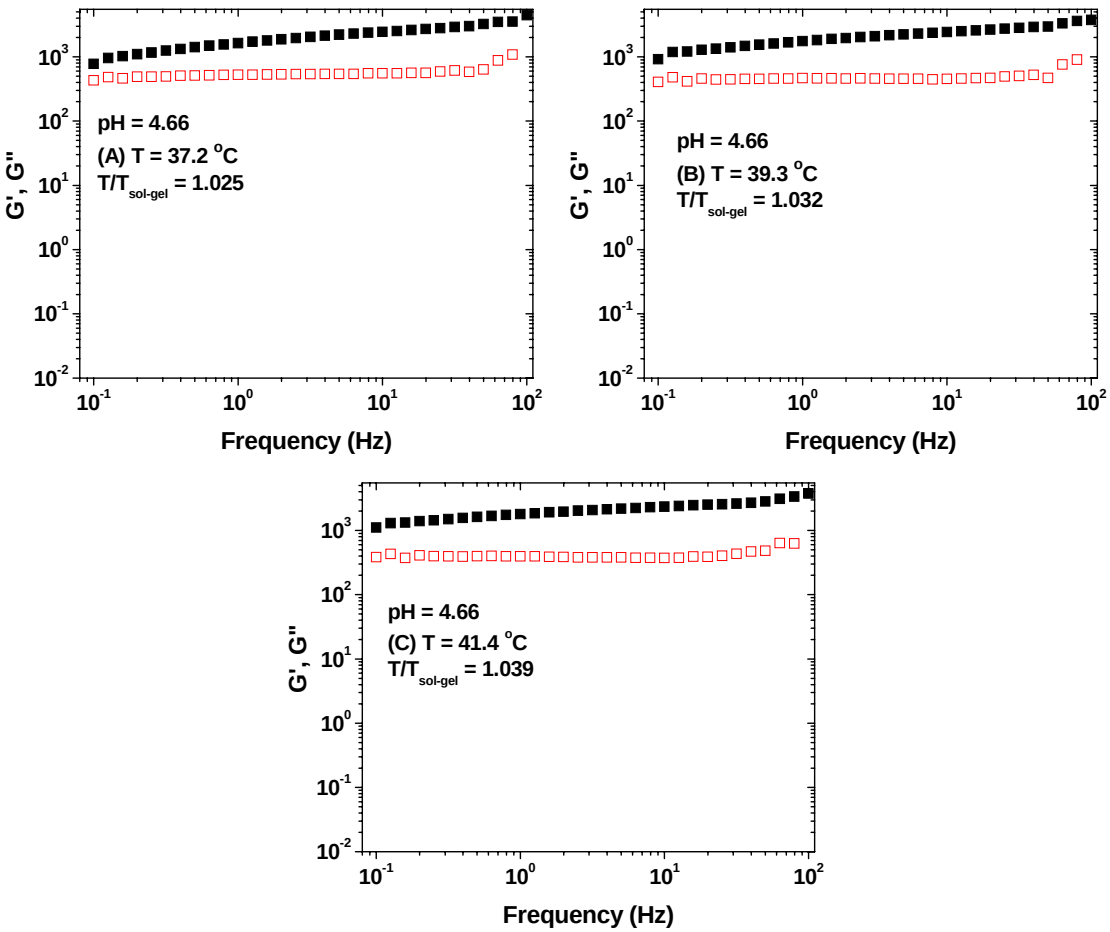

Figure B.30. Frequency dependences of dynamic storage modulus G' (■) and loss modulus G" (□) of a 10.0 wt% aqueous solution of P(DEGEA-*co*-AA)-*b*-PEO-*b*-P(DEGEA-*co*-AA) with pH of 4.66 obtained in the process of decreasing pH at (A) 37.2 °C ($T/T_{sol\text{-}gel}$ = 1.025), (B) 39.3 °C ($T/T_{sol\text{-}gel}$ = 1.032), and (C) 41.4 °C ($T/T_{sol\text{-}gel}$ = 1.039). A strain amplitude of 0.2 % was used in the frequency sweep experiments.

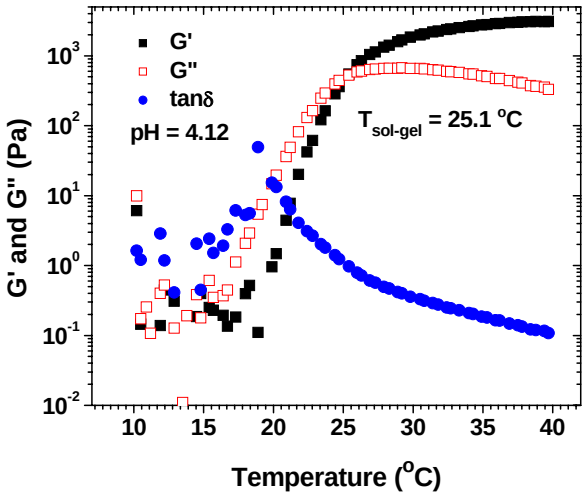

Figure B.31. Plot of dynamic storage modulus G' (■), dynamic loss modulus G" (□), and tanδ (●) versus temperature for a 10.0 wt% aqueous solution of P(DEGEA-*co*-AA)-*b*-PEO-*b*-P(DEGEA-*co*-AA) with a pH value of 4.12, which was obtained in the process of decreasing pH. The data were collected from a temperature ramp experiment performed using a heating rate of 3 °C/min, a strain amplitude of 0.2 %, and an oscillation frequency of 1 Hz.

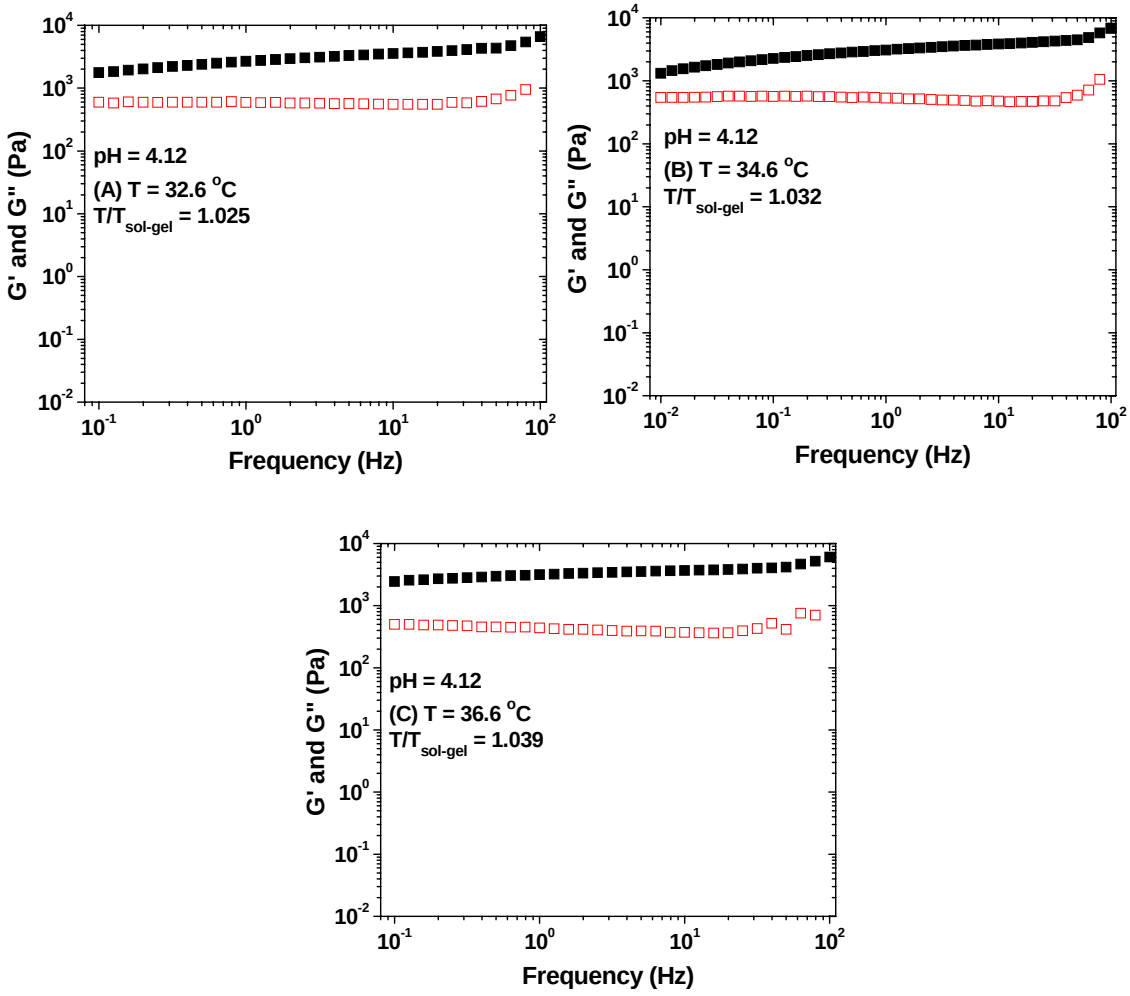

Figure B.32. Frequency dependences of dynamic storage modulus G' (■) and loss modulus G" (□) of the 10.0 wt% aqueous solution of P(DEGEA-*co*-AA)-*b*-PEO-*b*-P(DEGEA-*co*-AA) with pH of 4.12, obtained by the injection of 1.0 M HCl solution in the process of decreasing pH, at (A) 32.6 °C ($T/T_{sol\text{-}gel}$ = 1.025), (B) 34.6 °C ($T/T_{sol\text{-}gel}$ = 1.032), and (C) 36.6 °C ($T/T_{sol\text{-}gel}$ = 1.039). A strain amplitude of 0.2 % was used in the frequency sweep experiments.

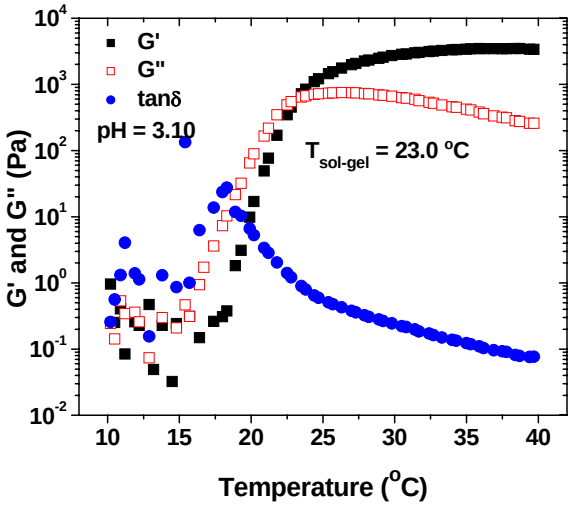

Figure B.33. Plot of dynamic storage modulus G' (■), dynamic loss modulus G" (□), and tanδ (●) versus temperature for a 10.0 wt% aqueous solution of P(DEGEA-*co*-AA)-*b*-PEO-*b*-P(DEGEA-*co*-AA) with a pH value of 3.10, which was obtained by the injection of 1.0 M HCl solution in the process of decreasing pH. The data were collected from a temperature ramp experiment performed using a heating rate of 3 °C/min, a strain amplitude of 0.2 %, and an oscillation frequency of 1 Hz.

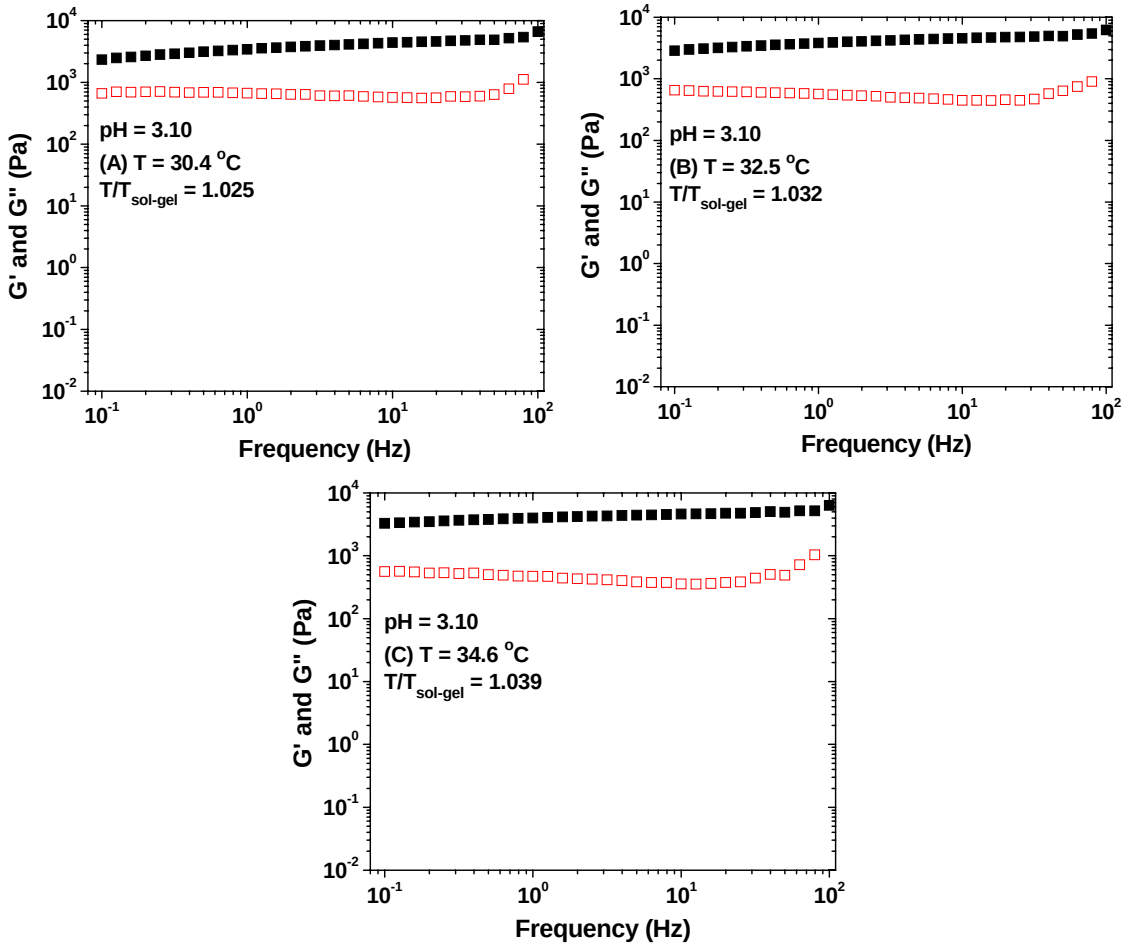

Figure B.34. Frequency dependences of dynamic storage modulus G' (■) and loss modulus G" (□) of the 10.0 wt% aqueous solution of P(DEGEA-*co*-AA)-*b*-PEO-*b*-P(DEGEA-*co*-AA) with pH of 3.10, which was obtained by the injection of 1.0 M HCl solution in the process of decreasing pH, at (A) 30.4 °C ($T/T_{sol\text{-}gel}$ = 1.025), (B) 32.5 °C ($T/T_{sol\text{-}gel}$ = 1.032), and (C) 34.6 °C ($T/T_{sol\text{-}gel}$ = 1.039). A strain amplitude of 0.2 % was used in the frequency sweep experiments.

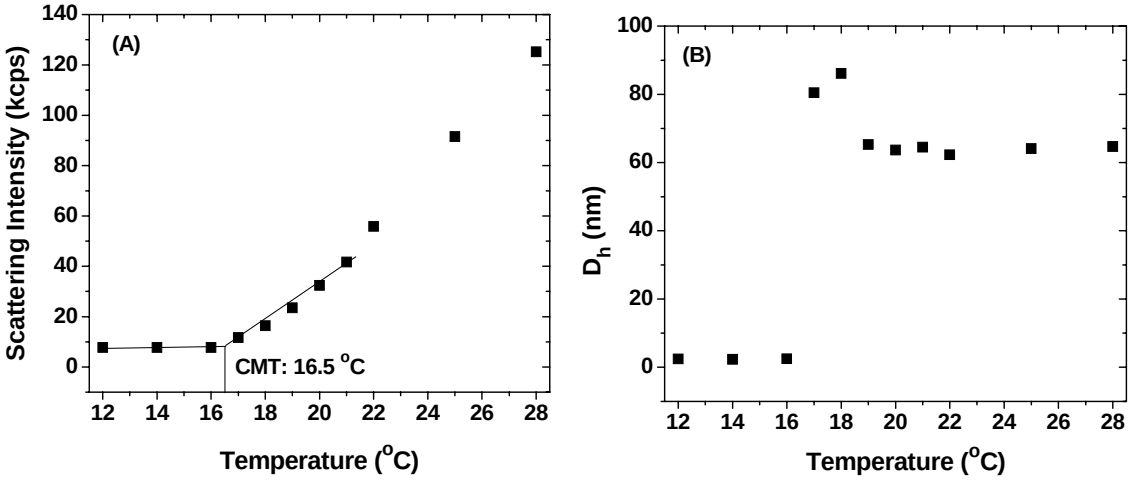

Figure B.35. Scattering intensity at scattering angle of 90° (A) and apparent hydrodynamic size D_h (B), obtained from CONTIN analysis, as a function of temperature in a dynamic light scattering study of 0.02 wt% solution of P(DEGEA-*co*-AA)-*b*-PEO-*b*-P(DEGEA-*co*-AA) in 10 mM KHP aqueous buffer at pH = 4.11.

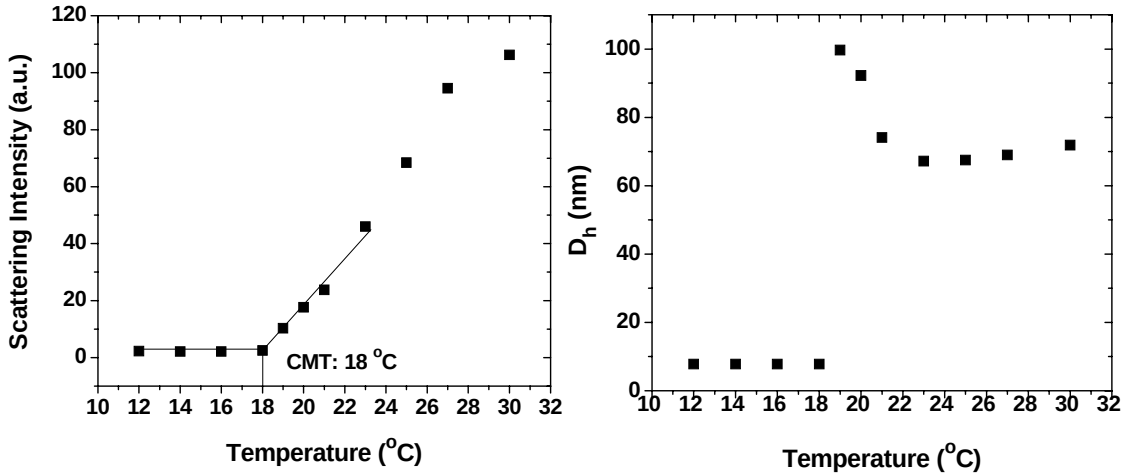

Figure B.36. Scattering intensity at scattering angle of 90° (A) and apparent hydrodynamic size D_h (B), obtained from CONTIN analysis, as a function of temperature in a dynamic light scattering study of 0.02 wt% solution of P(DEGEA-*co*-AA)-*b*-PEO-*b*-P(DEGEA-*co*-AA) in 10 mM KHP aqueous buffer at pH = 5.07.

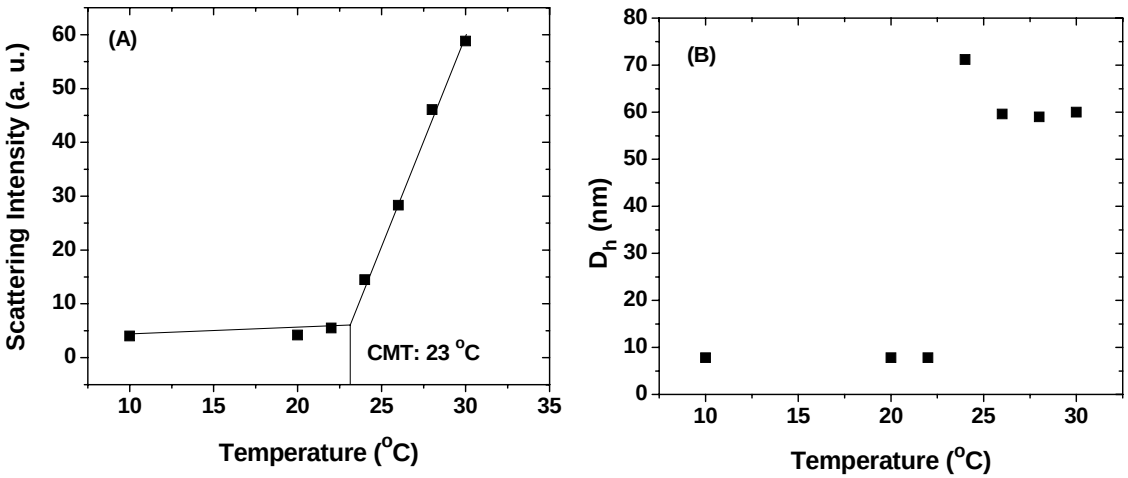

Figure B.37. Scattering intensity at scattering angle of 90° (A) and apparent hydrodynamic size D_h (B), obtained from CONTIN analysis, as a function of temperature in a dynamic light scattering study of 0.02 wt% solution of P(DEGEA-*co*-AA)-*b*-PEO-*b*-P(DEGEA-*co*-AA) in 10 mM KHP aqueous buffer at pH = 6.00.

Salt Effect Study

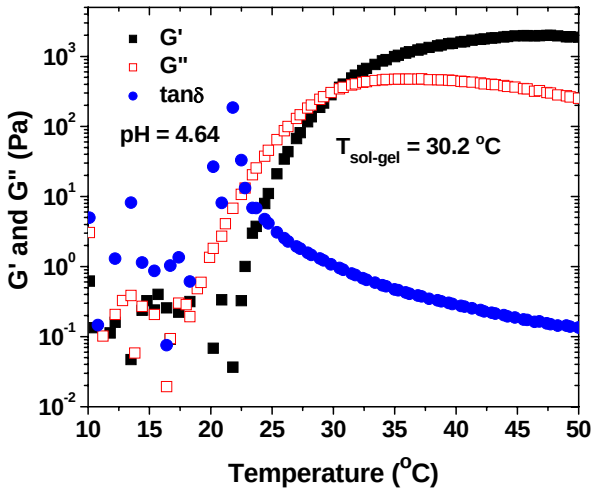

Figure B.38. Plot of dynamic storage modulus G' (■), dynamic loss modulus G" (□), and tanδ (●) versus temperature for a 10.0 wt% aqueous solution of P(DEGEA-*co*-AA)-*b*-PEO-*b*-P(DEGEA-*co*-AA) with a pH value of 4.64 without addition of KCl. The data were collected from a temperature ramp experiment performed using a heating rate of 3 °C/min, a strain amplitude of 0.2 %, and an oscillation frequency of 1 Hz.

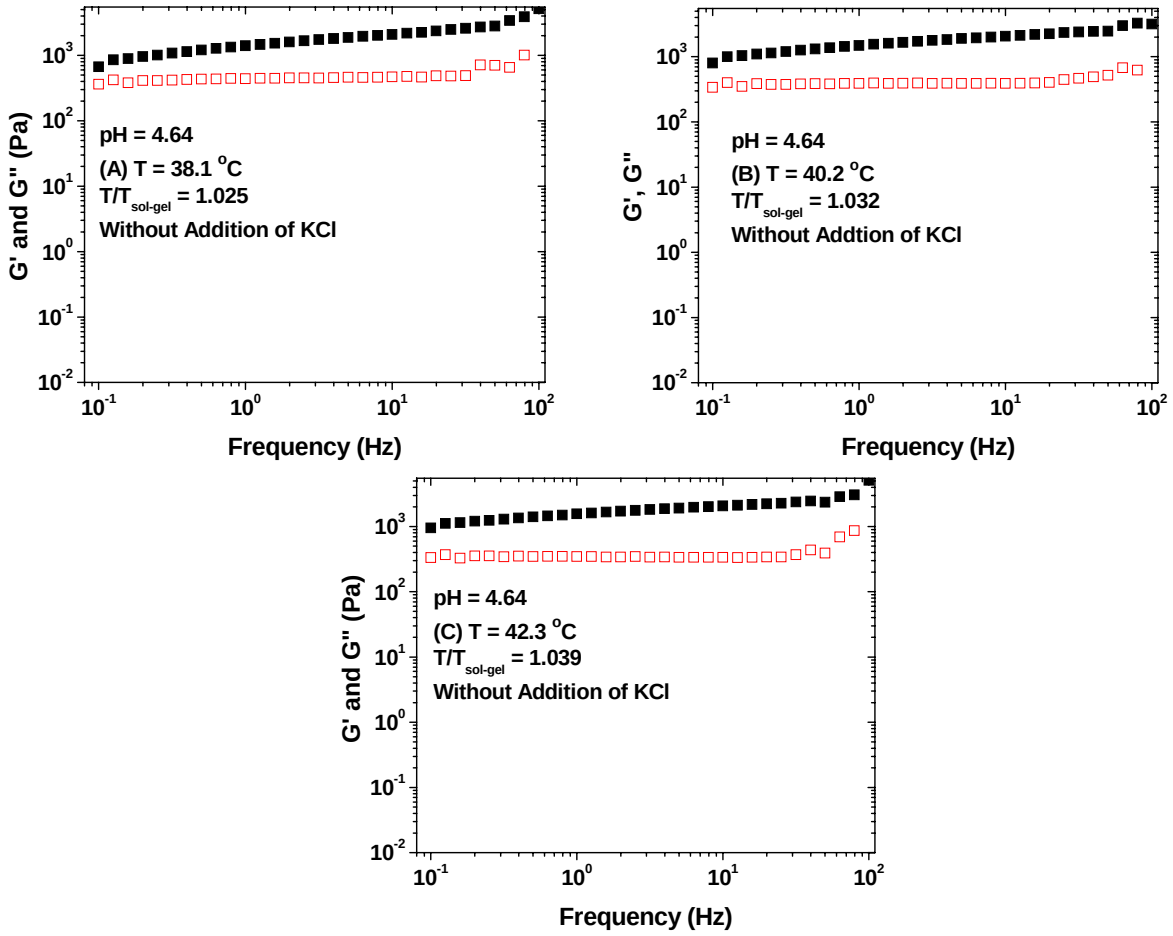

Figure B.39. Frequency dependences of dynamic storage modulus G' (■) and loss modulus G" (□) of a 10.0 wt% aqueous solution of P(DEGEA-*co*-AA)-*b*-PEO-*b*-P(DEGEA-*co*-AA) with pH of 4.64 without addition of KCl at (A) 38.1 °C ($T/T_{\text{sol-gel}}$ = 1.025), (B) 40.2 °C ($T/T_{\text{sol-gel}}$ = 1.032), and (C) 42.3 °C ($T/T_{\text{sol-gel}}$ = 1.039). A strain amplitude of 0.2 % was used in the frequency sweep experiments.

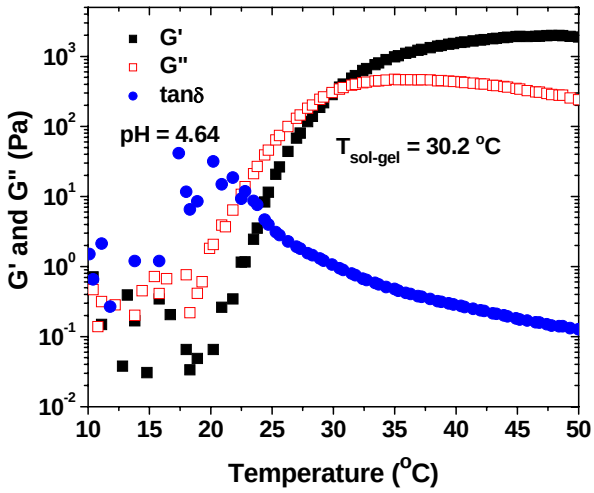

Figure B.40. Plot of dynamic storage modulus G' (■), dynamic loss modulus G" (□), and tanδ (●) versus temperature for a 10.0 wt% aqueous solution of P(DEGEA-*co*-AA)-*b*-PEO-*b*-P(DEGEA-*co*-AA) with a pH value of 4.64 after the addition of 20.4 mol% KCl with respect to the calculated amount of COOH/COOK. The data were collected from a temperature ramp experiment performed using a heating rate of 3 °C/min, a strain amplitude of 0.2 %, and an oscillation frequency of 1 Hz.

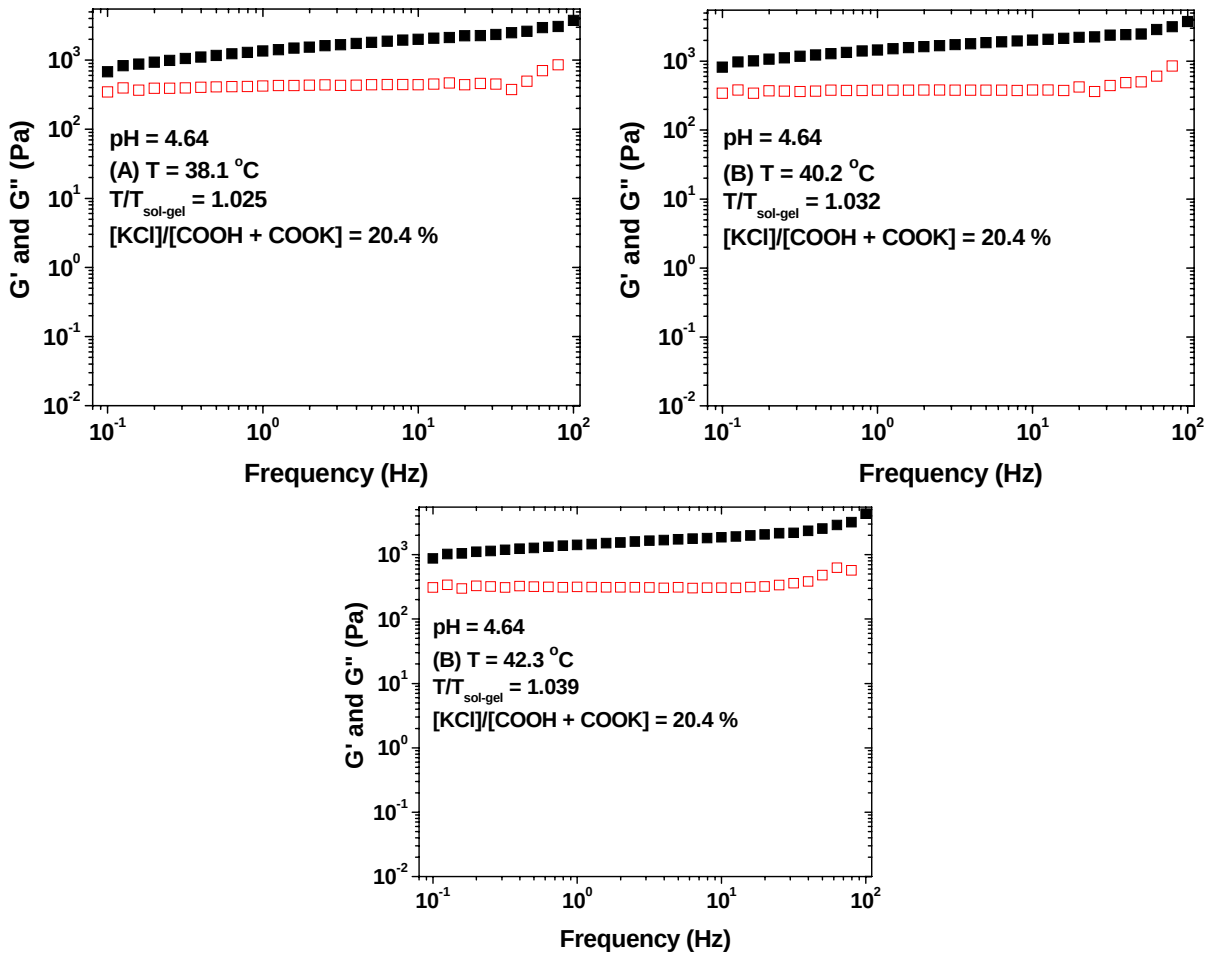

Figure S41. Frequency dependences of dynamic storage modulus G' (■) and loss modulus G" (□) of a 10.0 wt% aqueous solution of P(DEGEA-*co*-AA)-*b*-PEO-*b*-P(DEGEA-*co*-AA) with pH of 4.64 after the addition of 20.4 mol% KCl with respect to the calculated amount of COOH/COOK at (A) 38.1 °C ($T/T_{sol\text{-}gel}$ = 1.025), (B) 40.2 °C ($T/T_{sol\text{-}gel}$ = 1.032), and (C) 42.3 °C ($T/T_{sol\text{-}gel}$ = 1.039). A strain amplitude of 0.2 % was used in the frequency sweep experiments.

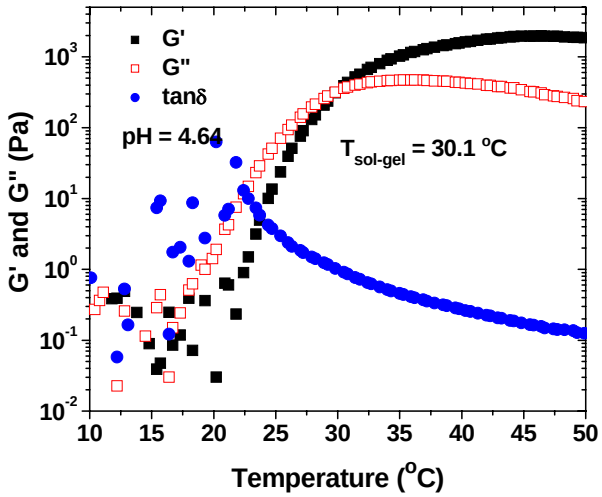

Figure B.42. Plot of dynamic storage modulus G' (■), dynamic loss modulus G" (□), and tanδ (●) versus temperature for a 10.0 wt% aqueous solution of P(DEGEA-*co*-AA)-*b*-PEO-*b*-P(DEGEA-*co*-AA) with a pH value of 4.64 after the addition of 59.6 mol% KCl with respect to the calculated amount of COOH/COOK. The data were collected from a temperature ramp experiment performed using a heating rate of 3 °C/min, a strain amplitude of 0.2 %, and an oscillation frequency of 1 Hz.

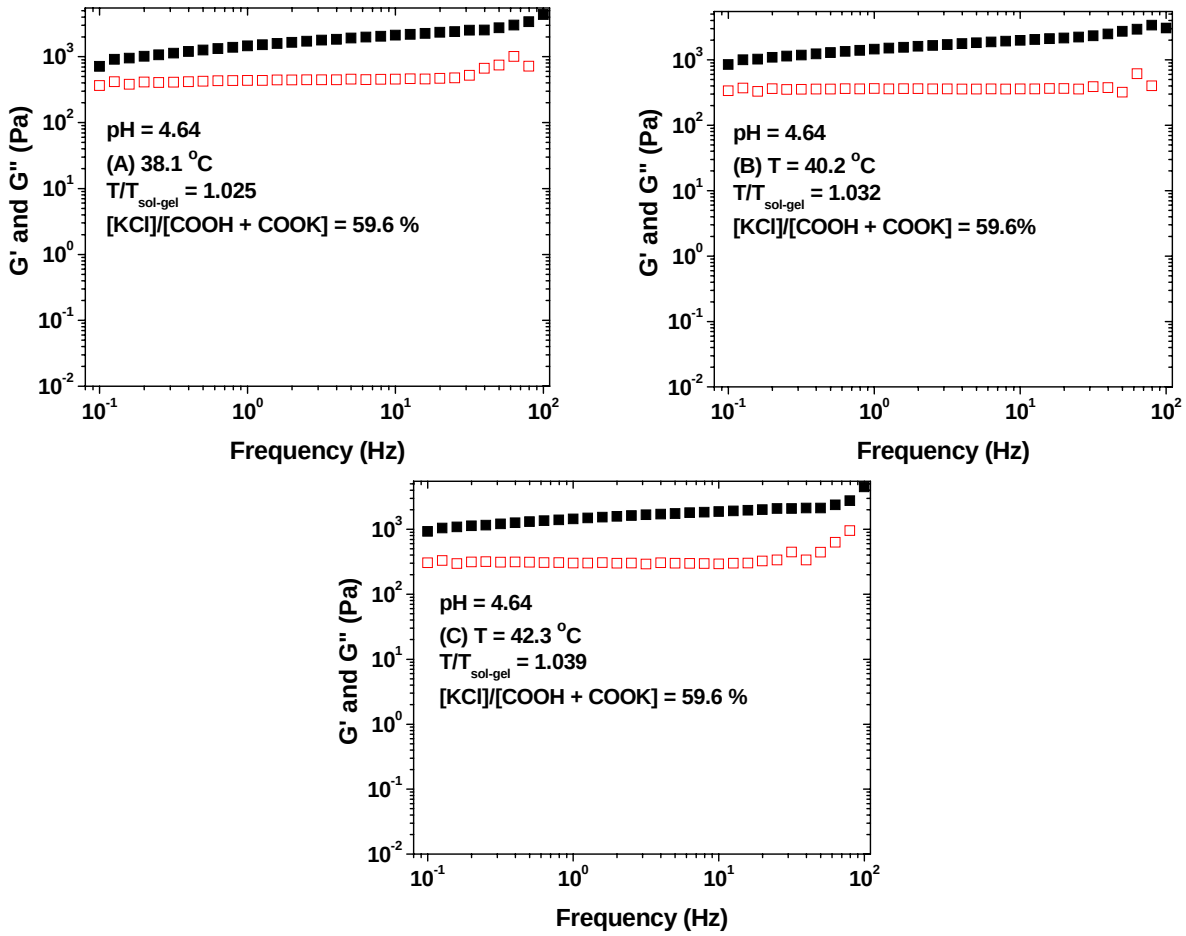

Figure B.43. Frequency dependences of dynamic storage modulus G' (■) and loss modulus G" (□) of a 10.0 wt% aqueous solution of P(DEGEA-*co*-AA)-*b*-PEO-*b*-P(DEGEA-*co*-AA) with pH of 4.64 after the addition of 59.6 mol% KCl with respect to the calculated amount of COOH/COOK at (A) 38.1 °C ($T/T_{sol\text{-}gel}$ = 1.025), (B) 40.2 °C ($T/T_{sol\text{-}gel}$ = 1.032), and (C) 42.3 °C ($T/T_{sol\text{-}gel}$ = 1.039). A strain amplitude of 0.2 % was used in the frequency sweep experiments.

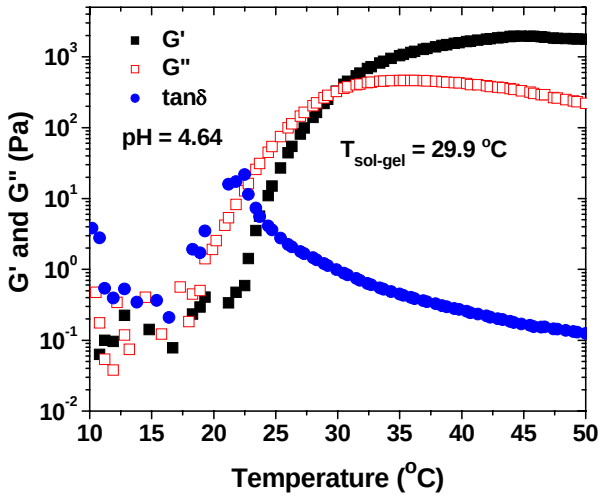

Figure B.44. Plot of dynamic storage modulus G' (■), dynamic loss modulus G" (□), and tanδ (●) versus temperature for a 10.0 wt% aqueous solution of P(DEGEA-*co*-AA)-*b*-PEO-*b*-P(DEGEA-*co*-AA) with a pH value of 4.64 after the addition of 100.9 mol% KCl with respect to the calculated amount of COOH/COOK. The data were collected from a temperature ramp experiment performed using a heating rate of 3 °C/min, a strain amplitude of 0.2 %, and an oscillation frequency of 1 Hz.

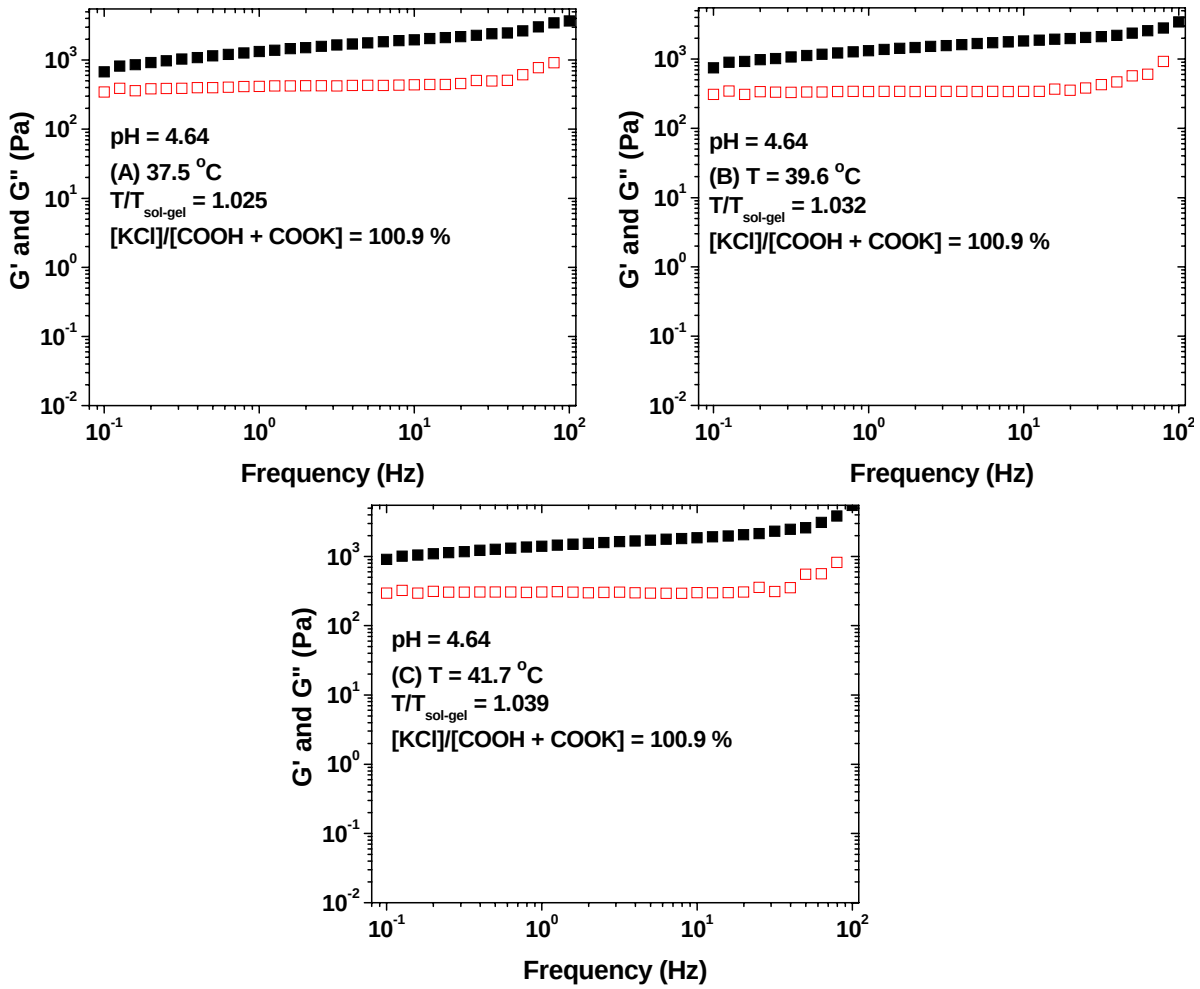

Figure B.45. Frequency dependences of dynamic storage modulus G' (■) and loss modulus G" (□) of a 10.0 wt% aqueous solution of P(DEGEA-*co*-AA)-*b*-PEO-*b*-P(DEGEA-*co*-AA) with pH of 4.64 after the addition of 100.9 mol% KCl with respect to the calculated amount of COOH/COOK at (A) 37.5 °C ($T/T_{sol\text{-}gel}$ = 1.025), (B) 39.6 °C ($T/T_{sol\text{-}gel}$ = 1.032), and (C) 41.7 °C ($T/T_{sol\text{-}gel}$ = 1.039). A strain amplitude of 0.2 % was used in the frequency sweep experiments.

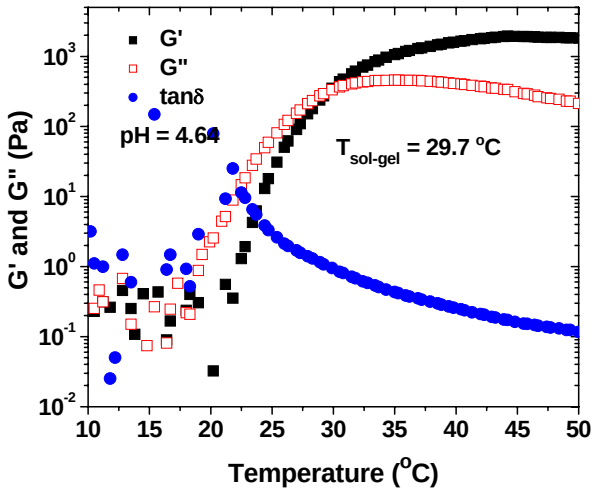

Figure B.46. Plot of dynamic storage modulus G' (■), dynamic loss modulus G" (□), and tanδ (●) versus temperature for a 10.0 wt% aqueous solution of P(DEGEA-*co*-AA)-*b*-PEO-*b*-P(DEGEA-*co*-AA) with a pH value of 4.64 after the addition of 151.4 mol% KCl with respect to the calculated amount of COOH/COOK. The data were collected from a temperature ramp experiment performed using a heating rate of 3 °C/min, a strain amplitude of 0.2 %, and an oscillation frequency of 1 Hz.

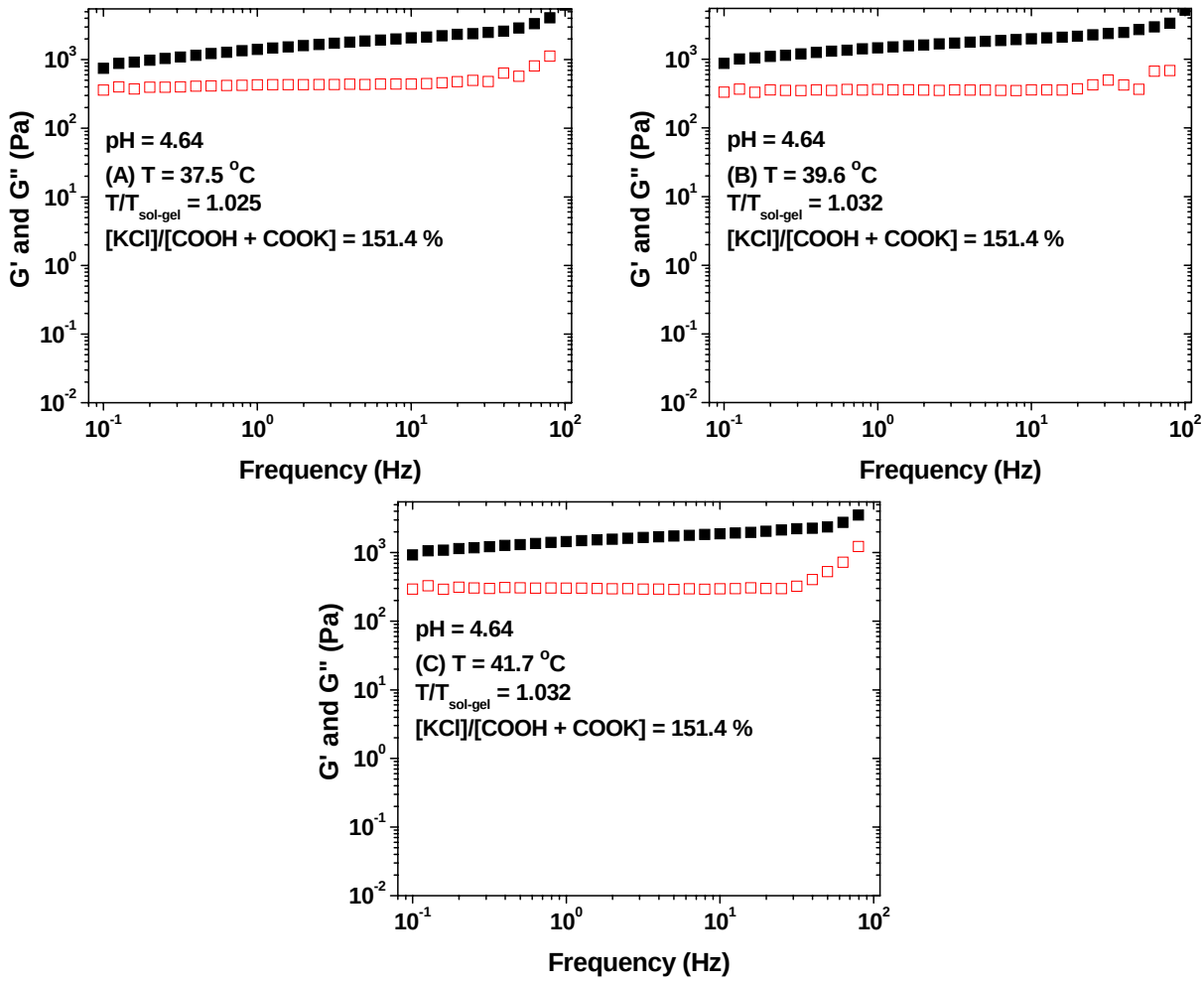

Figure B.47. Frequency dependences of dynamic storage modulus G' (■) and loss modulus G" (□) of a 10.0 wt% aqueous solution of P(DEGEA-*co*-AA)-*b*-PEO-*b*-P(DEGEA-*co*-AA) with pH of 4.64 after the addition of 151.4 mol% KCl with respect to the calculated amount of COOH/COOK at (A) 37.5 °C ($T/T_{sol\text{-}gel}$ = 1.025), (B) 39.6 °C ($T/T_{sol\text{-}gel}$ = 1.032), and (C) 41.7 °C ($T/T_{sol\text{-}gel}$ = 1.039). A strain amplitude of 0.2 % was used in the frequency sweep experiments.

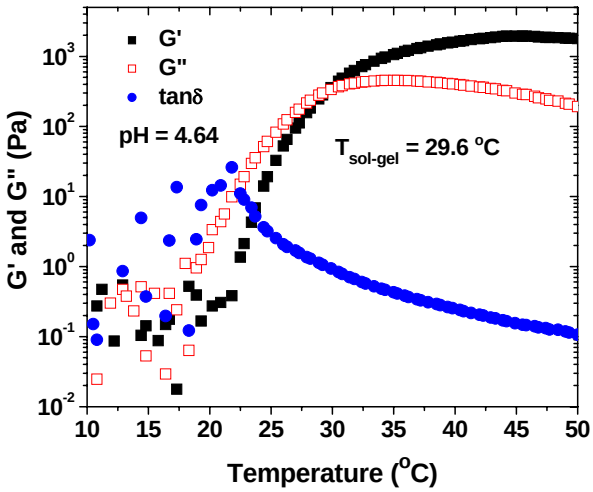

Figure B.48. Plot of dynamic storage modulus G' (■), dynamic loss modulus G" (□), and tanδ (●) versus temperature for a 10.0 wt% aqueous solution of P(DEGEA-*co*-AA)-*b*-PEO-*b*-P(DEGEA-*co*-AA) with a pH value of 4.64 after the addition of 200.8 mol% KCl with respect to the calculated amount of COOH/COOK. The data were collected from a temperature ramp experiment performed using a heating rate of 3 °C/min, a strain amplitude of 0.2 %, and an oscillation frequency of 1 Hz.

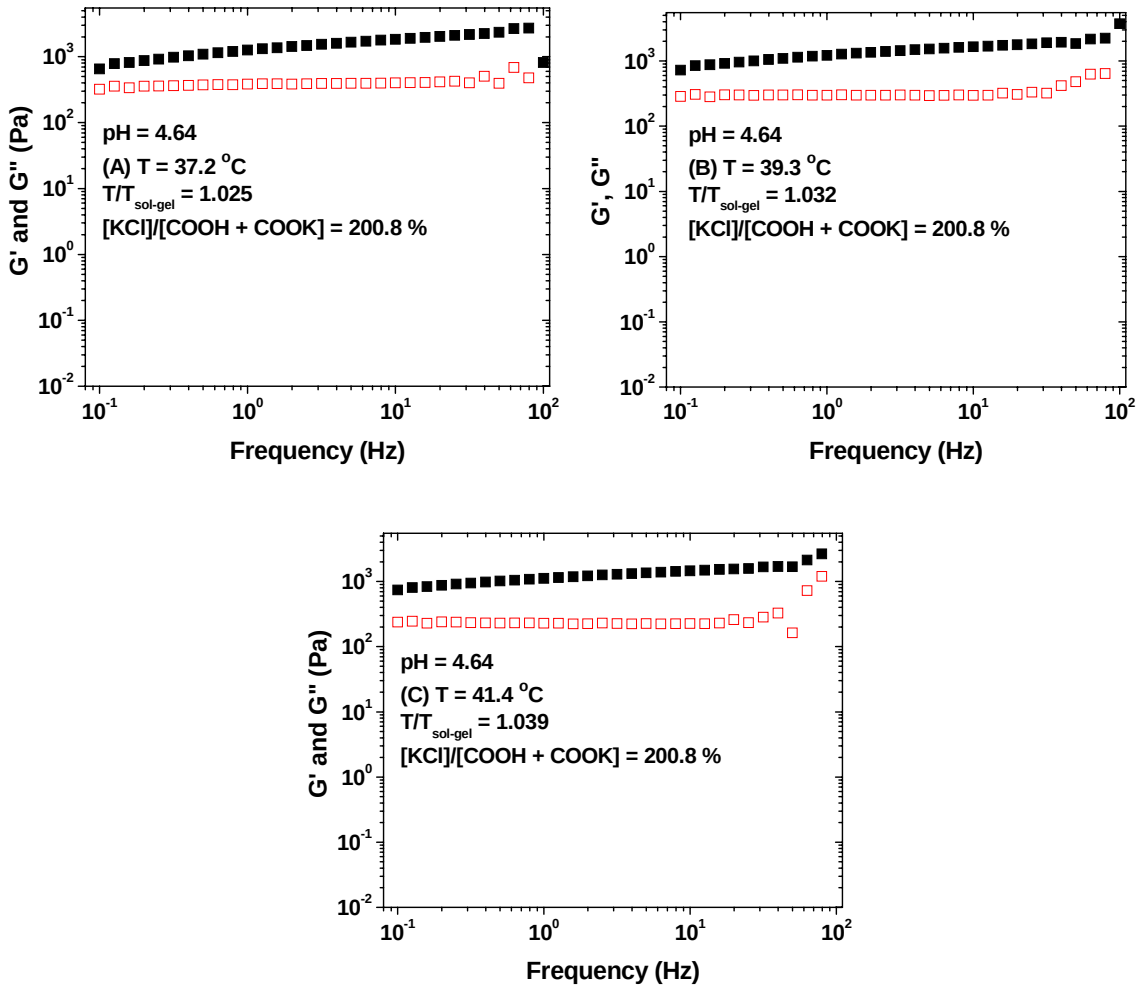

Figure B.49. Frequency dependences of dynamic storage modulus G' (■) and loss modulus G" (□) of a 10.0 wt% aqueous solution of P(DEGEA-*co*-AA)-*b*-PEO-*b*-P(DEGEA-*co*-AA) with pH of 4.64 after the addition of 200.8 mol% KCl with respect to the calculated amount of COOH/COOK at (A) 37.2 °C ($T/T_{sol\text{-}gel}$ = 1.025), (B) 39.3 °C ($T/T_{sol\text{-}gel}$ = 1.032), and (C) 41.4 °C ($T/T_{sol\text{-}gel}$ = 1.039). A strain amplitude of 0.2 % was used in the frequency sweep experiments.

Vita

Thomas G. O'Lenick was born in Ridgeview, New Jersey. He attended Georgia Southern University from 2000 to 2005, where he received a B.S. degree in Chemistry. In August, 2005, he enrolled as a graduate student in the Department of Chemistry at the University of Tennessee, Knoxville. He then joined Dr. Bin Zhao's group working on stimuli-sensitive hydrophilic block polymers. Thomas O'Lenick received a Doctor of Philosophy Degree in Chemistry from the University of Tennessee in May, 2011.